NASA-CR-54036

1282.

N64-25903

Code-1 Cat. 06

nasa Cr-54036

ELECTROMAGNETIC ALKALI METAL PUMP RESEARCH PROGRAM

Quarterly Progress Report 3

EDITED BY J. P. VERKAMP

prepared for

NATIONAL AERONAUTICS AND SPACE ADMINISTRATION

OTS PRICE

XEROX $ 10.10 ph

SPACE POWER AND PROPULSION SECTION
MISSILE AND SPACE DIVISION
GENERAL ELECTRIC
CINCINNATI 15, OHIO

Requests for copies of this report should be referred to:

National Aeronautics and Space Administration
Office of Scientific and Technical Information
Washington 25, D.C.
Attention: AFSS-A

NASA-CR-54036

ELECTROMAGNETIC ALKALI METAL PUMP RESEARCH PROGRAM

QUARTERLY PROGRESS REPORT 3

Covering the Period
December 27, 1963 to March 27, 1964

J. P. Verkamp, Manager
EM Pump Project

prepared for

NATIONAL AERONAUTICS AND SPACE ADMINISTRATION

Contract NAS 3-2543

May 22, 1964

Technical Management
NASA - Lewis Research Center
Nuclear Power Technology Branch
Robert T. Wainwright

SPACE POWER AND PROPULSION SECTION
MISSILE AND SPACE DIVISION
GENERAL ELECTRIC COMPANY
CINCINNATI, OHIO 45215

TABLE OF CONTENTS

TABLE OF CONTENTS - CONT'D

LIST OF ILLUSTRATIONS

LIST OF ILLUSTRATIONS - CONT'D

LIST OF TABLES

NOMENCLATURE

A	Cross-sectional area duct or a constant
A_1, A_2, A_3	Constants defined where used
B_i	3.19 I/zd
B_m	Average Flux density
C	Permeance constant
C_1	Constant defined where used
D	$\frac{\rho f}{\rho d}\left(\frac{2t}{a}\right)$ or Hydraulic diameter
I	Current
I_d	Current in the fluid directly between electrodes
I_f	Fringing current
I_m	Imaginary part of a complex conjugate
I_t	Current in the duct walls
K	Velocity heads
L	Length
M	Magnetomotive force
M_c	Total mmf produced by exciting coil
N_H	Hartmann Number
N_R	Reynolds Number
P	Pressure loss or developed pressure
P'	Defined where used
P_d	Pressure drop in duct
$P_{h\mu}$	Total pressure loss
P	Pressure loss, viscous
P_{Tr}	Pressure drop in transition section
P_o	Output pressure, net
Q	Flow in duct
R	Electrical resistance
R_c	Coil resistance
R_d	Resistance fluid in duct
R'_d	Defined where used
R_e	Resistance of duct outlet header
R_f	Resistance of fringing current path
R_ℓ	Resistance of duct outlet header
R_o	Resistance of duct inlet header
R_t	Resistance of duct walls
Re	Real part of a complex conjugate
V	Voltage
V_e	Voltage across duct fluid
V_g	Back emf
V_t	Volts per turn
W	Power
W_i	Input Power
W_o	Hydraulic output power
X	Defined where used or distance along X axis

NOMENCLATURE - CONT'D

a,b	Duct dimensions
c	Duct dimension or electrode length along duct
d	Mean duct diameter or gap between magnet poles
f	Frequency or force
f_h	Hydraulic drag on duct fluid
g	Total air or non-magnetic gap or gravitational constant
h	Velocity head
i	$\sqrt{-1}$
j	Current density
j_d	Current density in duct walls
j_f	Current density in duct fluid
ℓ	Effective duct length
t	Duct wall thickness
v	Fluid velocity
$\bar{v}$	Average fluid velocity
v_s	Synchronous velocity
w	2 f
x,y,z	Rectangular coordinate system
e	Log base e 2.72
α	Constant
$\dot{\beta}$	.1915 vC/ρ or constant
γ	Constant
δ	Friction factor
η	Efficiency
μ	Fluid viscosity or permeability of air gap
π	3.1416
ρ	Electrical resistivity
ρ_d	Electrical resistivity, duct walls
ρ_f	Electrical resistivity, duct fluid
σ	Fluid density
Φ	Constant
ϕ	Magnetic flux in core at distance x from duct inlet
VAR	Reactive power
P.F.	Power Factor

I. SUMMARY

The Space Power and Propulsion Section of the General Electric Company has been under contract to the National Aeronautics and Space Administration since June 27, 1963 for the performance of a research program to study electromagnetic pumps for application to Space Electric Power Plants.

This is the Third Quarterly Report for the program, covering the period from December 27, 1963 to March 27, 1964. The total program will include three principle phases. Phase I is primarily analytical. Phase II is experimental and will include manufacture and test of the best selections from Phase I. The final phase will evaluate the results of the first two phases. The entire program is estimated to require about thirty months to complete. However, the Phase I portion which is of primary interest here was allotted twelve months plus thirty days for final reporting.

The objectives of Phase I of the program are to determine the feasibility of using EM pumps in Space Electric Power Plants, establish the bases for selecting pumps for specific application, establish the bases for design of EM pumps applicable to space power plants, select pumps for construction and test and establish a test program for the selected pumps.

During the past quarter the most significant developments were:

2) Indication that the new design approach being developed by this program will produce pumps with about 1/10 the weight of previous pumps. (See Figure G-1.)

b) Development of a single phase induction pump particularly well suited to the high temperature primary coolant application (Figure G-4).

c) Indication that a boiler feed EM pump for the turbo-electric power plant could be competitive in weight with a canned motor - jet injector pump for the same application (Figure G-5).

Continuing the review of basic EM pump types and identifying their characteristics produced some qualitative information on the thermoelectromagnetic pump. This pump provides the simplicity of the D.C. conduction pump while eliminating the power supply problems of the D.C. pump. However, start up may be a problem and low efficiency of thermoelectric elements requires high heat flows and may lead to high weight.

Quantitative selection procedures were further developed. A general analysis of pump duct hydraulic pressure drop was completed. A graphical presentation of the results of the analysis was made relating hydraulic friction factor to the Hartmann Number as well as to the Reynolds Number. Thus the effects of flux density and fluid resistivity are included. This is the last of the general relationships planned for pump selection and design work under the present study.

Analytical methods specifically applicable to D-C conduction pump design and performance prediction were developed. The analyses cover both the electromagnetic and the permanent magnet machines.

Methods were developed for design and analysis of the single phase induction pump. To a great extent this was original work, although the suggestions of Watt[15] were used wherever applicable.

Further basic information required to support actual pump designs was accumulated and evaluated. Characteristics of soft magnetic materials and dielectric properties of gases were among these items. Reliability of the various pump types was surveyed. The results were tabulated in a chart which indicated the single phase induction pump to be most reliable.

Order of magnitude values for pump weights were obtained. A list of EM pumps produced and operated over the past ten years was prepared showing some of their characteristics. These pumps were compared in specific weight to the preliminary pump designs already produced by this program. As mentioned earlier an order of magnitude improvement appears possible.

More detailed weight information was developed for comparison and evaluation of the various pump types in the six specific applications selected for this program. Effects on weight of pump cooling, power factor, and power conditioning were determined.

Much of the above information as well as that presented in earlier progress reports was used to prepare a design of a D-C conduction pump for the condensate boost application. Compared to the helical induction pump presented in Quarterly Report No. 2 for the same application, the D.C. pump looked most attractive on a pumping system weight basis.

Similarly, a single phase induction pump design was initiated for service in the thermionic system primary coolant application. Preliminary design work has progressed sufficiently to permit estimation of weight and efficiency, both of which are attractive.

One other pump design was prepared. Primarily as a test of how competitive the EM pump is relative to canned motor pumps, a helical induction pump for boiler feed application was designed. Results of the design were compared with a canned motor pump for a similar application. The EM pump is competitive in weight.

The above results strongly suggests that further development of the EM pump is warranted. Plans for the Phase II work already begun in the second quarter were carried further in this quarter. A preliminary schedule of Phase II pump manufacture and test was prepared. It was based on two pumps.

Phase I schedule was again modified. The primary cause was the contractual change which extended the end date to August 3, 1964. In the over-all view, the program is now on schedule. However, to maintain the schedule, much work must be done next quarter in finalizing and summarizing the selection of pump types. Materials choices must be finalized and a large number of preliminary pump designs must be made.

II. INTRODUCTION

Until recently the use of electromagnetic pumps in space power plants using liquid metal working fluids had been generally considered unacceptable from a weight penalty standpoint. However in considering the reliability problems associated with other pumping methods, it appeared that a larger weight penalty might be accepted in order to gain the high reliability attainable with EM pumps.

In order to thoroughly evaluate the use of EM pumps in space power application, NASA established the Electromagnetic Alkali Metal Pump Research Program.

The program was divided into three phases as follows:

Phase I - Analytical phase consisting of (a) Evaluation of EM pumps for use in space power systems in both circulating and condensate boost applications, (b) Development of analytical methods to predict performance and to define optimum design, (c) Analytical methods for scaling EM pumps to meet future requirements, (d) Recommendations on the selection of one or more EM pumps for test, and (e) Definition of an EM pump test program.

Phase II - Experimental phase consisting of (a) Detailed design of selected pumps for test purposes, (b) Manufacture of the test pumps, (c) Design and manufacture of a suitable installation for testing the pumps, and (d) Performance of the test work and gathering and evaluation of the required data.

Phase III - Evaluation phase whereby an overall evaluation of EM pump performance and limitations will be presented as the final result of the program.

Contract NAS 3-2543 is for Phase I only. The evaluation, selection and analysis are guided by six particular pump applications. The design objectives stated for the selection of these pumps are quite specific and are based on the best estimates from present space power plant studies of the one megawatt level. The pumps are intended for use in space electric power generating systems of the turboelectric and thermionic types using certain alkali metals as the working fluids. The energy source is a nuclear reactor and the heat sink is a radiator in space. The design objectives for the various applications are shown in Table II-1.

The starting point for the program was a literature search to compile a summary of important previous work in the field of EM pumps. The results were presented in past quarterly reports. The principal value of this work was the compilation of all the many EM pump concepts that might fit the applications to be considered in the program. A total of 18 conceptual sketches and brief descriptions were presented. Along with this some initial analytical methods for performance prediction were developed.

Since selection of the pump requires considerable attention to the power plant characteristics, the initial step of integrating the pumps into the two reference power plants was also undertaken and described in past reports.

TABLE II-1

SPACE POWER PLANT EM PUMP APPLICATIONS

Application	Fluid Temp - °F			Flow - pps ... gpm			Press. Rise - psi ... ft.			Net Pos. Suction Press. - psi ... ft.			No. Pumps in Parallel	Developed Hydraulic Power - KW		
	Design Point	Study Range	Test Range	Design Point	Study Range	Test Range	Design Point	Study Range	Test Range	Design Point	Study Range	Test Range		Design Point	Study Range	Test Range
Turboelectric Condensate Boost Potassium	1200	1000 to 1400	1000 to 1400	1.5 ... 15.5	1-12 ... 10-125	1-10 ... 10-100	29.8 ... 100	3-60 ... 10-200	3-45 ... 10-150	2.98 ... 10	0-15 ... 0-50	0-15 ... 0-50	4	.20	.01-3	.01-2
Turboelectric Radiator Coolant NaK	1200	1000 to 1300	1000 to 1300	6 ... 60.0	3-36 ... 30-350	3-24 ... 30-230	25 ... 80.3	10-100 ... 30-320	10-100 ... 30-320	30 ... 96.7	20-40 ... 60-120	20-40 ... 60-120	16	.65	.13-15	.13-10
Turboelectric Radiator Coolant Lithium	1200	1000 to 1500	1000 to 1500	2 ... 30.3	1-12 ... 15-190	1-8 ... 15-125	20 ... 97.5	10-60 ... 50-300	10-40 ... 50-200	30 ... 146	20-40 ... 100-200	20-40 ... 100-200	16	.27	.06-5	.06-2.3
Thermionic Primary Coolant Lithium	1700	1200 to 2000	1200 to 1500	40 ... 647	35-200 ... 500-3000	35-100 ... 500-1500	6 ... 32.0	3-50 ... 15-250	3-10 ... 15-50	10 ... 52	5-20 ... 25-100	5-20 ... 25-100	1	2.3	.65-65	.65-13
Thermionic Radiator Coolant Lithium	1200	1000 to 1500	1000 to 1500	2 ... 30.3	1-12 ... 15-190	1-8 ... 15-125	20 ... 97.5	10-60 ... 50-300	10-40 ... 50-200	30 ... 146	20-40 ... 100-200	20-40 ... 100-200	16	.27	.06-5	.06-2.3
Thermionic Radiator Coolant Nak	1200	1000 to 1300	1000 to 1300	6 ... 60.0	3-36 ... 30-350	3-24 ... 30-230	25 ... 80.3	10-100 ... 30-320	10-100 ... 30-320	30 ... 96.7	20-40 ... 60-120	20-40 ... 60-120	16	.65	.13-15	.13-10

III. DISCUSSION

A. Electromagnetic Pump Characteristics

1. Introduction

To provide a basis for the choice of EM pump types having promise for particular space power applications, a listing and description of all the basic types of EM pumps was prepared. Largely qualitative in nature, it indicates the principal features and characteristics of each basic type EM pump. To attain comprehensive coverage, the following steps have been taken:

1. The available EM pump literature has been surveyed.
2. Principles and configurations analogous to electromagnetic devices have been sought.
3. The list has been extended by the principle of "duality"; that is analogies to other types of pumps, and to other electrical machinery.

Emphasis is placed on completeness with regard to basic types, although no attempt is made to cover the many variations in configuration detail possible within types.

2. Thermoelectromagnetic Pump

The literature survey and compilation of pump characteristics is essentially completed except for the thermoelectromagnetic or TEM pump. Actually this pump is a variation of the D.C. conduction pump which has already been thoroughly discussed. Therefore, the TEM pump will be considered here only in the manner in which it differs from the usual D.C. conduction configuration. Justification for presentation of the TEM pump as a separate type derives from the search for an answer to the one major weakness in the D.C. conduction pump.

One of the primary disadvantages of the D.C. conduction pump is the power conditioning associated with the low voltage-high current power required. The TEM approach eliminates this problem by obtaining power in the required form from a thermoelectric element mounted directly on the pump structure. The pumped fluid provides part of the thermal energy circuit required to drive the thermoelectric element. If the fluid is primary coolant, for example, the hot junction of the thermoelectric element is in contact with the hot fluid. The heat must then be removed from the cold junction by a cooler fluid such as the radiator coolant or by direct dissipation to space. Figure A-1 shows one arrangement suggested by S. Hufnagel(1). Only one couple is shown here, which in practice would provide no more than 0.1 volt. For higher voltages, several couples must be series connected. An interesting arrangement for primary coolant application was presented by D.C. Miley(2) whereby the thermoelements are incorporated in a heat exchanger between primary and secondary coolants. The heat exchanger and pump magnetic circuit are arranged in a toroid so that maximum use is made of the magnetic material. Possibly the entire structure could become part of the shielding surrounding a nuclear reactor. However, the life of the thermoelectric elements may be shortened by the high neutron flux.

Until recently thermoelectric devices had prohibitively low efficiencies. Now the new thermoelectric elements are available. Germanium-silicon has been operated successfully up to 1800°F. Its Carnot efficiency is about

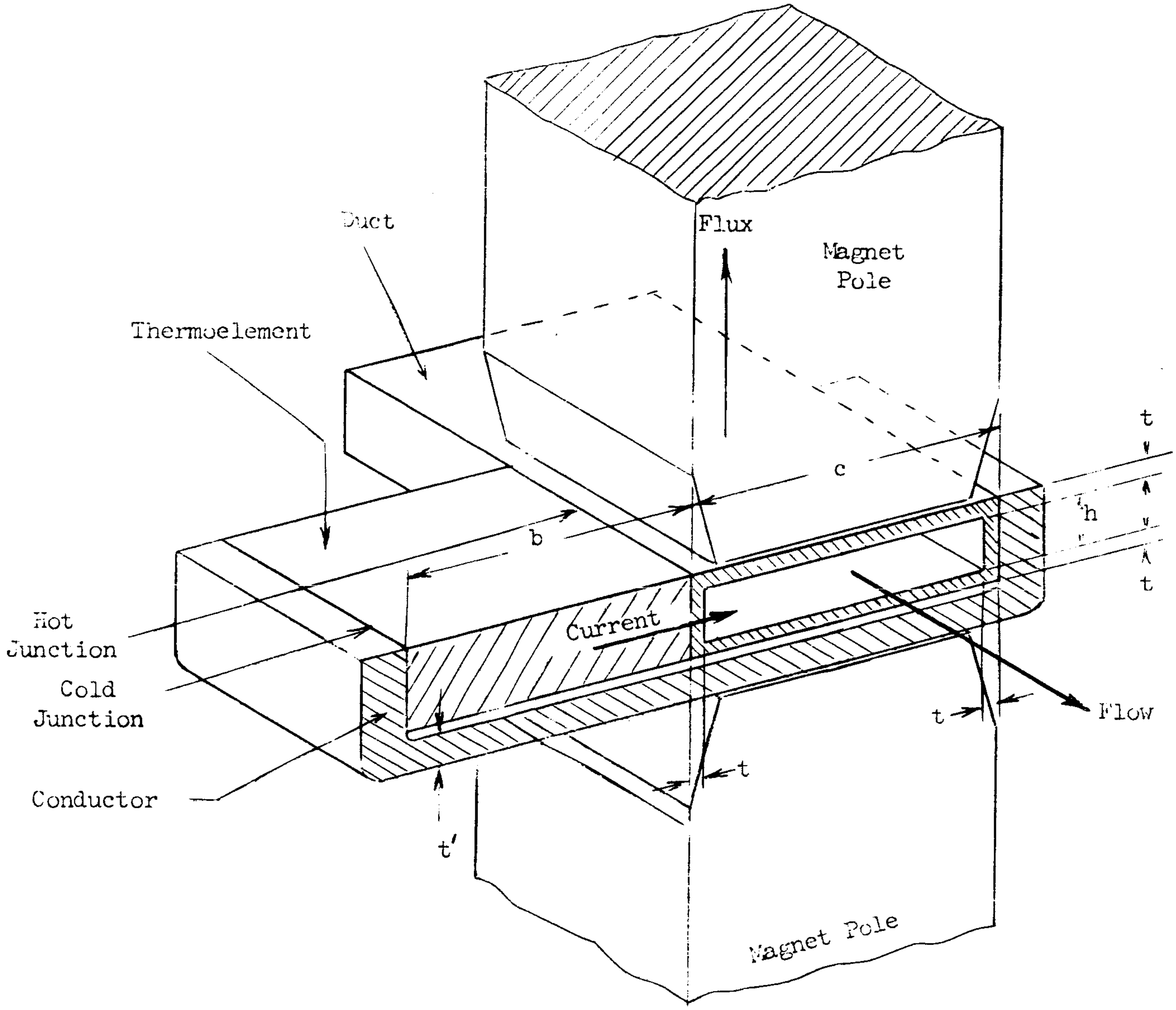

Figure A-1 Thermoelectromagnetic Pump

8% but in actual practice 3-4% is the rule. Germanium-silicon elements have performed well in vacuum.

Lead-teluride couples have a Carnot efficiency of 13% and realize 5-7% in practical applications[41][42]. The Lead teluride couples have a temperature limit of about 1200°F. Both types of elements will produce about 10 watts/lb. at best, which is less favorable than the 10 lb/KW weight penalty for power plus 2 lb/KW power conditioning weight presently estimated for the turboelectric system alternator. From this standpoint alone the TEM pumping system offers no significant advantage in specific weight over other EM pumping systems. Then, on adding, moreover, the cooling penalty for the high heat rejection rate, a substantial weight disadvantage must be accepted in gaining the power conditioning advantage. Such a trade off would probably be desirable for very small pumps.

The TEM pump has two special problems. Since the pumping action depends on heat supplied by the pumped fluid, a start up problem exists. Then, too, where good control of head and flow is required, either a throttling device must be used or auxiliary D.C. power must be supplied to a magnet coil to permit varying the magnetic flux. Compensation for temperature change in the fluid must also be considered. Overall the control of the TEM pump is complicated.

B. Pump Design Considerations

1. Introduction

This work is being presented in two major categories: General Relationships and Performance Prediction. The General Relationships Section contains those analyses applying broadly to all or several EM pump types. The Performance Prediction Section contains the performance prediction procedures used in pump development design requirements presented in Table II-1.

2. General Relationships

General analyses of pump efficiencies and duct specific power have been completed. Both analyses are quite general and lead to the development of literal expressions for electrical efficiency, duct efficiency and duct specific power. The assumptions made in these analyses were:

1. Hydraulic loss was neglected.
2. The magnetic material used was infinitely permeable and lossless.
3. Space and time harmonics were neglected.
4. End and side effects were neglected.
5. Fluid and duct wall currents were compensated.

The resultant generalized analytical relationships previously reported were presented graphically as curves plotted against slip.

a) Hydraulic Pressure Drop

1) Summary

One of the simplifying assumptions used in deriving the general relationships above was a negligible hydraulic loss. In actual pumps the hydraulic pressure drop may be quite significant. Consequently, a correction for this assumption must be made. Hydraulic pressure drop in an EM pump is due to entrance and exit losses and the viscous drag imparted to the fluid at the duct boundaries. Entrance and exit losses are usually expressed in terms of "velocity heads".

$$P_{he} = h \quad \frac{\sigma v^2}{2g} \tag{B-1}$$

The number of velocity heads lost, h , depends upon the details of the entrance and exit conditions, and may be approximated for a particular configuration by reference to various publications[3] [4].

Viscous loss is normally expressed in terms of the friction factor δ , the ratio of duct length to hydraulic diameter $\frac{L}{D}$, and velocity head. In a form of the Fanning equation,

$$P_{h\mu} = 4 \; \delta \; (\frac{L}{D}) \; \frac{\sigma v^2}{2g} \tag{B-2}$$

With the usual flow conditions, friction factor is a function of Reynolds number N_R, duct surface conditions, and duct curvature. When a conducting fluid flows through a magnetic field, circulating currents flow within the fluid introducing an additional body force on the fluid which influences the velocity distribution across the duct. This tends to modify the friction factor. An analysis of hydraulic pressure drop for laminar flow of a viscous conducting fluid flowing in a straight duct through a magnetic field is given in this section. The result for the friction factor is:

$$\delta = \frac{8 \; N_H^2}{N_R} \left[\frac{1}{N_H \; \text{Coth} \; N_H - 1} \right] \tag{B-3}$$

where N_H, the Hartmann number,[5] is given in consistent units by

$$N_H = \frac{B \; D}{4 \sqrt{\frac{\rho_f \mu}{g}}} \tag{B-4}$$

in conventional units,

$$N_H = 30.4 \frac{\left(\frac{B}{10^3}\right) D}{\sqrt{\rho_f \mu}} \qquad \text{(B-5)}$$

Equation (B-3) is plotted in Figure B-1. A similar solution for the friction factor when flow is turbulent has not been developed. Physical reasoning and a limited amount of test data on mercury indicate that the magnetic field has very little effect on the firction factor when flow is turbulent.

For turbulent flow, the equation due to von Karman

$$\frac{1}{\sqrt{\delta}} = 4.0 \log_{10}(N_R \sqrt{\delta}) - 0.4 \qquad \text{(B-6)}$$

seems appropriate. This equation which neglects magnetic field effects and considers only smooth ducts is plotted in Figure B-1.

The effect of duct curvature upon flow is to increase the value of Reynolds number at which transition from laminar to turbulent flow occurs and to increase the friction factor, particularly for laminar flow. In Reference 6, Schlichting gives the effect of curvature as increasing friction factor by the multiplier

$$1 + 0.075\, N_R \left[\frac{\text{Rad. of Cross-Section}}{\text{Radius of Curvature}}\right]^{\frac{1}{4}} \qquad \text{(B-7)}$$

No information is available in the literature concerning the effect of duct curvature when the Hartmann No. is other than zero. The increase in friction factor due to curvature is due to secondary flow patterns arising from the centrifugal force field set up by the variations in fluid velocity across the duct cross-section.(3)(6)

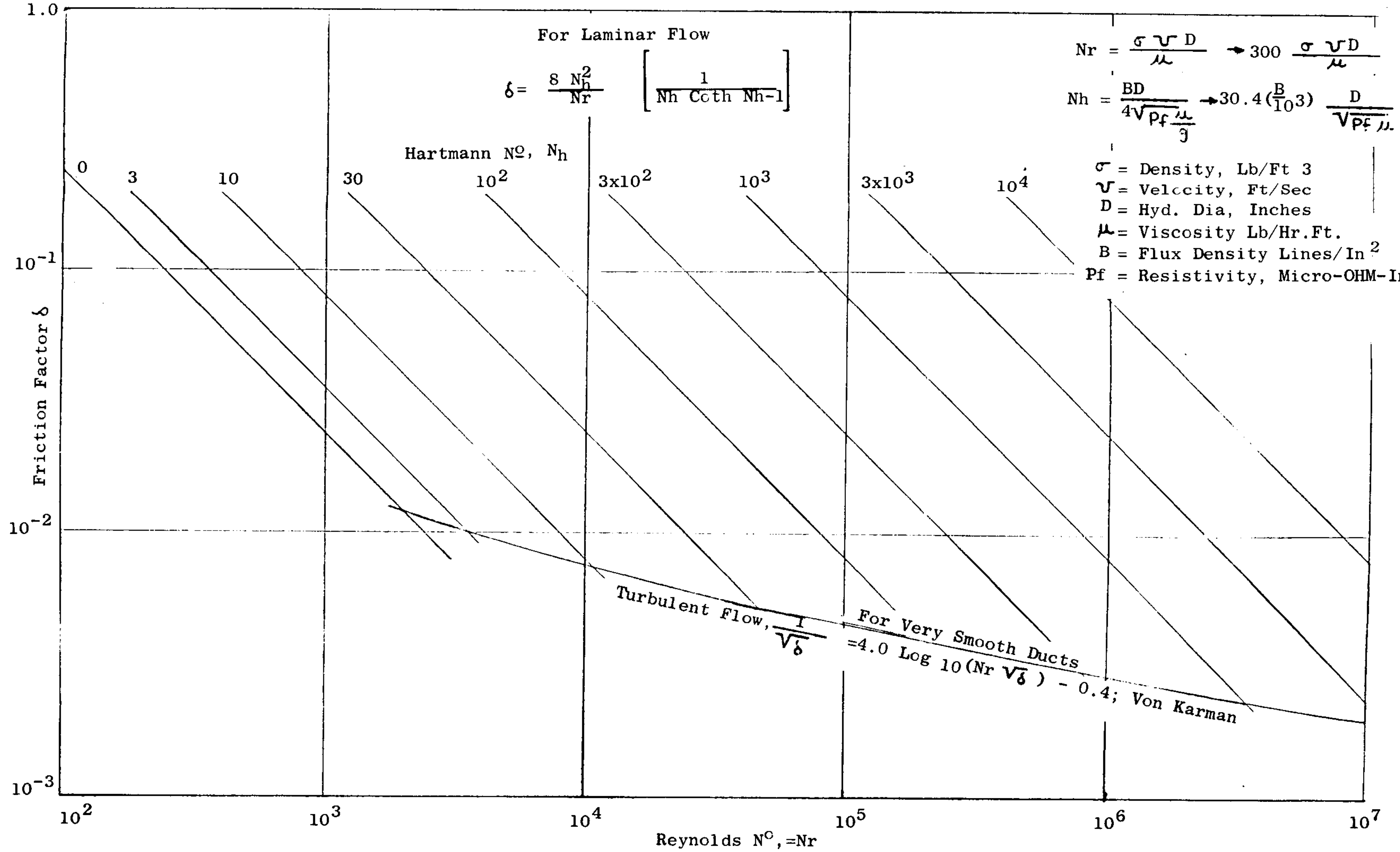

Figure B-1 Friction Factor Flow of Conducting Fluid in a Magnetic Field

When a conducting fluid flows in a transverse magnetic field, velocity variations across the duct are reduced by the eddy current magnetic field reaction, hence, it is reasonable to expect the effect of curvature to decrease with increasing Hartmann number.

It is interesting to observe the effect of a magnetic field upon the velocity distribution for laminar flow. The velocity distribution across a wide rectangular duct is shown in Figure B-2 for the range of practical values of Hartmann number. This velocity distribution is given by Equation B-21. By the viscous force relationship, higher values of pressure drop are associated with the higher velocity gradients at the boundaries.

b) Analysis of Magnetic Field Effect

Consider the elementary duct section shown in Figure B-3

Assume:

1. The field moves in the z-direction at a constant velocity v_s.
2. The duct and air gap height in the y-direction are much less than the other duct dimensions and the pole pitch so there are no variations in the field with respect to x and y.
3. Flow is laminar. Velocity, v , varies only with y.
4. Current density has an x-component only and there are no conditions external to the elementary duct section shown which influence current density.

Then taking the center of the duct section at y = 0, the current density anywhere, is

$$j = \frac{B(v_s - v)}{\rho_f} \tag{B-8}$$

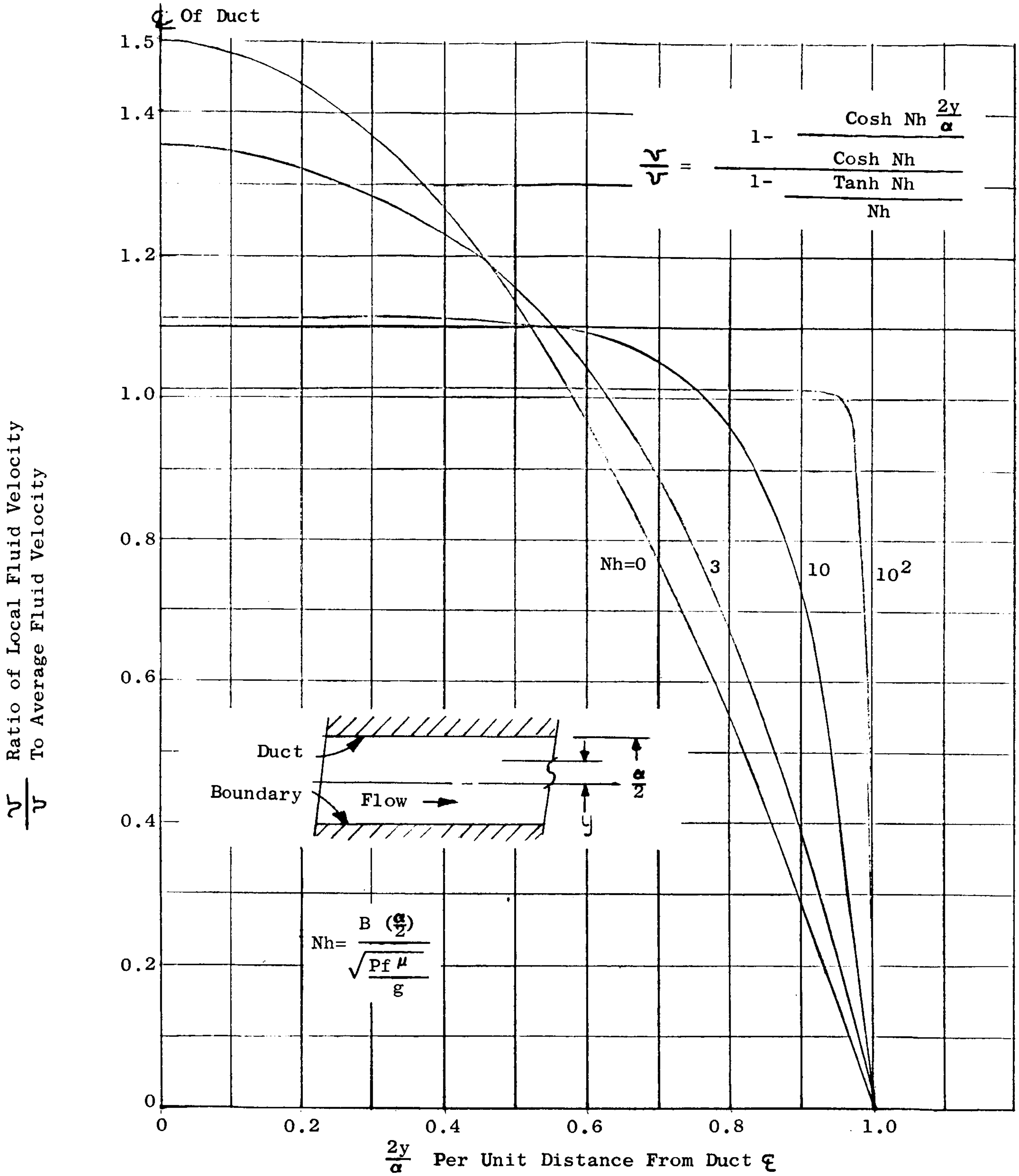

Figure B-2 Fluid Velocity Profile in a Rectangular Duct As A Function of Hartmann Number (Laminar Flow)

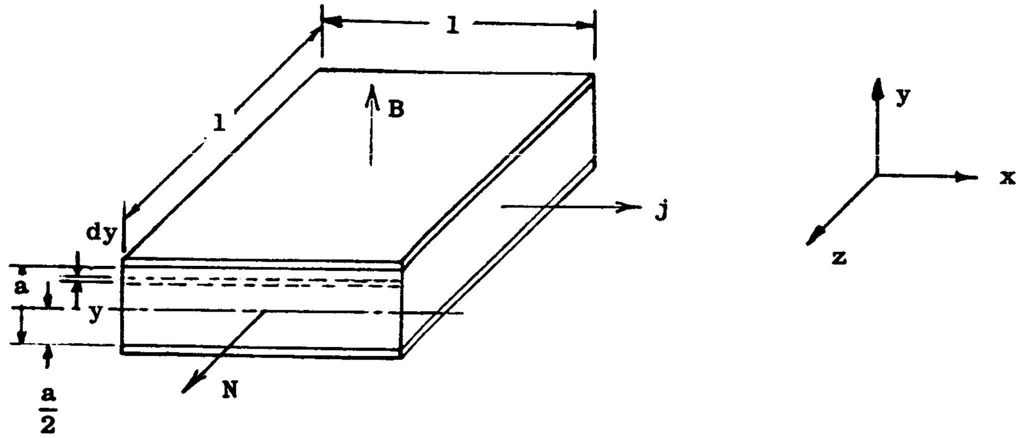

Figure B-3 Elementary Duct Section

The body force, therefore, on an element bounded by x-z planes at y and y + dy is

$$f_b = B\,j\,dy = \frac{B^2\,(v_s - v)}{\rho_f}\,dy \tag{B-9}$$

The viscous force on the element is

$$f_\mu = \mu/g\,\frac{\partial^2 v}{\partial y^2}\,dy \tag{B-10}$$

The total force on the element is

$$f = f_b + f_\mu = \frac{B^2\,(v_s - v)}{\rho_f}\,dy + \mu/g\,\frac{\partial^2 v}{\partial y^2}\,dy \tag{B-11}$$

It is a necessary condition for laminar flow that the pressure across any cross-section perpendicular to the flow be constant. This requires that

$$\frac{\partial f}{\partial y} = 0 = -\frac{B^2}{\rho_f}\,\frac{\partial v}{\partial y} + \mu/g\,\frac{\partial^3 v}{\partial y^3} \tag{B-12}$$

Writing these partial differentials as total differentials, in accordance with the assumptions,

w

$$-\frac{B^2}{\rho_f}\,\frac{dv}{dy} + \mu/g\,\frac{d^3\,v}{dy^3} = 0 \tag{B-13}$$

The solution of this differential equation may be written

$$v = A_1 + A_2 \cosh\alpha\,y + A_3 \sinh\alpha\,y \tag{B-14}$$

where

$$\alpha = \frac{B}{\sqrt{\rho_f\,\mu/g}} \tag{B-15}$$

Since v is an even function of y,

$$A_3 = 0$$

Thus

$$v = A_1 + A_2 \cosh \alpha y \tag{B-16}$$

When $y = \pm \frac{a}{2}$, $v = 0$

Thus
$$A_2 = - \frac{A_1}{\cosh \alpha \frac{a}{2}} \tag{B-17}$$

and

$$v = A_1 \left[1 - \frac{\cosh \alpha y}{\cosh \alpha \frac{a}{2}} \right]$$

$$\bar{v} = A_1 \left[1 - \frac{\tanh \alpha \frac{a}{2}}{\alpha \frac{a}{2}} \right] \tag{B-18}$$

and

$$v = \bar{v} \left[\frac{1 - \frac{\cosh \alpha y}{\cosh (\alpha \frac{a}{2})}}{1 - \frac{\tanh (\alpha \frac{a}{2})}{(\frac{\alpha a}{2})}} \right] \tag{B-19}$$

The dimensionless constant

$$\frac{\alpha a}{2} = \frac{B\left(\frac{a}{2}\right)}{\sqrt{\frac{\rho_f \mu}{g}}} = N_H \tag{B-20}$$

is called the Hartmann number.(6)

In terms of the Hartmann number

$$v = \bar{v} \left[\frac{1 - \dfrac{\cosh(N_H \frac{2y}{a})}{\cosh N_H}}{1 - \dfrac{\tanh N_H}{N_H}} \right] \tag{B-21}$$

The net hydraulic drag on the fluid in the duct is

$$f_h = - \frac{2\mu}{g} \left. \frac{dv}{dy} \right|_{y = \frac{a}{2}} \tag{B-22}$$

$$= \frac{4N_H \mu}{ga} \left[\frac{\tanh N_H}{1 - \dfrac{\tanh N_H}{N_H}} \right] \bar{v} \tag{B-23}$$

In terms of pressure drop per unit length of flow path

$$P_h = \frac{f_h}{a} = \frac{4\, N_H^2 \mu}{ga^2} \bar{v} \left[\frac{1}{N_H \coth N_H - 1} \right] \tag{B-24}$$

Equation (B-2) stated:

$$P_{h\mu} = 4\, \delta\, \frac{\sigma v^2}{2g} \left(\frac{L}{D}\right) \tag{B-2}$$

Equating these expressions for pressure drop,

$$4\, \delta\, \frac{\sigma \bar{v}^2}{2g} \left(\frac{L}{D}\right) = \frac{4 \mu\, N_H^2\, \bar{v}}{g\, a^2} \left[\frac{1}{N_H \coth N_H - 1} \right] \tag{B-25}$$

Introducing Reynolds number,(6)

$$N_R = \frac{\sigma v\, D}{\mu} \tag{B-26}$$

it follows from Equation (B-25) that

$$\delta = \frac{8 N_H^2}{N_R} \left[\frac{1}{N_H \coth N_H - 1} \right] \tag{B-27}$$

For large values of N_H, this expression becomes

$$\delta = \frac{8 N_H}{N_R} \tag{B-28}$$

Equation (B-27) may be written

$$\delta = \frac{8 N_H^2}{N_R} \left[\frac{\tanh N_H}{N_H - \tanh N_H} \right]$$

Expanding tank N_H in a Taylor Series, for small values of N_H,

$$\delta = \frac{8 N_H^2}{N_R} \left[\frac{N_H - \frac{N_H^3}{3} + \frac{2}{15} N_H^5 - \frac{17}{315} N_H^7 + \ldots}{\frac{N_H^3}{3} - \frac{2}{15} N_H^5 + \frac{17}{315} N_H^7 + \ldots} \right]$$

Then $\lim_{N_H \to 0} \delta = \frac{24}{N_R}$ (B-29)

This is the classical expression given for friction factor, in the absence of magnetic field effects, for laminar flow in a wide rectangular duct. (7)

Expressing Equation (B-20) in general terms,

$$N_H = \frac{B\ D}{4 \sqrt{\rho f \frac{\mu}{g}}} \tag{B-4}$$

(The use of a simple hydraulic diameter is sufficiently accurate here so it is felt that the use of different hydraulic diameters for N_H and N_R and for viscous and turbulent flow regimes cannot be justified at this time.)

In the units indicated below:

$$N_H = 30.4 \frac{\left(\frac{B}{10^3}\right) D}{\sqrt{\rho_f \mu}} \tag{B-5}$$

For the alkali metals,

$$0.3 < \mu < 2$$

$$5 < \rho_f < 50$$

Then, for reasonable values of D and B , say

$$0.4 < D < 4$$

$$5 < \left(\frac{B}{10^3}\right) < 30$$

The Hartmann Number then is:

$5 < N_H < 3000$, approximately

with:

B in lines/inches^2 D in inches

ρ_f in micro-ohm-inches μ in lb/ft-hr.

3. Performance Prediction

The foregoing general relationships are most useful in the conceptual design and preliminary analysis stages of the pump research work. More detailed methods of analysis for the particular types of pumps have been developed under the designation of Performance Prediction Methods. Many of these are iteritive methods and lend themselves well to computer programming.

a) Direct Current Conduction Pump

The d-c conduction electromagnetic pumps considered below are of the type shown in the sketch of Figure B-4 . The fluid enters the pump by way of an inlet transition section leading to a pumping section of rectangular cross section and constricted area. Here the interaction between the current and the magnetic field produces an increase in fluid pressure, and the fluid flows on through the outlet transition section to the pump outlet.

The magnetic field and current relationships are shown in the sketch. The magnetic field may be provided by a permanent magnet, particularly in small-size pumps, or by an electromagnet. If an electromagnet is used its exciting winding is usually connected in series with the current electrodes. If the duct is made of conducting material, current is introduced into the fluid by electrodes attached to the outside of the duct walls. If the duct is of non-conducting material the electrodes extend through the walls and make contact directly with the fluid.

The equivalent electrical circuit for this pump is shown in Figure B-4. The resistance, R_d, represents the resistance of the fluid directly between

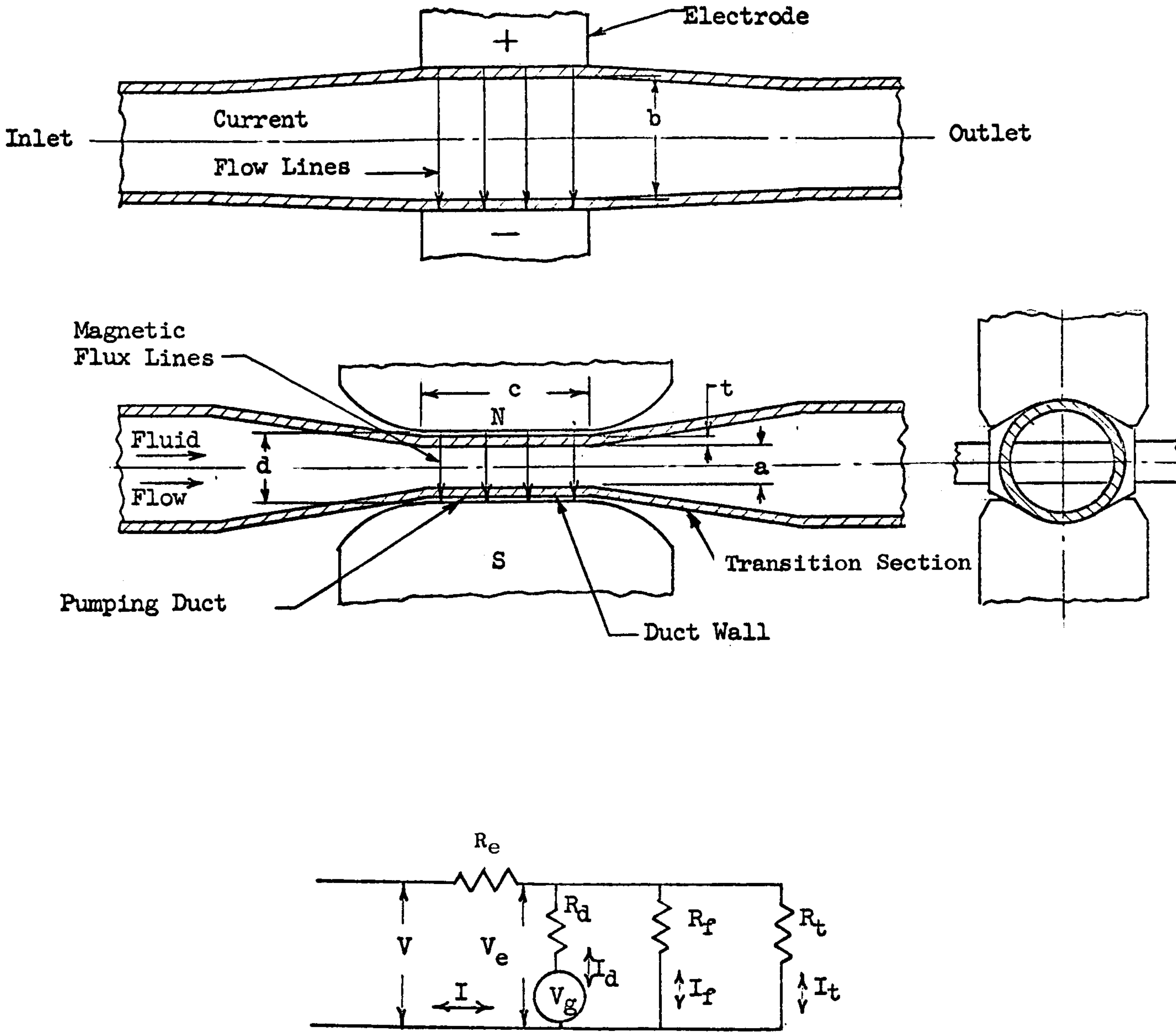

Figure B-4 D.C. Conduction Pump & Equivalent Circuit the electrodes. The current, I_d, through this portion of the fluid reacts with the magnetic field to produce the increase in pressure in the fluid. The flow of fluid through the magnetic field generates a back emf, V_g, which opposes the flow of current I_d. The resistance R_f represents the resistance of the two parallel fringing current paths from the ends of the electrodes through the fluid out into the transition sections around the magnetic field region. Current in these paths, I_f, does not contribute to the development of pressure in the fluid except as the fringing magnetic field may extend into that region. R_t represents the resistance of the current path through the duct walls from electrode to electrode. The current in this path, I_t, does not contribute to the development of pressure in the fluid. The resistance R_e represents the resistance of the electrodes through which the entire current passes. It includes the resistance of the joint between the electrode and the duct wall and a part of the resistance through the thickness of the duct wall. Part of the resistance through the thickness of the duct wall and contact resistance between the duct wall and the fluid may be included in R_d and R_f. If the duct is made of non-conducting material there is no duct wall current, and the electrodes contact the fluid directly. If the magnetic field is produced by a series electromagnet, R_e, includes the resistance of the magnet coil.

The magnet poles may be tapered back from the pumping portion of the duct to extend the fringing magnetic field into the region of fringing current as shown in Figure B-4 . This tends to reduce the fringing current and the fringing field contributes to the pressure rise by reacting with the fringing current. Non-conducting separators (not shown) may be located in the transition sections to block much of the fringing current.

The calculation of voltage, current and power required to produce a desired flow and pressure rise in a pump of known construction and dimensions involves the following steps:

1) Calculation of internal pressure drop.
2) Calculation of total pressure rise necessary.
3) Calculation of magnetic field.
4) Calculation of current, voltage, power and efficiency.
5) Corrections for "armature reaction" effects.

These steps will be discussed and methods of calculation described in the order tabulated above.

1) Calculation of Internal Pressure Drop

There is a pressure drop in the pump, due to hydraulic losses in the duct and transition sections, which must be added to the net pressure rise developed by the pump in order to obtain the total pressure rise to be generated in the duct by the current and magnetic field.

The loss in the duct portion of the pump where the pumping takes place may be calculated as follows:

$$P_d = C_f c \quad \frac{2 \sigma v^2}{g d_d \times 144} \tag{B-30}$$

$$d_d = 2a\,b/\,(a+b) \tag{B-31}$$

The value of C_f may be materially affected by the presence of the magnetic field crossing the duct. The effect is to increase the hydraulic loss when the flow is laminar and to increase the value of the Reynolds number at which transition from laminar to turbulent flow occurs. **The hydraulic loss is not significantly affected by the magnetic field after turbulent flow is established.**

The relationships between friction factor, Reynolds number and Hartmann number were developed and illustrated in Figures B-1 and B-2.

Calculation of pressure drop in the duct by means of these relationships does not take into account losses occurring at the ends of the duct. These may be a significant proportion of the total in d-c conduction pumps because the ducts are usually only a few diameters long. They depend upon the shape of the transition sections connecting to the duct, and may be conveniently included as part of the losses in these sections.

Pressure drop in the transition sections can be calculated for conical, square, or rectangular shapes. The accuracy of results for a circular-to-rectangular shape, in the presence of the fringing magnetic field, may be poor. The drop may be estimated by assuming an arbitrary number of velocity heads loss.

$$P_{Tr} = \frac{K\sigma v^2}{144 \times 2g} \qquad \text{(B-32)}$$

The value of K may be estimated by comparing the pump with a Venturi meter. For Venturi meters with diameter ratios of 25 to 50% an entrance cone of 21 deg.

and an exit cone of 5 to 7 deg. the overall pressure loss is given[4] as 10 to 20% of the differential pressure.

$$P_{Tr} = 0.2 \frac{\sigma}{144} \left[\frac{v^2 - v_o^2}{2\,g}\right] = 0.2\frac{\sigma}{144} \left[1 - \left(\frac{A}{A_1}\right)^2\right] \frac{v^2}{2g} \qquad \text{(B-33)}$$

$$P_{Tr} = 0.2 \left[1 - .0625\right] \frac{\sigma}{144} \frac{v^2}{2g}, \quad \left(\frac{A}{A_1} = \frac{1}{4}\right) \qquad \text{(B-34)}$$

$$K = 0.2(1 - .0625) = 0.187$$

The loss in a pump where the cross-section changes from circular to rectangular and back to circular along with the reduction and expansion of area, combined with the presence of the fringing magnetic field, would be greater than that occurring in a Venturi meter of nearly ideal shape. A value of 0.5 is suggested for K.

2) Calculation of Total Pressure Rise Necessary

The pressure drops calculated for the duct and **transition sections**, when combined and added to the net pressure rise desired between the inlet and outlet of the pump will give the total pressure rise that must be developed in the duct.

3) Calculation of the Magnetic Field

The magnetic fields of importance to the pump characteristics are the field crossing the duct between electrodes, and the fringing fields extending into the transition sections. These may be obtained by established procedures of magnetic circuit calculation. This involves a determination of the magnetic permeance of the gap across the duct between magnet poles, of the fringing flux paths across the transition section, of the fringing flux paths from the sides of the magnet poles, and of any other leakage flux paths in the magnetic circuit. These are important if a permanent magnet is used for excitation, in order to calculate the total flux being supplied by the magnet. Permanent magnet calculation procedures are described by Parker and Studders(8), Chapter 4. Chapter 5 of the same book describes procedures for calculating magnetic permeance of fringing and leakage flux paths. Roters(9), in his Chapter 5, also describes procedures for calculating magnetic permeance of fringing and leakage flux paths. Permanent magnet excitation is generally used only in small pumps. The fringing and leakage permeances are used in calculation of an electromagnet to obtain the total flux and the amount of magnetomotive force absorbed in the magnet circuit.

The current between electrodes in the fluid and in the duct wall has a distorting effect on the magnetic field, increasing the field strength at the entrance to the duct and decreasing it at the exit end. This in turn affects the current distribution along the duct, producing maximum current density in the region of lower field strength and reducing the total pressure developed. Large pumps in which this effect is significant may be equipped with compensating conductors which return the current through the gap close beside its paths through the fluid and the duct wall, cancelling out most of the distortion. Equations are given by Blake(10) by which the effect on output pressure, output power and electrical losses can be approximated for an uncompensated pump. These are given in paragraph 5.

4) Calculation of Current, Voltage, Power and Efficiency

Assume first that the pump is either of the permanent magnet type or is separately excited, so that the gap flux density is fixed and has been calculated as outlined in preceding paragraphs. Let P = pressure in psi developed in the pump, equal to the prescribed terminal pressure plus the hydraulic pressure loss which has been determined as above outlined. Let v = the velocity of flow in ft./sec. in the duct, calculated from the prescribed flow to be delivered by the pump at the prescribed pressure. The equivalent circuit of Figure B-4 obtains

$$P = \frac{BI_d}{a} \times 8.85 \times 10^{-8} \text{ psi} \qquad \text{(B-35)}$$

$$I_d = \frac{Pa}{B} \times 0.1132 \times 10^{8} \text{ amp.} \qquad \text{(B-36)}$$

$$V_g = B\ v\ b \times 12 \times 10^{-8} \text{ volts} \qquad \text{(B-37)}$$

$$V_e = I_d\ R_d + V_g \text{ volts} \qquad \text{(B-38)}$$

$$I_f = \frac{V_e}{R_f} \text{ amp.} \qquad \text{(B-39)}$$

$$I_t = \frac{V_e}{R_t} \text{ amp.} \qquad \text{(B-40)}$$

$$I = I_d + I_f + I_t \text{ amp.} \qquad \text{(B-41)}$$

$$V = V_e + IR_e \text{ volts at terminals} \qquad \text{(B-42)}$$

$$W_i = VI \text{ watts input} \qquad \text{(B-43)}$$

(This does not include power for a magnetizing coil)

$$P_o = P - P_h \text{ psi output} \tag{B-44}$$

$$W_o = P_o\, Q \times 0.435 \text{ watts hydraulic output} \tag{B-45}$$

$$\eta = \frac{W_o}{W_i} \tag{B-46}$$

(This does not include magnetizing coil power)

Calculation of R_d, R_f and R_t is discussed in a following paragraph.

Consider now a series excited pump in which the gap flux density is proportional to the pump current.

$$B = CI \tag{B-47}$$

$$I_d = \frac{Pa}{CI} \times 0.1132 \times 10^8 \text{ amp.} \tag{B-48}$$

$$V_g = CI\,v\,b \times 12 \times 10^{-8} \text{ volts} \tag{B-49}$$

$$V_e = CI\,v\,b \times 12 \times 10^{-8} + \frac{PaR_d}{CI} \times 0.1132 \times 10^8 \text{ volts} \tag{B-50}$$

$$I = I_d + I_f + I_t \text{ amp.} \tag{B-51}$$

$$I = \frac{Pa}{CI} \times 0.1132 \times 10^8 + \frac{CIvb}{R_f} \times 12 \times 10^{-8} + \frac{PaR_d}{CIR_f} \times 0.1132 \times 10^8$$
$$+ \frac{CIvb}{R_t} \times 12 \times 10^{-8} + \frac{PaR_d}{CIR_t} \times 0.1132 \times 10^8 \text{ amp.} \tag{B-52}$$

$$I^2 \left(1 - Cvb\left(\frac{1}{R_f} + \frac{1}{R_t}\right) \times 12 \times 10^{-8}\right) = \frac{PaR_d}{C}\left(\frac{1}{R_d} + \frac{1}{R_f} + \frac{1}{R_t}\right)$$
$$\times 0.1132 \times 10^8 \tag{B-53}$$

$$I = \sqrt{\frac{PaR_d \left(\frac{1}{R_d} + \frac{1}{R_f} + \frac{1}{R_t}\right) \times 0.1132 \times 10^8}{C \left(1 - Cvb\left(\frac{1}{R_f} + \frac{1}{R_t}\right) \times 12 \times 10^{-8}\right.}} \text{ amperes} \tag{B-54}$$

Using above equations, calculate I_d, V_g, V_e, I_f, I_t

$$V = V_e + IR_e \text{ terminal volts} \tag{B-55}$$

$$W_i = VI \text{ watts input} \tag{B-56}$$

$$P_o = P - P_h \text{ psi output} \tag{B-57}$$

$$W_o = P_o @ \times 0.435 \text{ watts output} \tag{B-58}$$

$$\eta + \frac{W_o}{W_i} \tag{B-59}$$

The calculation of the resistances R_d, R_f, and R_t is discussed by Blake[10] and Watt[11], and curves given to aid in the calculations. They involve the assumptions that the duct is of uniform cross-section, rectangular in shape, and the resistance is not affected by the presence of the magnetic field. It is assumed in applying these curves that the magnet poles extend over the same axial length of the duct as the electrodes. The value of R_d is affected by the magnetic field in an uncompensated pump where the current distribution is changed by the field. A correction for this effect is given in a following paragraph. The value of R_f is affected by the fringing magnetic field which affects the fringing current distribution. It is also affected by the changing cross-section of the transition sections in which the fringing current paths lie; so that the value of R_f obtained from the curves is approximate.

No suitable method of correction for these effects is available. The value of R_t is not affected by the magnetic field and is affected only slightly by changes in cross-section of the transition sections. The value of R_e depends upon the arrangement of the electrodes, the connecting buses, and the magnetizing coil, and can be calculated by established procedures. The contact resistance between the electrode and the duct wall depends upon the construction but is usually negligible. The above calculations for R_d and R_f assume good wetting of the duct wall by the fluid, with negligible contact resistance between the fluid and the wall. The resistance of the duct wall to the flow of current through its thickness from the electrode to the fluid may be conservatively approximated by assuming that all the electrode current flows straight through from electrode to fluid.

If fringe-current baffles are used in the pump to reduce the fringe current, the effective value of R_f is greater than would be obtained from the curves of Blake[10] and Watt[11]. The baffles are insulating plates placed in the transition sections parallel to the fluid flow but perpendicular to the fringe current flow, dividing the transition sections into two or more parallel channels. They may extend from the ends of the transition sections, or further, to reduce current flow around the outer ends. The value of R_t is not appreciably affected by the presence of the baffles. The values of R_d and R_f may be approximated by using a value of b equal to the width of each separate parallel channel, calculating from Ref. (10) and (11) values of R_d and R_f for each channel, and adding together the values thus found to get the net effective value. Interchange of current between the fluid and the tube walls near the baffles is neglected.

5) Correction for Armature Reaction Effects

The distortion of the magnetic field and current distribution by the current in the fluid is discussed by Blake,[10] Watt,[11] Woodrow,[12] and Barnes.[13] Approximate corrections for this effect taken from equations developed by Blake are given here. The total developed pressure may be expressed as follows:

$$P = \frac{B_m I_d}{a}\left(1 - \frac{B_i}{B_m}\ \frac{\beta \coth \beta - 1}{\beta}\right) \times 8.85 \times 10^{-8} \text{ psi} \qquad \text{(B-60)}$$

$$R'_d = R_d\ \beta \coth \beta \qquad \text{(B-61)}$$

R_d = value of R_d as found from curves of Figure B-5.

$$\beta = .1915\ vC/\rho \qquad \text{(B-62)}$$

v = fluid velocity in the duct, ft/sec

c = electrode length along the duct, inches

ρ = electrical resistivity of the fluid, micro-ohm-inches

B_i is the value of the flux density at the edges of the magnet poles, (at the entrance to and exit from the duct), which would be produced by the current through the magnet gap alone. Strictly speaking, the current I should include only I_d and the portion of duct wall current between the poles. The overall accuracy of the correction, however, does not warrant the extra calculation to obtain these values.

B_m may be obtained by assuming that the distortion of current distribution does not affect the total flux and making the calculation as if the current

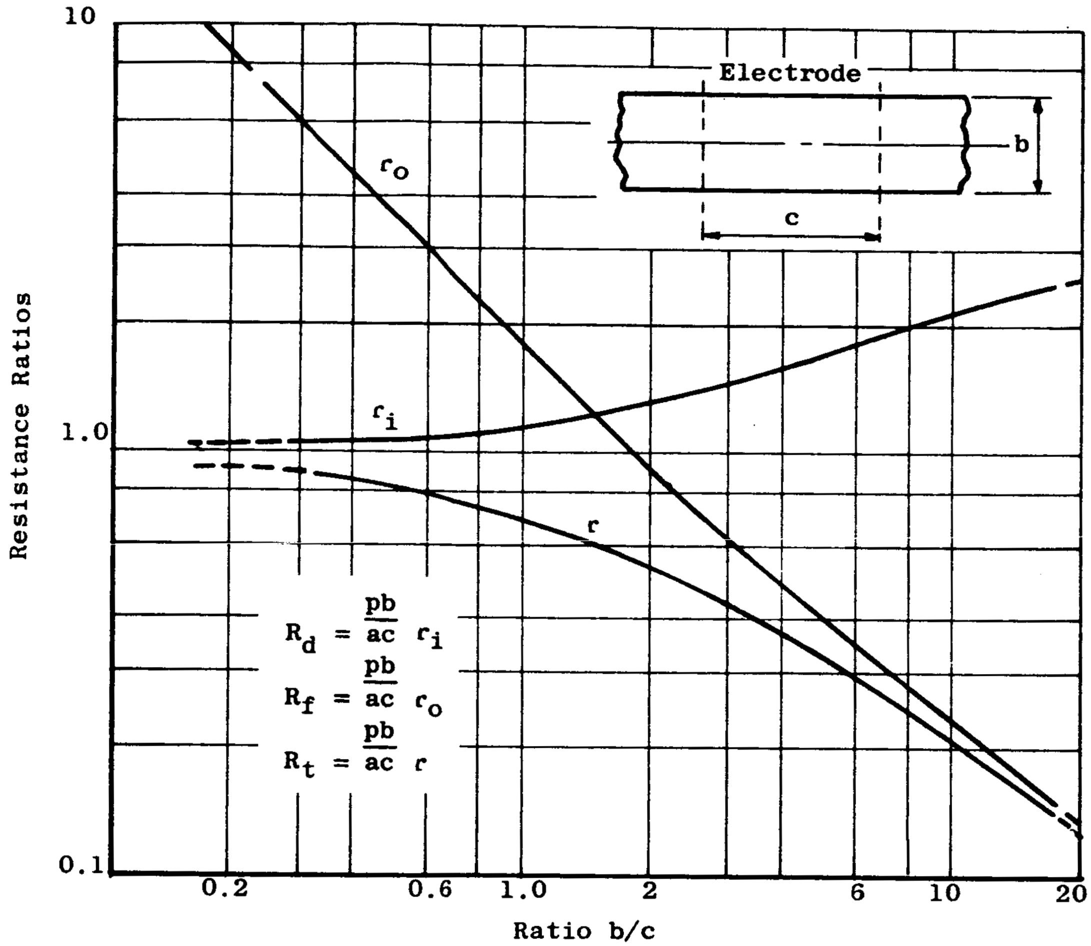

Figure B-5 Theoretical Fringing Resistance Ratios for Conduction Pumps, Without Magnetic Field Source: Reference (11) distribution were not distorted. The total electrode current may be assumed to flow in a half turn adding to or subtracting from the external gap magnetomotive force, depending upon the geometry of the electrode connections. This is an approximation as the distortion of current distribution will affect the total flux.

Plots of $\beta \coth \beta$ and of $\frac{\beta \coth \beta - 1}{\beta}$ are given in Figure B-6 as functions of β to assist in determining the correction factors.

For series connected D-C electromagnet pumps the ratio of B_i/B_m is nearly constant

$$\frac{B_i}{B_m} = \frac{3.91I/2d}{CI} = \frac{1.955}{Cd} \tag{B-63}$$

$$\text{Let } X = \left(1 - \frac{B_i}{B_m} \frac{\beta \coth \beta - 1}{\beta}\right) = \left(1 - \frac{1.955}{Cd} \frac{\beta \coth \beta - 1}{\beta}\right) \tag{B-64}$$

$$\text{Let } P' = P/X \tag{B-65}$$

Then Equations (B-47) - (B-59) may be used to include the effects of armature reaction by substituting P', (B-65), and R'_d, (B-61) for P and R_d.

For permanent magnet or separately excited pumps B_m is constant, but B_i varies with current. It is necessary to first calculate the currents as if there were no armature, obtain an approximate value of B_i and of X, then repeat with P' and R'_d. It may be necessary to then revise the values of B_i, X, and P' and again repeat the calculation.

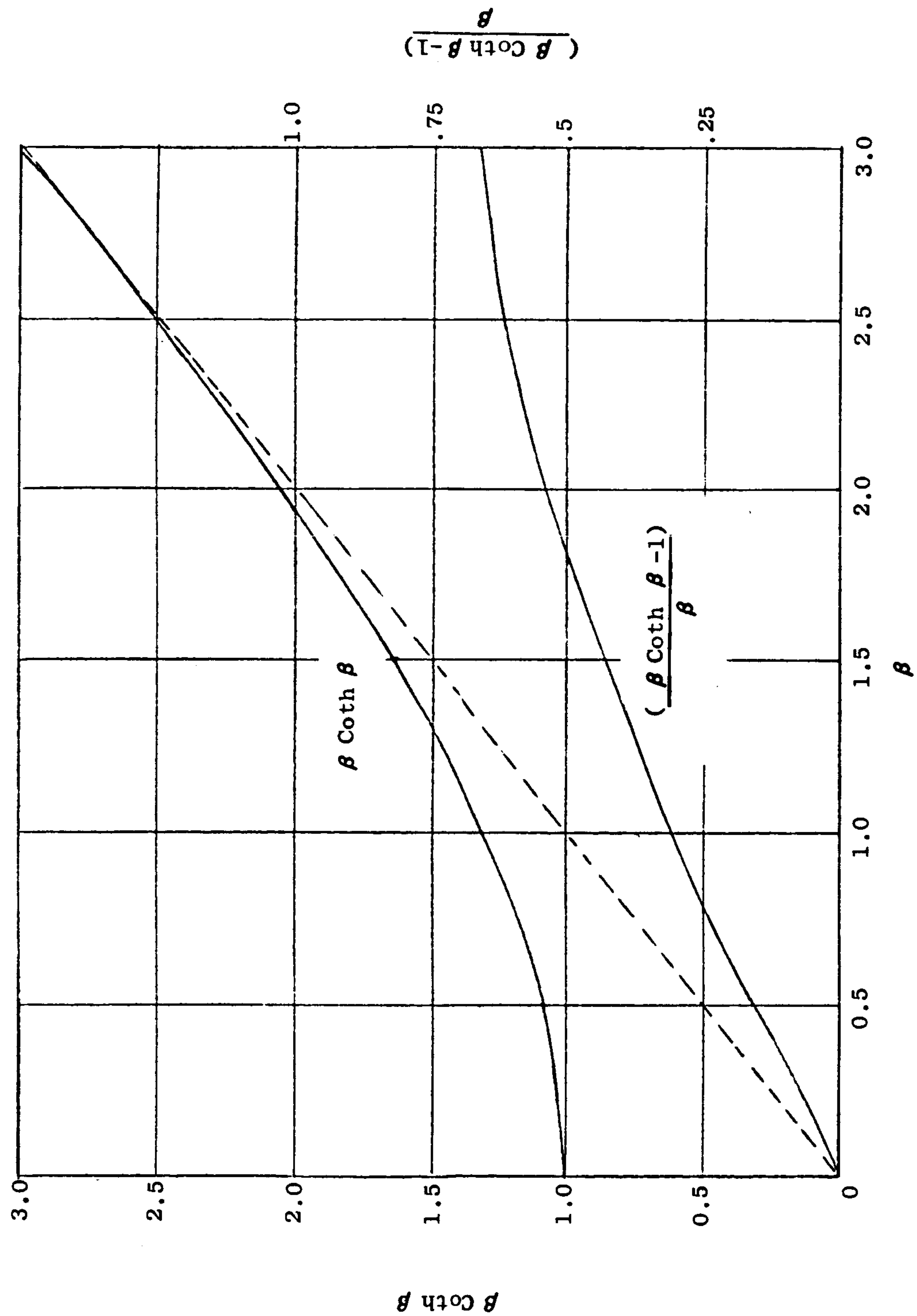

Figure B-6 β Coth β and $\frac{(\beta \text{ Coth } \beta - 1)}{\beta}$ vs β

b) Single Phase Induction Pump

An analysis by D. A. Watt of a single phase induction pump with an annular duct was published in Reference (14) in 1953. Reference (15), a declassified edition of Reference (14), was published in 1956. The configuration treated in these references is shown in Figure B-7.

A more compact configuration developed during the course of this EM pump design study is shown in Figure B-8. From an electromagnetic viewpoint this configuration is equivalent to that studied by Watt. It is more compact and more symmetrical, hence better suited to space applications where size, weight, and volt ampere requirements must be minimized. As illustrated in Figure B-8, both the duct and the exciting coil are annular in form. The basic magnetic flux pattern is axial and radial, hence the laminations must be oriented with their major dimensions lying in planes passing through (or near) the axial centerline of the pump. Multiple inlet and outlet pipes are desirable to minimize hydraulic and electromagnetic inlet and exit losses. The symmetry of the configuration of Figure B-8 is such that the complex arrangement of chokes described by Watt in the reference to minimize circulating currents in the configuration of Figure B-7 are not necessary provided entry and exit pipes are arranged with appropriate symmetry.

Other compact single phase induction pump configurations similar to that of Figure B-8 are shown in Figures B-9 and B-10. The configuration of Figure B-9 Type B, is somewhat more compact than Type A, but this compactness is achieved at the expense of poorer performance. Type C, shown in Figure B-10, has exciting coils located at each end of the annular duct.

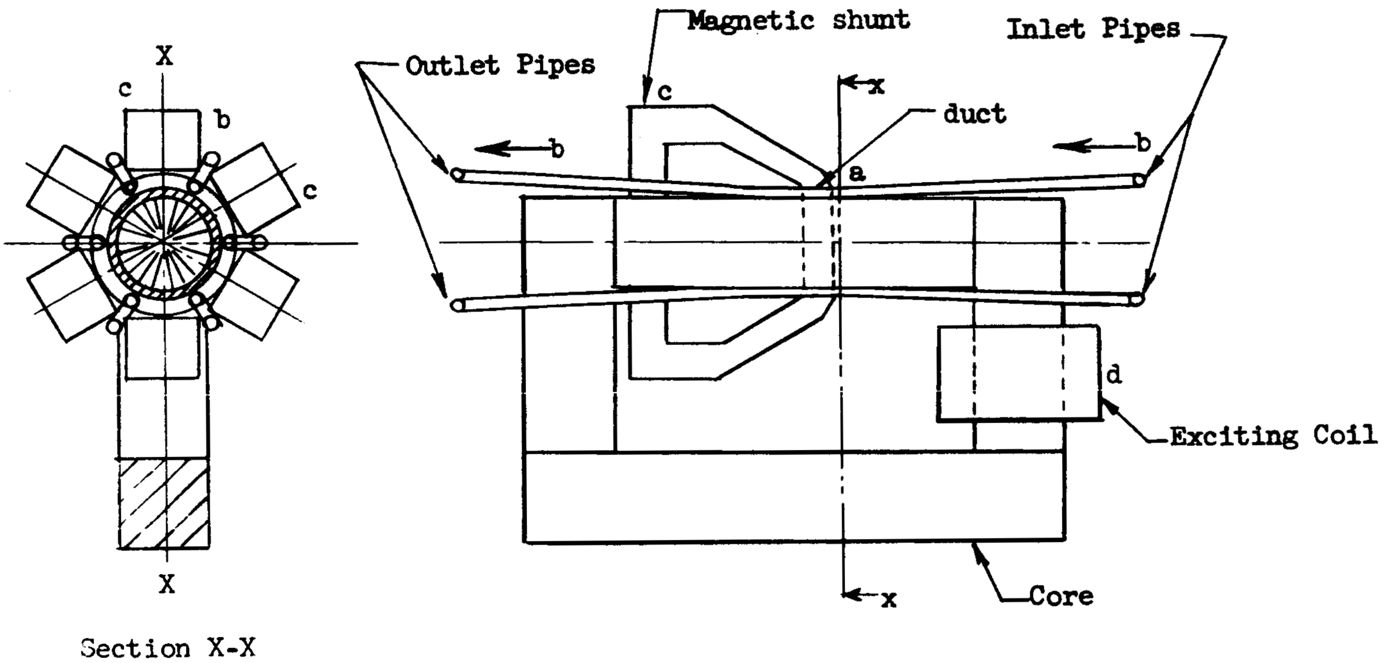

Figure B-7 Single Phase Induction Pump Studied by Watt

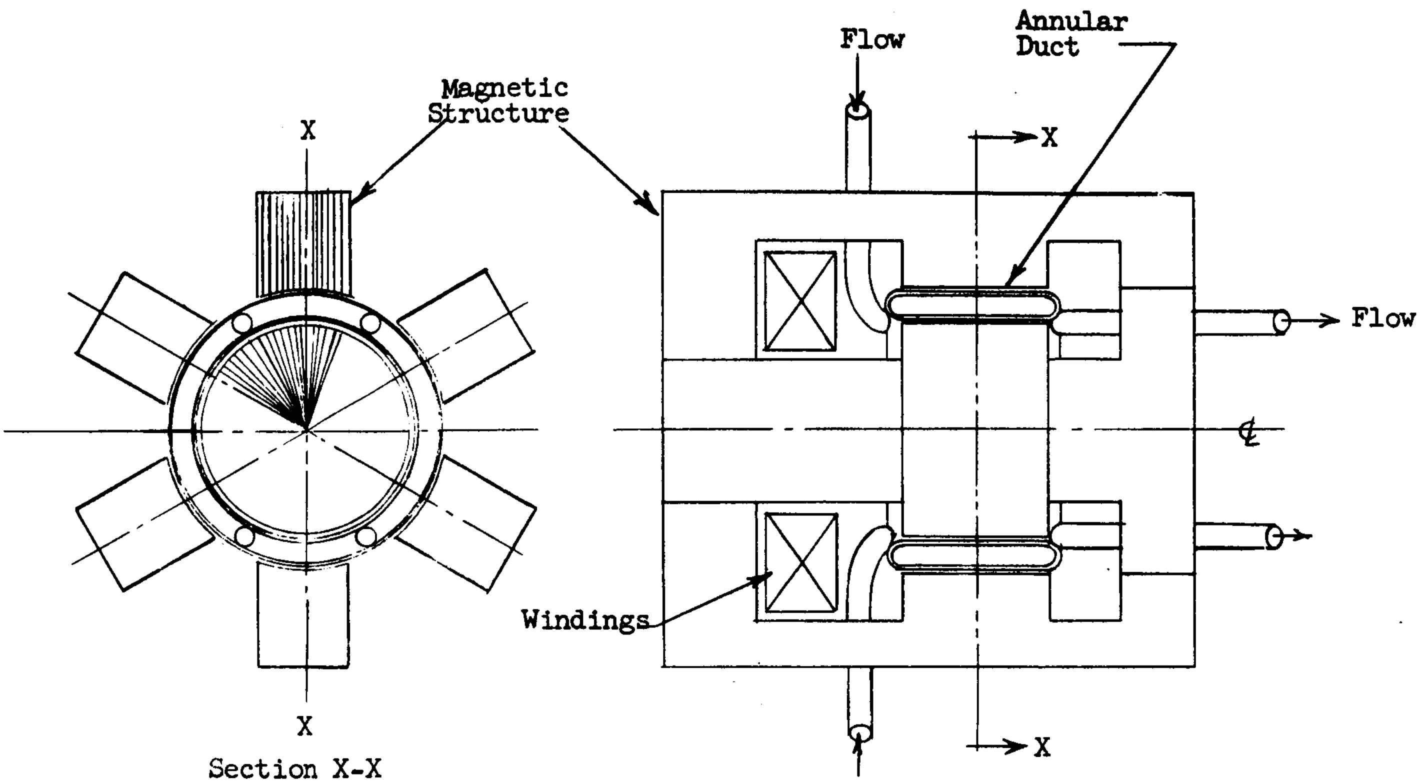

Figure B-8 Single Phase Induction Pump, Type A

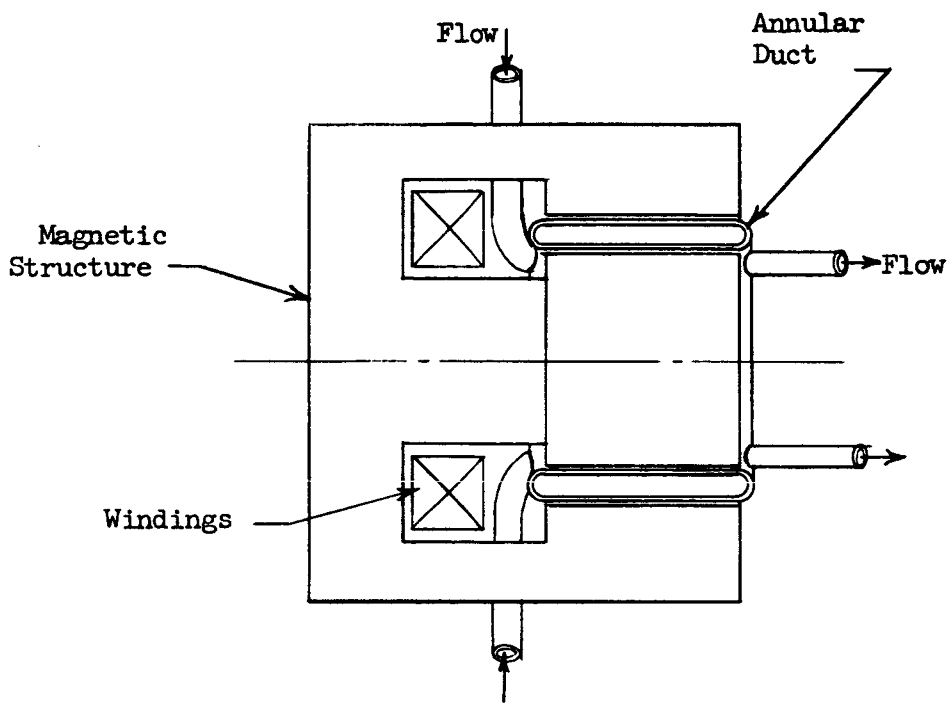

Figure B-9 Single Phase Induction Pump, Type B

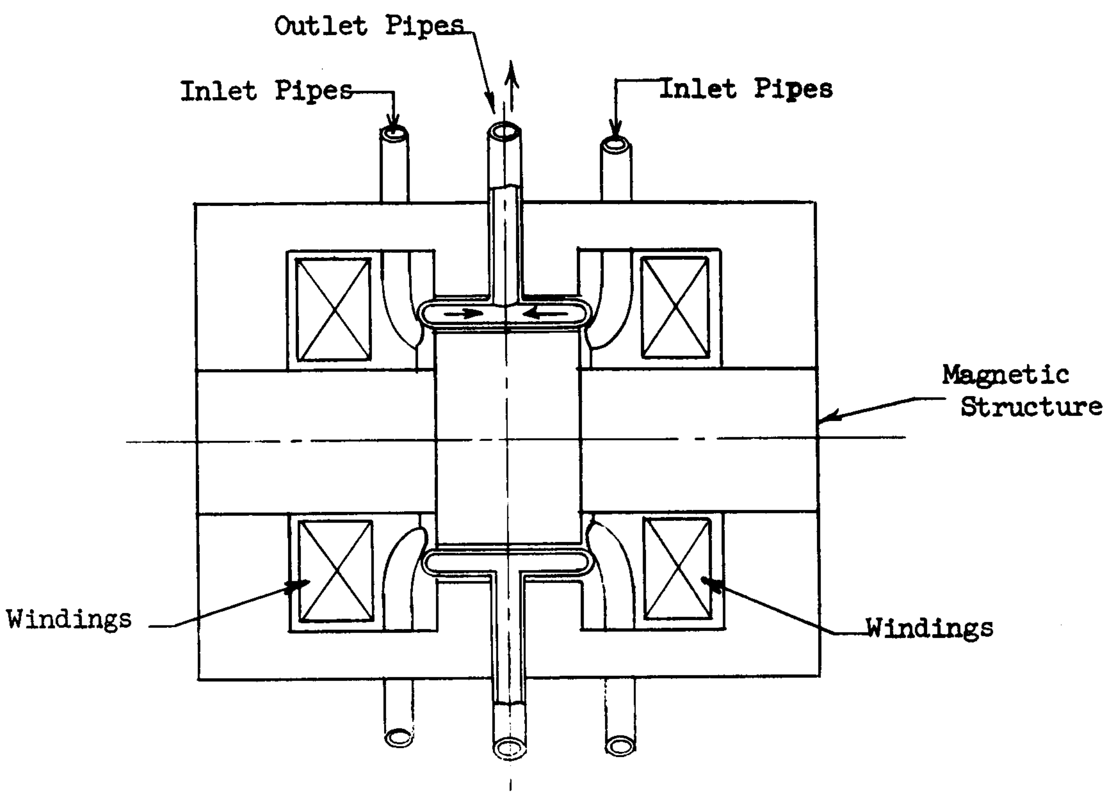

Figure B-10 Single Phase Induction Pump, Type C

When these coils are connected with their mmf's aiding, considering axial flux, Type C may be shown to be equivalent to two pumps of Type A, connected back to back. Similarly, when the coils are connected with their mmf's opposing, Type C may be shown to be equivalent to two pumps of Type B, connected back to back. In either case, pumping is from the ends of the duct toward the middle. Type C does not appear to have any significant advantages relative to Types A and B.

The analysis of the performance of single phase induction pumps Types A and B proceeds along similar lines and is carried through concurrently below. Throughout this analysis the following assumptions are made:

1. The annular duct and air gap configuration is treated as an equivalent rectangular configuration as shown in Figure B-11 This introduces negligible error as the duct diameter will normally be several integral multiples of the air gap radial height.
2. The flux density in the air gap is assumed to have a y-component only.
3. The fringing flux field at each end of the duct is neglected.
4. The permeability of the magnetic core is assumed infinite during the analysis of the air gap region. A correction for mmf drop in the core may be made later.
5. Fluid and duct walls are assumed to be isotropic and non-magnetic, having permeabilities the same as free space.
6. The fluid velocity is assumed to have an x-component only and to be independent of y and z.

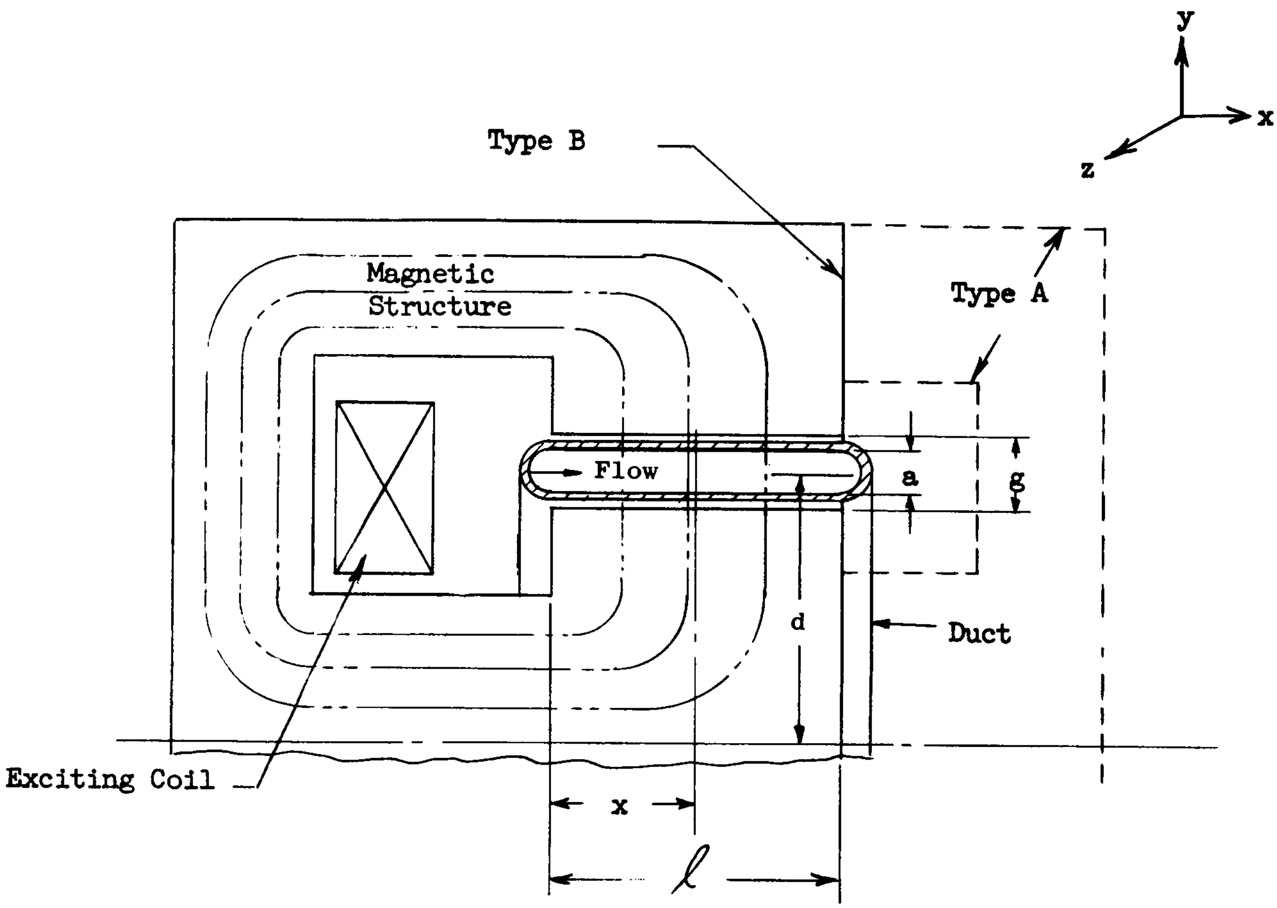

Figure B-11 Equivalent Configuration for Annular Duct Design

The nomenclature presented with the Table of Contents is used. All sinusoidally varying quantities are rms. Any consistent system of units applies to the analysis. The results are expressed in terms of the units indicated.

The following basic relationships may be written for the configuration of Figure B-11,

$$B = - \frac{1}{\pi d} \frac{\partial \phi}{\partial x} \tag{B-66}$$

$$j_f = - \frac{1}{\pi d \rho_f} \left(\frac{\partial \phi}{\partial t} + v \frac{\partial \phi}{\partial x} \right) \tag{B-67}$$

$$j_d = - \frac{1}{\pi d \rho_d} \frac{\partial \phi}{\partial t} \tag{B-68}$$

$$\frac{\partial B}{\partial x} = \frac{\mu}{g} \left(a \ j_f + 2t \ j_d \right) \tag{B-69}$$

For an assumed configuration and fluid velocity, these equations relate the four unknowns, B, ϕ, j_f, and j_d. They may be combined to yield one equation in one unknown, ϕ

$$\frac{\partial^2 \phi}{\partial x^2} = \frac{\mu a}{\rho_f g} \left[\left(1 + \frac{2t}{a} \frac{\rho_f}{\rho_d}\right) \frac{\partial \phi}{\partial t} + v \frac{\partial \phi}{\partial x} \right] \tag{B-70}$$

Assuming the exciting voltage to be sinusoidal in time and fluid velocity to be constant, the system is linear and the resulting flux ϕ will also be sinusoidal in time. Thus, it may be written

$$\phi = R_e \left(\underline{\Phi} \ e^{\ iwt} \right), \tag{B-71}$$

and $$\frac{\partial \phi}{\partial t} = R_e \left\{ i w \Phi e^{iwt} \right\} \qquad \text{(B-72)}$$

where Re $\left\{ A \right\}$ signifies "the real part" of A.

For convenience, let

$$D_1 = \left[1 + \frac{2t}{a} \frac{\rho_f}{\rho_{cl}} \right] \qquad \text{(B-73)}$$

Then, substituting these relationships in Equation (B-70), and dropping the Re $\left\{ A \right\}$ designation for convenience, in the conventional manner, Equation (B-70) may be written

$$\frac{\partial^2 \Phi}{\partial x^2} - \frac{\mu a v}{\rho_f g} \frac{\partial \Phi}{\partial x} - j \frac{w \mu D_1 a}{\rho_f g} \Phi = 0 \qquad \text{(B-74)}$$

The solution of this equation is

$$\Phi = \Phi_1 e^{\alpha_1 x} + \Phi_2 e^{\alpha_2 x} \qquad \text{(B-75)}$$

Where $$\alpha_1 = \gamma 1 + i\beta_1 = \frac{\mu a v}{2 \rho_f g} \left\{ 1 - \sqrt{1 + i \frac{4 w \rho_f g D_1}{\mu a v^2}} \right\} \qquad \text{(B-76)}$$

$$\alpha_2 = \gamma 2 + i\beta_2 = \frac{\mu a v}{2 \rho_f g} \left\{ 1 + \sqrt{1 + i \frac{4 w \rho_f g D_1}{\mu a v^2}} \right. \qquad \text{(B-77)}$$

It is apparent that

$$\beta_1 = - \beta_2$$

Φ_1 and Φ_2 are constants which depend upon the boundary conditions. It is convenient to proceed with the analysis of the pump performance, expressing the performance in terms of these constants. Their evaluation in terms of the boundary conditions for pumps Type A and B will be covered later.

It is convenient to introduce a dimensionless constant C_1, where

$$C_1 = \frac{\Phi_2}{\Phi_1} \tag{B-78}$$

Equation (B-75) may then be written

$$\Phi = \Phi_1 \left\{ e^{\alpha_1 x} + C_1 \; e^{\alpha_2 x} \right\} \tag{B-79}$$

Substituting now from Equation (B-79) in Equations (E-66) (B-67) and (B-68) we may write

$$B = -\frac{\Phi_1 \alpha_1}{\pi d} \left[e^{\alpha_1 x} + \frac{\alpha_2}{\alpha_1} C_1 \Sigma^{\alpha_2 x} \right] \tag{B-80}$$

$$j_f = -\frac{\Phi_1 w}{\pi d \rho_f} \left[\left(\frac{v}{w}\alpha_1 + i\right) e^{\alpha_1 x} + \left(\frac{v}{w}\alpha_2 + i\right) C_1 e^{\alpha_2 x} \right] \tag{B-81}$$

$$j_d = -\frac{\Phi w}{\pi d \rho_d} \left(e^{\alpha_1 x} + C_1 \; e^{\alpha_2 x} \right) \tag{B-82}$$

The pressure developed by the pump is given by the product of the flux density and the current density in the fluid, integrated over the length of the pump duct. This pressure varies sinusoidally in time. The average value of the pressure is given by the expression

$$p = \mathrm{Re} \left\{ \int_o^{\ell} -j_f \, \overline{B} \, dx \right\} \tag{B-83}$$

where $\bar{B}$ is the complex conjugate of B

Thus

$$p = Re\left\{- \frac{w\Phi_1\bar{\Phi}_1\bar{\alpha}_1}{(\pi d)^2\rho_f}\int_0^{\ell}\left[(\frac{v}{w}\alpha_1 + i)\, e^{\alpha_1 x} + (\frac{v}{w}\alpha_2 + i)\, C_1\, e^{\alpha_2 x}\right]\right.$$

$$\left.\left[e^{\bar{\alpha}_1 x} + C_1 (\frac{\bar{\alpha}_2}{\bar{\alpha}_1})\, e^{\bar{\alpha}_2 x}\right] dx\right\} \qquad \text{(B-84)}$$

The expression of Equation (B-84) may be expanded, integrated and expressed as follows:

$$p = -\frac{w}{\rho_f}\left[\frac{|\Phi_1|}{\pi d}\right]^2 R_e\left\{(\frac{v}{w}\alpha_1 + i)\left[\frac{\bar{\alpha}_1(e^{2\alpha_1\ell}-1)}{2\alpha_1} + \bar{\alpha}_2\ \bar{C}_2\right] + (\frac{v}{w}\alpha_2 + i)\right.$$

$$\left.\left[\ |C_1|^2\ \frac{\bar{\alpha}_2\,(e^{2\alpha_2\ell}-1)}{2\alpha_2} + \alpha_1\, C_2\right]\right\} \qquad \text{(B-85)}$$

where

$$C_2 = C_1\left[\frac{e^{(\bar{\alpha}_1 + \alpha_2)\ell}-1}{\bar{\alpha}_1 + \alpha_2}\right] \qquad \text{(B-86)}$$

and $|A|$ means "the absolute value of A".

It is apparent from Figure (B-10) that the total flux entering the duct is the value of the flux at x = 0 and the total mmf produced by the exciting coil, neglecting iron drop, may be written in terms of the air gap flux density at x = 0 and the mmf produced by the inlet duct header. Thus

$$\Phi_T = \Phi_1 \left\{ 1 + C_1 \right\} \tag{B-87}$$

$$M_c = \frac{g}{\mu} B \Big/_{x=o} + \frac{iw\Phi_T}{R_o} \tag{B-88}$$

Thus, from Equation (B-80)

$$M_c = -\frac{w\Phi_1}{R_o} \left\{ \left(\frac{gR_o}{w\mu\pi d}\alpha_1 - i\right) + \left(\frac{gR_o}{w\mu\pi d}\alpha_2 - i\right) C_1 \right\} \tag{B-89}$$

Assuming a single turn exciting coil, the component of applied voltage corresponding to the flux ϕ_T is

$$V_t = \frac{\partial \Phi_t}{\partial t} = iw\Phi_1 \left[1 + C_1 \right] \tag{B-90}$$

The total input power to the air gap region is

$$W_m = R_e \left\{ M_c \bar{V}_t \right\} \tag{B-91}$$

or, using Equation (B-89) and (B-90)

$$W_m = \frac{w^2\Phi_1\bar{\Phi}_1}{R_o} R_e \left\{ i\,(1 + \bar{C}_1) \left[\frac{g\,R_o}{w\mu\pi d}\alpha_1 - i + \left(\frac{g\,R_o}{w\mu\pi d}\alpha_2 - i\right) C_1 \right] \right\} \tag{B-92}$$

Also

$$VAR_m = \frac{w^2\Phi_1\bar{\Phi}_1}{R_o} \operatorname{Im} \left\{ i\,(1+\bar{C}_1) \left[\left(\frac{g\,R_o}{w\,\mu\,\pi d}\alpha_1 - i\right) + \left(\frac{g\,R_o}{w\mu\,\pi d}\alpha_2 - i\right) C_1 \right] \right\} \tag{B-93}$$

Where $\operatorname{Im} \left\{ A \right\}$ signifies "the imaginary" of A.

If the exciting coil resistance, on a one turn basis is R_c, the coil loss may be written

$$W_c = \left| M_c \right|^2 R_c \tag{B-94}$$

The total loss is the sum of W_m and W_c

$$W_T = W_m + W_c \tag{B-95}$$

The power output is given by the product of developed pressure and flow. Thus, in consistent units, efficiency and power factor may be written

$$\eta = \frac{pQ}{W_T} \tag{B-96}$$

$$P.F. = \frac{W_T}{\sqrt{\overline{VAR}_m^{\,2} + \overline{W}_T^{\,2}}} \tag{B-97}$$

The turn voltage is

$$V_t = \sqrt{\frac{\overline{VAR}_m^{\,2} + \overline{W}_T^{\,2}}{M_c}} \tag{B-98}$$

The analysis is now complete except for further consideration of the constants, Φ_1, and C_1, which are defined by Equation (B-79), repeated for convenience.

$$\Phi = \Phi_1 \left\{ e^{\alpha_1 x} + C_1 e^{\alpha_2 x} \right\} \tag{B-79}$$

One boundary condition common to both pumping configurations Type A and B is that the total flux entering the duct, Φ_T, is the value of Φ at $x = 0$.

This condition has been expressed in Equation (B-87)

$$\Phi_T = \Phi_1 (1 + C_1) \tag{B-87}$$

A second boundary condition is imposed at the outlet end of the duct, at $x = \ell$.

For pump Type A, the mmf drops around a closed path crossing the duct at $x = \ell$ and returning to the starting point by way of the magnetic core to the right of the duct (Figure B-7) yield this relationship.

$$I_\ell = - \frac{g B}{\mu}\Bigg/_{x=\ell} = \frac{g \alpha_1}{\mu \pi d} \Phi_1 \left[e^{\alpha_1} + \frac{\alpha_2}{\alpha_1} C_1 e^{\alpha_2} \right] \tag{B-99}$$

where I_ℓ is the current in the outlet duct header, having resistance R_ℓ. I_ℓ flows by virtue of the voltage induced by the flux at $x = \ell$. Thus,

$$I_\ell = - \frac{iw\Phi}{R_\ell}\Bigg/_{x=\ell} = - \frac{iw\Phi_1}{R_\ell} \left[e^{\alpha_1} + C_1 e^{\alpha_2} \right] \tag{B-100}$$

Combining Equations (B-88) and (B-89), and solving for C_1,

For Type A

$$C_1 = - \frac{\left(\frac{g R}{w \mu \pi d} \alpha_1 + i\right)}{\left(\frac{g R}{w \mu \pi d} \alpha_2 + i\right)} e^{(\alpha_1 - \alpha_2)\ell} \tag{B-101}$$

For pump Type B, the boundary condition at $x = \ell$ is more obvious. Neglecting fringing flux, the flux at $x = \ell$ must be zero. Thus for Type B, from Equation (B-79) at $x = \ell$,

$$C_1 = - e^{(\alpha_1 - \alpha_2)\ell} \tag{B-102}$$

Summary of Performance Equations

The equations relating the performance of a single-phase induction pump of either Type A or Type B to the parameters of the configuration and the fluid pumped are extracted from the foregoing analysis and listed below. The equations in the analysis are correct in any consistent system of units. Constants have been introduced into the equations listed below to correspond to the units indicated in the Nomenclature. These equations have the same numbers as the corresponding equations in the analysis, except that a lower case "a" has been added as a suffix.

$$D_1 = \left[1 + \frac{2t}{a} \frac{\rho_f}{\rho_d} \right] \quad \text{dimensionless} \tag{B-73a}$$

$$\left.\begin{aligned}
D_2 &= \sqrt{1 + i\, 5.475 \frac{f \rho_f g D_1}{a v^2}} \\
\alpha_1 &= \gamma_1 + i\beta_1 \\
\alpha_2 &= \gamma_2 + i\beta_2 \\
\gamma_1 &= 0.1915 \frac{av}{\rho_f g} \left[1 + R_e\,(D_2) \right] \\
\gamma_2 &= 0.1915 \frac{av}{\rho_f g} \left[1 + R_e\,(D_2) \right] \\
\beta_1 &= -\beta_2 = 0.1915 \frac{av}{\rho_f g}\, I_m\,(D_2)
\end{aligned}\right\} \quad \begin{matrix}(B76a)\\(B77a)\end{matrix}$$

For pump Type A,

$$C_1 = -\left[\frac{1.588 \times 10^6 \left(\frac{g\, R\ell}{fd}\right)^{\alpha_1} + i}{1.588 \times 10^6 \left(\frac{g\, R\ell}{fd}\right)^{\alpha_2} + i} \right] e^{(\alpha_1 - \alpha_2)\ell} \quad \text{dimensionless}$$

For pump Type B,

$$C_1 = - e^{(\alpha_1 - \alpha_2)\ell} \quad \text{, dimensionless}$$

$$C_2 = C_1 \left[\frac{e^{(\bar{\alpha}_1 + \alpha_2)\ell} - 1}{\bar{\alpha}_1 + \alpha_2} \right] \quad \text{, inches} \qquad \text{(B-86a)}$$

$$\Phi_T = \Phi_1 \left\{ 1 + C_1 \right\} \quad \text{, megalines} \qquad \text{(B-87a)}$$

$$p = - 562.5 \frac{f \left|\Phi_1\right|^2}{d^2 \rho_f} \operatorname{Re} \left\{ (1.91 \frac{\alpha_1 v}{f} + i) \left[\frac{\bar{\alpha}_1 (e^{2\gamma_1 \ell} - 1)}{2\gamma_1} + \bar{\alpha}_2 \bar{C}_2 \right] \right.$$

$$\left. + (1.91 \frac{\alpha_2 v}{f} + i) \left[\bar{\alpha}_2 \frac{(e^{2\gamma_2 \ell} - 1)}{2\gamma_2} \left|C_1\right|^2 + \bar{\alpha}_1 C_2 \right] \right\} \quad \text{psi}$$

$$G = \left[1.588 \times 10^6 \left(\frac{gR_o\alpha_1}{f\,d}\right) - i \right] + \left[1.588 \times 10^6 \left(\frac{gR_o\alpha_2}{f\,d}\right) - i \right] C_1$$

, dimensionless

$$M_c = - 0.0628 \frac{f \Phi_1}{R_o} G \quad \text{, amperes} \qquad \text{(B-89a)}$$

$$KW_m = 3.95 \times 10^{-6} \frac{\left[f \left|\Phi_1\right| \right]^2}{R_o} \operatorname{Re} \left\{ i\,(1 + C_1)\,G \right\} \quad \text{, kilowatts} \qquad \text{(B-92a)}$$

$$KVAR_m = 3.95 \times 10^{-6} \frac{\left[f \left|\Phi_1\right| \right]^2}{R_o} \operatorname{Im} \left\{ i\,(1 + C_1)\,G \right\} \quad \text{, kilovars} \qquad \text{(B-93a)}$$

$$KW_c = 10^{-3} \left|M_c\right|^2 R_c \quad \text{, kilowatts} \qquad \text{(B-94a)}$$

$$KW_T = KW_m + KW_c \quad \text{, kilowatts} \qquad \text{(B-95a)}$$

$$V_t = 10^3 \frac{\sqrt{(KW_T)^2 + (KVAR_m)^2}}{M_c} \qquad \text{(B-98a)}$$

$$P.F. = \frac{KW_T}{\sqrt{(KW_T)^2 + (KVAR_m)^2}} \quad \text{, dimensionless} \tag{B-97a}$$

$$\text{Efficiency} = \eta = \frac{0.435\ p\ Q}{10^3\ KW_T} \quad \text{, dimensionless} \tag{B-96a}$$

It follows from Equations (B-79) and (B-80) that the flux at $x = \ell$, Φ_ℓ, and gap flux density at $x = 0$ and $x = \ell$, B_o and B_ℓ, respectively, are

$$\Phi_\ell = \Phi_1\, e^{a_2 \ell} \left\{ e^{(\alpha_1 - \alpha_2)\ell} + C_1 \right\} \quad \text{, megalines} \tag{B-79a}$$

$$\left.\begin{aligned} B_o &= -\,10^3\, \frac{\Phi_1 \alpha_1}{\pi d} \left\{ 1 + \frac{\alpha_2}{\alpha_1} C_1 \right\} \quad \text{, kilolines/in}^2 \\ B_\ell &= -\,10^3\, \frac{\Phi_1 e^{\alpha_2} \alpha_1}{\pi d} \left\{ e^{(\alpha_1 - \alpha_2)\ell} + \frac{\alpha_2}{\alpha_1} C_1 \right. \quad \text{, kilolines/in}^2 \end{aligned}\right\} \tag{B-80a}$$

C. Materials and Processes

1. Introduction

In order to provide support primarily to the pump design effort and insure compliance with the state-of-the-art requirement on materials selection and application, a materials and processes function was included. The principal work here consists of uncovering and evaluating suitable sources of materials properties data then selecting and compiling the data for the convenience of the pump designer.

In Quarterly Progress Report No. 1 a grouping of the data to be sought was outlined. Group A was to be a broad selection suitable to conceptual design and initial selection work. Group B was to be more carefully selected but restricted to only those materials applicable to pumps chosen for further study. Finally Group C would be those properties which are of interest only in detailed design or become available incidental to the search for Groups A and B data. Information presented below falls into the Group A category. Further selection is now in progress for Group B and will appear in subsequent reports.

2. Properties of Gases

The heat transfer design approach for polyphase induction pumps as discussed in Quarterly Progress Report No. 2 calls for a gas filled stator cavity. Choice of gases for this application requires attention to thermal conductivity, dielectric strength and chemical stability in the expected environment. Helium being the obvious choice from the view of thermal conductivity and stability its dielectric strength was investigated first and some comparisons to other gases made as presented below.

The investigation was based on the following design considerations:

(a) Enclosure is to be filled to one atmosphere of pressure at room temperature.

(b) Maximum temperature of stack, conductor and gas is expected to be $800^{\circ}F$.

(c) Minimum separation of conductors is .001 inch, conductor coated with glass roving, ceramic particles, ceramic "film" or other insulating material.

(d) Radiation: 10^7 Rads; 10^{12} to 10^{14} NVT.

The locations of particular concern are the slots where turn, phase, and coil to ground voltages may exist, and at end loops close to each other. From a thermal conductivity standpoint, helium is good; but of the commonly available gases on which dielectric information is readily available, it is the poorest electrically. At the pressure and gaps indicated, the DC sparkover voltages are as shown in G. A. Farrall's survey of Paschen curve information, Research Lab. Memo-Report P215, dated December, 1959:

Gas	Volts		
@ 760 Torr @ R.T.	.010" Gap	.002" Gap	.001" Gap
Helium	350	210	280
Neon	360	250	260
Argon	590	290	270
Hydrogen	950	400	310
Air	1700	620	450

These data are plotted in Figure C-1.

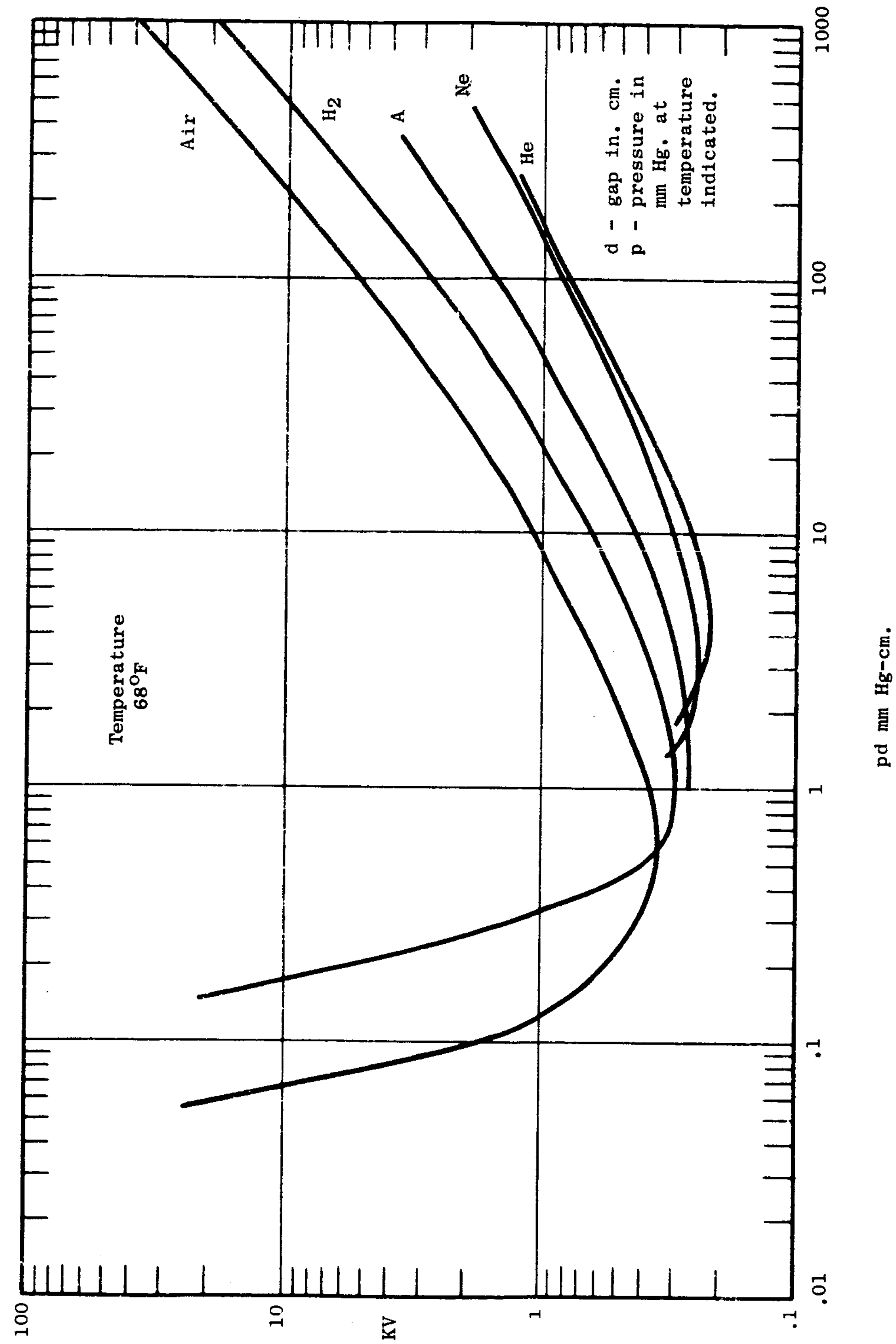

Figure C-1 Paschen Curves

It must be emphasized that these values are for: (1) uniform electrical field, (2) the gas only, and (3) D.C. voltages.

For small gaps only small errors are incurred by considering the D.C. value as peak A.C. value. Somewhat larger variations may occur with different electrode materials, at this and smaller pressure and gap distance products. Oxide and other coatings on electrodes usually reduce the sparkover values. However, very significant reductions may result from the following:

(a) Non-uniformity of field: In most electrical equipment a non-uniform field is usual. The EM pump is likely to be no different. A reduction of 30% in the above values is not unusual.

(b) Interposed material in the gap: No serviceable high temperature conductor insulation of a truly film nature, similar to Formex for low temperature, is known. Even chemically formed oxide films do not ensure a completely unbroken film. Whether the conductors are spaced by oxide film, by attached ceramic granules, or by inorganic fibers, such matter represents an interposed material of higher dielectric constant between the electrodes. It is uncertain at the moment if these should be calculated as equivalent to an interposed film plus gas gap in series or as equivalent to a shunting surface between electrodes. In either case there is some probability of overstressing the gas to cause corona or breakdown. Estimated reduction of flashover voltage for this cause is a miminum of 30%.

(c) Radiation: Although helium (and nitrogen) per se are not subject to damage at the radiation fluxes involved, the gap flashover voltage will likely be somewhat lower because of the high irradiation of the gap and electrode materials.

(d) Impurities in the gas: The nature of the impurity(ies) governs whether the breakdown voltage is increased or decreased. Most impurities degrade the dielectric properties.

The conclusion is that in helium turn to turn breakdown, etc. is likely not to exceed 50 V RMS 60 cy. This appears to be very marginal. In the case of solid material slot liners the division of voltage between solid and possible gas gaps appears to be less disadvantageous, but still may be considered marginal. Even if non-porous separators between phase or other conductors in the same slot or external to slots are capable of withstanding corona attack, corona effects on the inevitable impurities in the enclosed atmosphere may have deleterious effects; and, certainly corona or sparking is undesirable from a communications standpoint.

Possible Solutions:

Several solutions immediately suggest themselves.

(a) Increase the gap.

(b) Increase the filling pressure.

(c) Add other gases to improve the dielectric properties with minimum interference with heat transfer.

(d) Combinations of above.

The first two, within reasonable limits, will increase the breakdown strength but not in direct ratio; see curves, Figure C-1. The third possible solution requires examination. The approximate improvement possible with the addition of nitrogen or octofluoropropane (C_3F_8) to helium is indicated in Figure C-2. The crux of the situation is the possibility of radiation damage to the gas and consequent deterioration of properties or attack on other materials. Sulfur hexafluoride (SF_6) addition would appear to be suitable from dielectric and thermal conductivity standpoints, but SF_6 is believed to be sufficiently radiation sensitive to be unsuitable. In addition, the expected 800°F is uncomfortably close to the start of dissociation (450°C). Heavier gases which might be more desirable from the standpoint of dielectric and thermal conductivity properties are also more complex and usually more subject to radiation damage. C_3F_8 has been suggested by Sharbaugh at Research Lab as possibly radiation suitable. CF_4 (Freon 14) has been suggested by Dutton of Medium Transformet Dept. as another possibility on the basis that it is a saturated compound. Insufficient evidence is at hand at the moment to draw sound conclusions about any of the additions other than nitrogen.

3. <u>Magnetic Materials</u>

This electromagnetic pump project is intended to cover "state-of-the-art" materials and, as power frequencies in the order of 60 cycles are required, as indicated by earlier work on the program, the search for material information

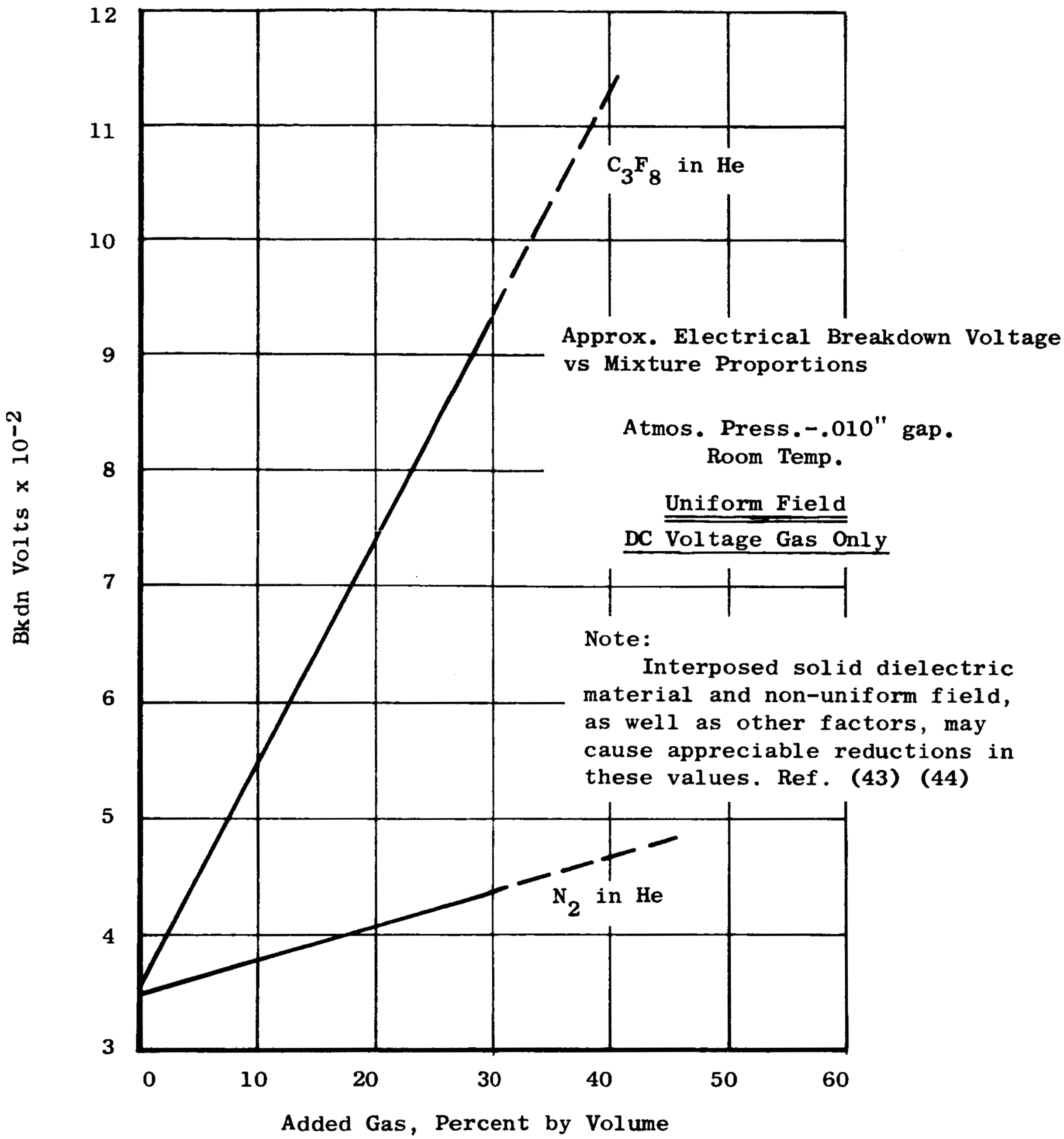

Figure C-2 Electrical Breakdown Voltages for Helium Mixture is narrowed somewhat. At this point it is well to restate the present tentative main requirements for the magnetic materials:

Operating temperature of magnetic material: 800°F or 1300°F.

Atmosphere: Vacuum, or nitrogen or other inert gas at ca 40 PSIA at temp.

Lowest weight consistent with reasonable magnetic flux carrying capability, watt loss and exciting volt-amperes, and consistent with reliability and other conditions of operations and environment.

Power supply: 10 to 100 cycles per second, 1 phase or 3 phase.

Magnetic flux: unidirectional for D.C. devices; simple alternating for 1 phase devices; alternating and rotating for 3 phase devices.

Fast neutron radiation exposure: 1×10^{-8} nvt.

Consideration of the possible materials and the available test information to support a proper choice of one or more of them provides little choice; few of the probable candidate materials have been tested at elevated temperature in the absence of air. There have been a number of reports of tests, mostly in the period of 1957 through 1960, at 932°F, a few at temperatures up to 1382°F, but usually in air; the exceptions to air tests are found in Ref. 21 and 40 (Co alloys only), and 22. Uncertainty regarding processing details and variations for some of the tests reported makes difficult the reconciliation of apparently anomalous differences. Despite the scarcity of entirely satisfactory test information, there is data which is indicative of probable behavior under the required conditions.

The Bibliography lists most of the reports and articles examined. Excerpts will be more fully presented in later reports.

The properties of primary interest for EM pumps are:

Curie temperature

Normal magnetization curves vs. temperature

Core loss vs. induction vs. temperature

Exciting volt-amperes vs. induction vs. temperature

Variation of stress sensitivity with temperature

Magnetic anisotrophy

Aging characteristics

It should also be noted that many magnetic materials are notorious for sensitivity to various conditions. Among these are:

a) non-uniform and uniform stresses

b) small chemical variations

c) processing variables, particularly heat treatment

d) surface conditions and inclusions

e) radiation

4. Discussion of Property Information

(a) Curie Temperature

The Curie point of a magnetic material is the first criterion for selection of a magnetic material. Usually the material must be held well below the Curie temperature to obtain useful properties. Tables III-1 thru III-4 reproduce information from references (18) and (19), and summarize partial data on a variety of materials. However, Pasnak and Lundsten (20), Figure C-3, indicates that the maximum high flux density usefulness of Supermendur is in the order of 1112°F. Helms (36) shows

Table III-1 Magnetic and Thermal Properties of Electrical Steel Sheets(a) (Ref. 18, Table 1, Pg. 788)

AISI type	Maximum core loss, watts per pound at 60 cycles(b): Induction, 10 kilogausses: 29 gage, (0.014 in.)	26 gage, (0.0185 in.)	24 gage, (0.025 in.)	Induction, 15 kilogausses: 29 gage, (0.014 in.)	26 gage, (0.0185 in.)	24 gage, (0.025 in.)	Saturation induction, B-H or 4 π Is, gausses	Residual induction, gausses, Bmax=10,000	Coercive force, oersteds, Bmax=10,000	Thermal conductivity at 20C, cal/sq cm/cm/°C/sec
M-43	1.30	1.55	1.98	3.90	4.20	5.25	21,300	8200	-0.94	0.097
M-36	1.17	1.35	1.70	3.30	3.60	4.40	21,100	8700	-0.85	0.073
M-27	1.01	1.14	1.30	2.46	2.74	3.09	20,600	6700	-0.79	0.047
M-22	0.82	0.94	1.10	2.00	2.26	2.63	20,300	6700	-0.69	0.043
M-19	0.72	0.83	0.97	1.78	2.03	2.35	20,000	6300	-0.55	0.039
M-17	0.65	0.75	(c)	1.62	1.86	(c)	19,900	5250	-0.33	0.038
M-15	0.58	0.68	(c)	1.46	1.71	(c)	19,500	5000	-0.25	0.036
M-14	0.52	(c)	(c)	1.33	(c)	(c)	19,200	4600	-0.20	0.034
M-8	(d)	(c)	(c)	0.80	(c)	(c)	20,100	....	....	0.043
M-7	(d)	(c)	(c)	0.73	(c)	(c)	20,100	....	....	0.043
M-6	(d)	(c)	(c)	0.66	(c)	(c)	20,100	....	....	0.043
M-5	(d)	(c)	(c)	0.60	(c)	(c)	20,100	....	....	....
Iron *							21,600		1.0	
Cobalt *							17,000		10.0	
Nickel *							6,500		0.7	

* (Ref. 19, Table II)
(a) For silicon contents, see Table III-2. (b) Standard tests on all hot rolled sheets (M-43 to M-14 inclusive) are made on samples cut half with and half across the rolling direction. (d) Transformer grades not normally now produced in the heavier gages. (d) Grain-oriented grades produced to a maximum core loss at 15 kilogausses only and tested in the rolling direction. Also produced in 0.012 in. thickness with maximum core losses at 15 kilogausses of 0.78 for M-8, 0.71 for M-7, 0.64 for M-6, and 0.58 for M-5.

Table III-2 Silicon Contents, Properties and Applications of Electrical Steel Sheets (Ref. 18, Table 2, Pg. 788)

AISI type	Nominal silicon content, %	Density(a), grams per cu cm	Electrical resistivity, microhm-cm	Alternate designation	Some characteristics and applications
M-50	0.40	7.85	18	Field	Not subject to magnetic requirements; pole pieces and electrical apparatus for intermittent operation
M-43	0.95	7.82 to 7.78	20 to 28	Armature	High core loss but good permeability at high inductions; small motors, pole pieces, and relays
M-36	1.40	7.80 to 7.75	24 to 33	Electric	Lower core loss than M-43, excellent permeability at high inductions; rotating machines including a-c and d-c motors
M-27	2.35	7.76 to 7.67	32 to 47	Motor	Good punching properties; continuous-duty, high-efficiency motors (10 to 1000 hp), small transformers
M-22	3.00	7.70 to 7.64	41 to 52	Dynamo	Good ductibility, intermediate magnetic quality; stators of high-efficiency rotating machines, intermittent-duty transformers, high-reactance cores
M-19	3.20	7.70 to 7.62	41 to 56	Transformer 72	Moderately high permeability at all inductions; communications equipment, high-efficiency fractional-horsepower motors
M-17	3.40	7.68 to 7.60	45 to 58	Transformer 65	Intermediate properties; transformers to 1000 kva
M-15	4.00	7.68 to 7.54	45 to 69	Transformer 58	Low core loss, excellent permeability at low and moderate inductions
M-14	4.50	7.60 to 7.54	58 to 69	Transformer 52	Lowest core loss of nonoriented grades, high permeability at low inductions; distribution and power transformers, high-efficiency rotating machines
M-8	3.00	7.68 to 7.64	....	Oriented 80 or Tran-Cor 2 X	Grain-oriented sheets, M-8, M-7, M-6 and M-5, have highly directional magnetic properties, lowest core loss andhighest permeability available when flux path is parallel to rolling direction; highest-efficiency distribution and power transformers and large generators.
M-7	3.00	7.68 to 7.64	45 to 52	Oriented 73 or Tran-Cor 3 X	
M-6	3.00	7.68 to 7.64	45 to 52	Oriented 66	
M-5	3.00	7.68 to 7.64	45 to 52	Oriented 60	
Iron	*		9.7		
Cobalt	*		6.3		
Nickel	*		6.8		

* (Ref. 19, Table II) (a) For magnetic testing, ASTM recommends the use of one of the following assumed values of density: 7.85, 7.75, 7.65 or 7.55, depending on the silicon content of the steel being use.

Table III-3. Magnetic and Physical Properties of Alloys with Moderately High Permeability at Low Field Strength and High Electrical Resistance (Ref. 18, Table 3, Pg. 788)

Alloy(a)	Permeability: Initial	Permeability: Maximum	B value at max permeability	Hysteresis loss, ergs per cu cm per cycle	Residual induction, gausses	Coercive force, oersteds	Saturation, gausses	Resistivity, microhm-cm	Specific gravity, g per cu cm
Thermenol	6,000	60,000	1500	....	2,070	0.018	6,100	162	6.58
16 Alfenol	4,000	80,000	3500	76.4	4,000	0.044	8,000	153	6.50
12 Alfenol	2,370	20,600	....	....	......	0.10	13,320	...	....
Sinimax	2,200	50,000	5400	400	5,500	0.06	11,000	90	7.70
Monimax	3,000	60,000	6200	800	8,900	0.06	14,500	80	8.27
Supermalloy	55,000 min	300,000 min	4000	20	4,000 to 5,500	0.006	6,800 to 7,800	65	8.77
4-79 Moly-Permalloy, Hymu 80	20,000 min	90,000 min	4000	200	4,000 to 5,500	0.003	7,000 to 7,800	58	8.74
Mumetal	20,000 min	100,000	2000	....	2,300	0.30	6,500	60	8.58
1040 alloy	20,000 min	100,000	2000	200	2,400	0.20	6,000	56	8.76
High Permalloy 49, A-L 4750, Armco 48, Hipernik	5,000	70,000	4500	300	10,000	0.50	16,000	48	8.25
45 Permalloy	2,500	25,000	....	....	....	0.25	16,000	45	8.17
Iron *						1.0	21,600	9.7	
Cobalt *						10.0	17,000	6.3	
Nickel *						0.7	6,500	6.8	

* (Ref. 19, Table II)

Table III-4. Typical Magnetic Properties for Various Iron-Nickel and Iron-Cobalt Alloys (Ref. 18, Table 7, Pg. 790)

Material	Nominal composition(a)	Typical anneal(b)	Permeability: At B = 20	Permeability: Maximum	Saturation induction, gausses	Coercivity, H_e, oersteds	Retentivity, B_r, gausses	Approx Curie temperature, F	Resistivity, microhm-cm
45 Permalloy	45 Ni	1920 F	2,500	30,000	16,000	0.20	8,000	825	50
		H_2, 2150 F	4,000	50,000	16,000	0.06	8,000	825	50
4750 alloy	47 to 50 Ni	H_2, 2050 F	4,000	50,000	16,000	0.07	8,000	896	50
Armco 48, Ni	47 to 50 Ni	H_2, 2050 F	4,000	50,000	16,000	0.07	8,000	896	50
Carpenter 49 alloy	47 to 50 Ni	H_2, 2050 F	4,000	50,000	16,000	0.07	8,000	896	50
Hipernik	50 Ni	H_2, 2200 F	4,500	70,000	16,000	0.05	8,000	896	50
Conpernik	50 Ni	....	1,500	2,000	16,000	....	....	896	50
Deltamax	50 Ni (c)	H_2, 1825 F	....	150,000	15,600	0.10	14,500	896	50
48 Orthonik	50 Ni (c)	H_2, 1825 F	....	60,000	15,600	0.20	14,500	896	50
Hipernik V	50 Ni (c)	H_2, 1825 F	....	50,000	15,600	0.20	14,000	896	50
Monimax	48 Ni, 3 Mo	H_2, 2050 F	2,000	35,000	15,000	0.10	....	...	50
Sinimax	43 Ni, 3 Si	H_2, 2050 F	3,000	35,000	11,000	...	....	...	80
78 Permalloy	78 Ni	1920 F	8,000	100,000	10,700	0.05	6,000	1075	90
4-79 Permalloy	79 Ni, 4 Mo	2000 F, Q	20,000	100,000	8,700	0.05	5,000	790	16
Hymu 80	79 Ni, 4 Mo	2000 F, Q	20,000	100,000	8,700	0.05	5,000	790	55
Supermalloy	79 Ni, 5 Mo	2375 F, H_2, Q	75,000	800,000	8,000	0.005	5,000	...	55
Mumetal	77 Ni, 5 Cu, 1.5 Cr	2050 F	20,000	100,000	6,500	0.05	3,000	...	60
Permendur	50 Co	1470 F	800	5,000	24,500	2.00	14,000	...	60
2V Permendur	49 Co, 2 V	1470 F	800	4,500	24,000	2.00	14,000	...	7
Hiperco	35 Co plus 1	....	650	10,000	24,200	1.00	13,000	1796	27
	to 2% others							...	28
Supermendur	49 Co, 2 V	....	....	60,000	24,000	0.20	21,500	1796	27
2-81 Moly Permalloy powder	81 Ni, 2 Mo	1200 F	125	130	....	...	....	...	16 x 10^6
Carbonyl iron powder	....	....	60	150	....	...	....	...	10 x 10^6
Iron *	....	....	....	5000	21,600	1.0	....	1418	9.7
Cobalt *	....	....	....	250	17,000	10.0	....	2066	6.3
Nickel *	....	....	....	8000	6,500	2.7	....	677	6.8

* (Ref. 19, Table II) (a) Remainder iron plus deoxidizer. (b) H_2 = annealed in hydrogen, Q = quenched or controlled cooled. (c) Grain oriented.

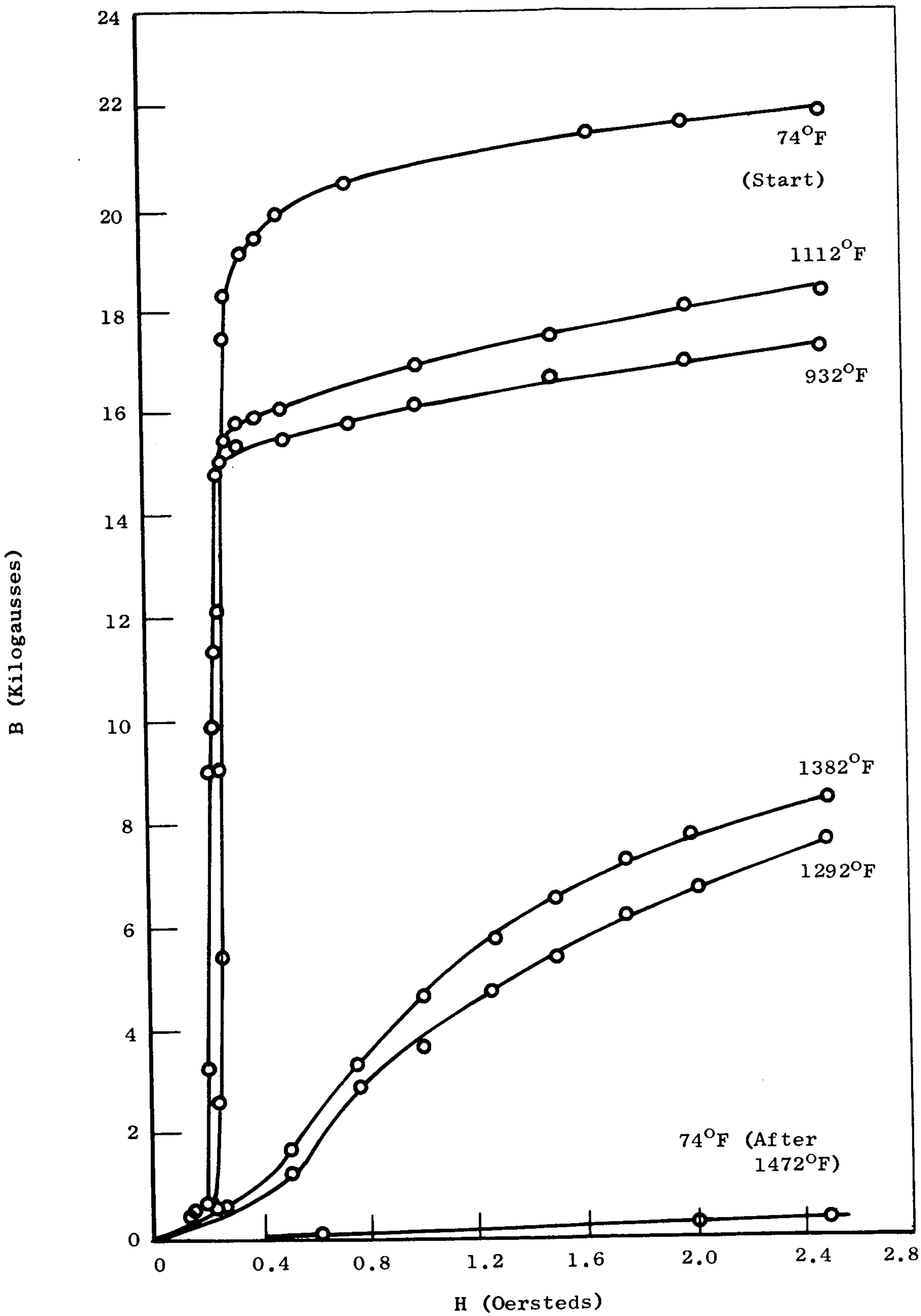

Figure C-3 D.C. Induction Curves of Supermendur in the Temperature Range of 24°C - 750°C (Source: Reference 20, Figure 25) a Curie temperature range of 1418°F to 1292°F for silicon iron alloy with a silicon weight percentage range of 0 to 6% (Fig. C-4). The information at hand indicates that silicon iron and cobalt iron alloys are the materials primarily of interest.

(b) Normal Magnetization and Normal Permeability

These parameters are primarily of use for d-c applications and can indicate maximum useful flux densities in apparatus. They can also furnish some useful clues to a-c performance. Although most of the elevated temperature reports reviewed do not show normal magnetization or permeability curves, Clark and Fritz (27) show this information to 932°F (See Figs. C-5 and C-6, for .018" and .025" thick sheet, respectively).

(c) Core Loss and Excitation; Aging

Core loss and excitation volt-amperes are of interest in determining the engineering performance of a proposed design. There appears to be relatively little information available on high temperature core loss and even less published data on excitation volt-amperes. Much of the data are on small laminations of the E-I or U-I form, some are on ring punchings, some on square hole or "picture frame" punchings, and some on spirally wound cores. The cores were mostly in the order of two pounds or less total weight. The core losses measured could therefore be affected by cross-fluxing at corners, saturation or cross-fluxing at lamination gap locations, averaging influence of ring or square hole punchings, etc., as well as other conditions such as stress, low interlaminar resistance and atmosphere. Harms and Fraser (26) made loss, excitation and aging tests. Their data are typical of the information confirmed by others, notably Clark and

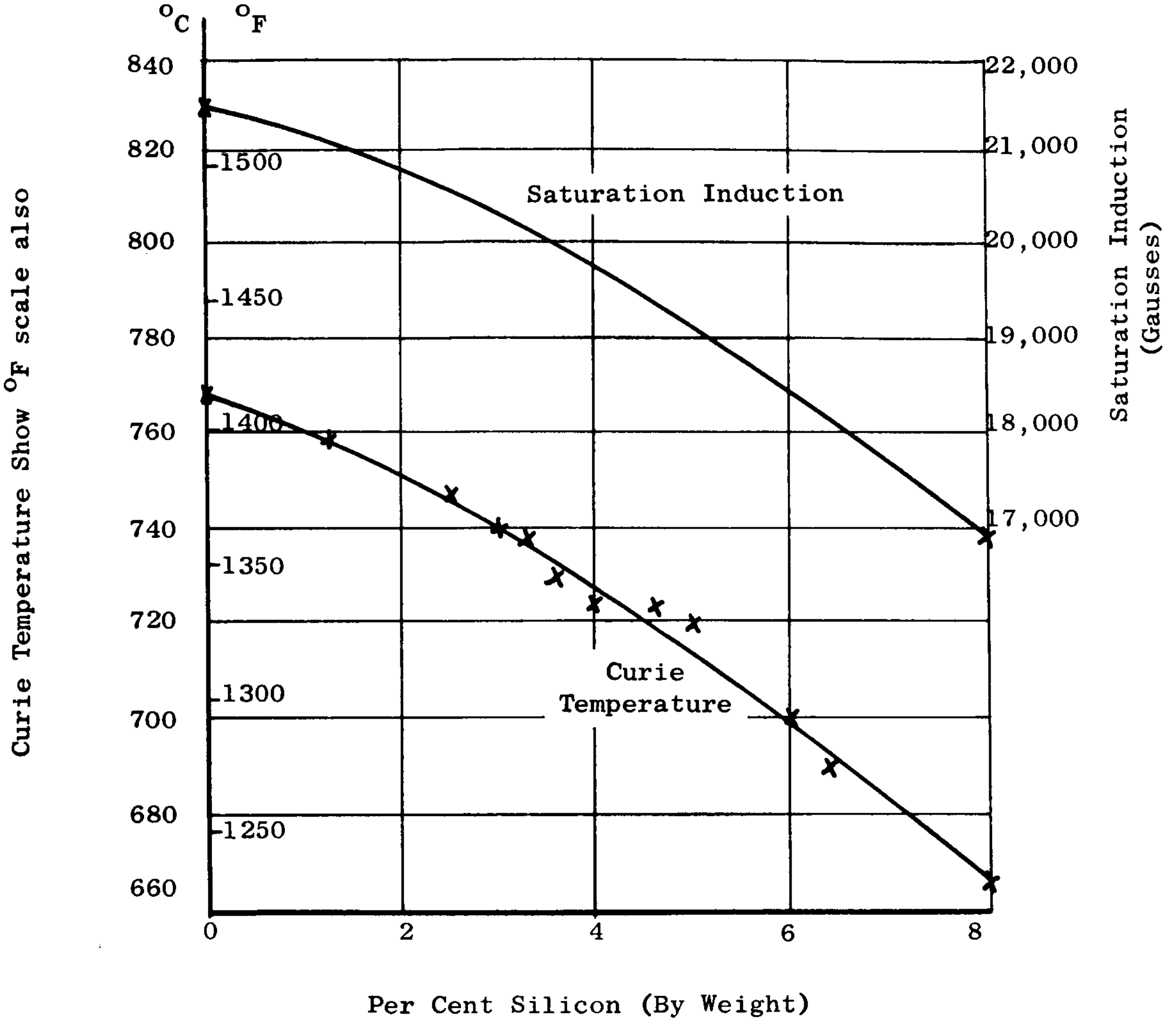

Figure C-4 Variation of Important Properties of Iron-Silicon Alloys with Composition (Source: Reference 36, Figure 8)

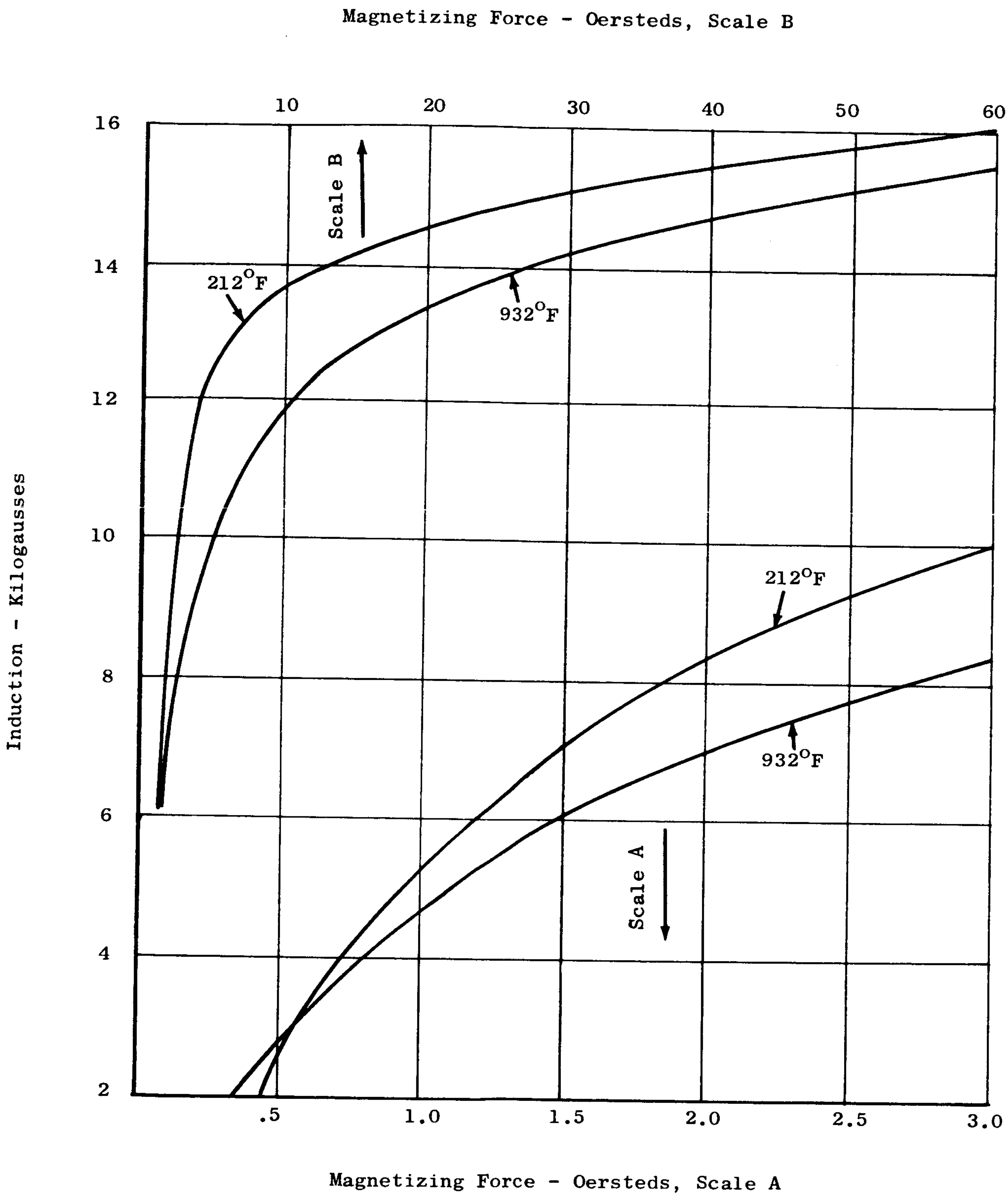

Figure C-5 Normal Magnetization Curves at Various Temperatures 3.6% Silicon-Iron (Source: Reference 27, Figure 9)

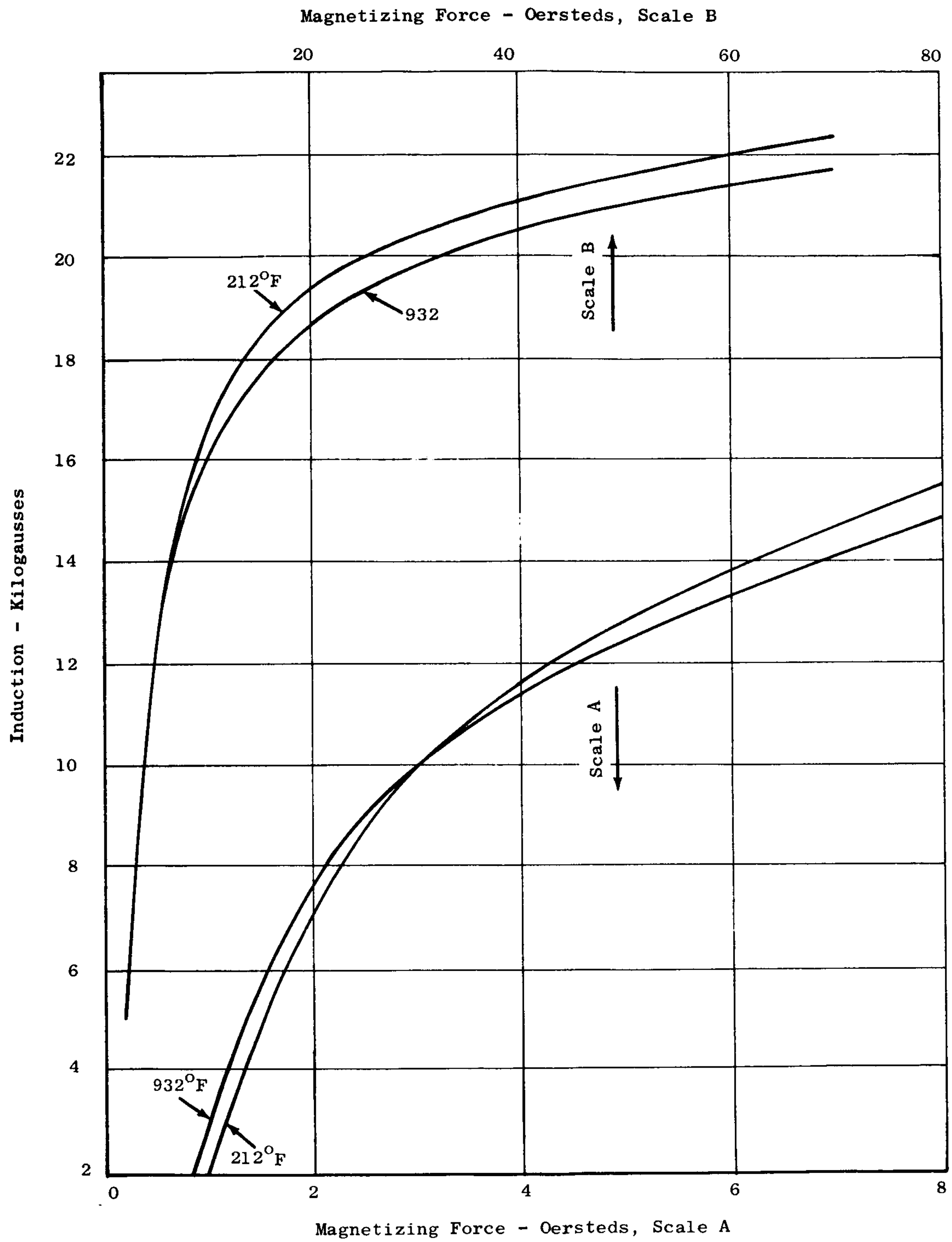

Figure C-6 Normal Magnetization Curves at Various Temperatures Hiperco 27 (Source: Reference 27, Figure 25)

Fritz (27), showing lowered core loss with increased temperature; increased temperature results in higher A.C. excitation at high inductions and lower excitation at lower inductions, with a relatively constant value at about 55,000 lines per square inch. A.C. loss and excitation in cobalt steels are appreciably higher than in silicon steels at inductions up to about 15 kilograms.

(d) Aging Tests

Harms and Fraser (26) (grain oriented silicon steel), and Greene, et al (25) (oriented and non-oriented silicon steel and cobalt steel), reported relatively short aging tests, both sets in air at 932°F (1000 hrs.) and 600°C (600 hrs.) respectively. Both show degradation, partially due to temperature alone, partly probably due to oxidation. Silicon steels appear to be affected in the order of 10 to 25% of both core loss and excitation at 60 cycles, depending on the quality of the inter-laminar insulation; cobalt steel appears to be affected in the order of 10 to 15%; both experiments were run in air. The conclusion of both sets of investigators was that at temperatures in the neighborhood of 932°F and for times in the 1000 hours range, the silicon irons did not age sufficiently to preclude their use.

(e) Other Properties

Other properties, which may require further documentation, are:

1) Stress sensitivity and magnetostriction (inverse manifestations of the same phenomenon); oriented material is more sensitive than non-oriented; cobalt alloys are more sensitive than silicon steels; stress sensitivity generally reduces with increasing temperature.

2) Magnetic anisotrophy: Bozorth (16) showing the loss in a direction 70° from the rolling direction of grain oriented silicon steel to be 240% of the loss in the rolling direction, at 15 kilograms; also see Kaplan (30) showing 300% higher losses due to rotational magnetic flux compated to the loss due to induction in the rolling direction only; no data were found to support clearly the opinion that loss and excitation anistropy will decrease with increasing temperature.

3) Radiation effects; virtually no effect on alloys of interest here, but cobalt will become highly radioactive under neutron exposure.

(f) Comments

1) All data available are on samples or cores with no gaps or very small gaps in the magnetic circuit, and most are directed toward transformer type apparatus for operation at 932°F, for relatively short times (500 to 1000 hours). With a large magnetic circuit gap, such as would occur in an electromagnetic pump, the benefit of a high permeability material, compared with a relatively low one, is essentially lost.

2) Almost all data at elevated temperature are in air. Two reports on cobalt alloys indicate damage due to oxidation, but experimental data also indicate that this is due primarily to mechanical strain induced in tape wound cores due to oxidation. It is virtually certain that the silicon alloy aging degradation is due primarily to oxidation.

3) It is obvious from the normal magnetization vs. temperature curves that the cobalt alloys have a higher flux carrying capability than the silicon iron alloys, and that they suffer less (in air) with temperature elevation and aging compared to room temperature values. On the other hand, the cobalt alloys, at the same temperature and flux density, have higher core loss and exciting volt-amperes at 60 cycle than the silicon-irons, within reasonable portions of their saturation flux densities.

4) The kind of magnetic circuit employed will govern the use of oriented vs. non-oriented material when use of a silicon-iron alloy is indicated. Cross-grain losses and exciting currents in oriented material are inferior to with-grain values and may also be inferior to those of non-oriented material, depending on the grade of steel used.

5) In magnetic circuits which have rotational fluxes, the losses may be substantially higher than those calculated on the basis of conventional sample loss measurements.

6) Cobalt-iron alloys, in general, have much higher magnetostriction than do silicon-iron alloys. From available data, magnetostriction would be expected to decrease with temperature elevation, approaching zero with approach to Curie temperature.

7) The cost of cobalt-iron lamination stock is in the order of thirty times that for silicon-iron.

8) If relatively low flux densities are required in an EM pump, the use of some non-oriented silicon steels may be considered for use at 1292°F.

9) Obviously, some compromises will have to be made by the designer as no one material is outstanding in all properties such as induction, loss, excitation, anisotropy, magnetostriction, radioactivity, aging, weight, cost and reliability.

(g) Recommendations

1) Considering all properties, silicon steel seems to be the best choice for 800°F. One exception may have to be taken to a choice of grain oriented silicon steel. For polyphase cylindrical stator induction pumps and perhaps, also, for linear induction pumps, non-oriented silicon steel alloys may be preferable. See the discussion under anisotropy.

2) For application at 1300°F and above, apparently, a cobalt alloy probably is necessary. Hiperco 27, Reference (24), or equal, seems indicated, although the vendor's information (Page 3 and 4 reproduced here) does not extend beyond 932°F. Also see comment 7 above.

3) Aging tests on candidate materials (oriented and non-oriented silicon steels and Hiperco 27) should be made on samples of geometry appropriate to expected useful EM pump designs, in both vacuum and inert atmospheres at 800°F and 1300°F (or other appropriate temperatures) for periods of time sufficient to demonstrate stability or

continuing instability. Suitability of several insulative coatings should also be verified.

4) If magnetic material power loss can be an important factor in performance, the effects of cross-flux and rotational flux at elevated temperature should be investigated on samples similar to those above.

5) If the construction of the pump is such that magnetostriction might influence the reliability of the pump, the elevated temperature magnetostrictive effects, particularly in the case of cobalt-iron alloys, should be looked into more carefully.

D. Power Conditioning

1. Introduction

In considering electrical equipment for space power plant application the available power form is of primary importance. Power conditioning is frequently required. In the past reports it was established that high performance EM pumps generally require low voltage D.C. or relatively low frequency A.C. The power forms available in space power plants are shown in Table III-5.

2. Performance and Weight

Several power conditioning systems have been identified for use in the two types of power plants of interest to this program. A frequency changer and a rectifying system have been described in earlier reports.

In Quarterly Report NO. 2 a comparison was presented of the A.C. induction pump and the D.C. conduction pump as applied to the thermionic power plant. In the comparison several assumptions were made. Since then further design work on EM pumps has required modification of values used in the earlier comparison. The modified evaluation is presented below.

In the thermionic power plant, power is available at 100V D.C.. Therefore either A.C. or D.C. pumps will require power conditioning. The comparison of the weights for conditioning equipment in the earlier report was accompanied by a description of the electrical components and circuitry. This information has been deleted here and a simple comparison chart substituted.

TABLE III-5

SPACE POWER PLANT EM PUMPS

POWER SUPPLIES

System	Power Source	Power Form	Fraction of Reactor Thermal Pwr.	Weight Penalty for Power Consumed
Turboelectric	Alternator	500-1000V A.C.-2000 cps	10%	10 lb/KW c
Turboelectric	Thermo-electric Device "A"	Low Voltage D.C.	100%	0.5 lb/KW th.
Turboelectric	Thermo-electric Device "B"	Low Voltage D.C.	100%	0 lb/KW th.
Turboelectric	Turbo-alternator shaft	24,000 RPM	11%	9 lb/KW mech.
Thermionic	Bus Bar	100-200V D.C.	10%	9 lb/KW e
Thermionic	Thermo-electric Device "A"	Low Voltage D.C.	100%	0.5 lb/KW th.
Thermionic	Thermo-electric Device "B"	Low Voltage D.C.	100%	0 lb/KW th.

Note: Thermoelectric Device "A" provides low voltage D.C. power for EM Pump operation by thermoelectric elements operating on the temperature difference between primary coolant and radiator coolant.

Thermoelectric Device "B" provides low voltage D.C. power for EM Pump operation by thermoelectric elements operating on the temperature difference between primary coolant and space.

POWER CONDITIONING SPECIFIC WEIGHT

THERMIONIC SYSTEM

AC vs. DC PUMPS

	DC Pumps		AC Pumps	
	Original	Revised 3/27	Original	Revised 3/27
Hydraulic Power - KW				
Primary Coolant	2.3	Same	2.3	Same
Radiator Coolant	4.3	Same	4.3	Same
Total	6.6	Same	6.6	Same
Pump Efficiency - %	33	20	20	15
Pump Input - KW	20	33	33	44
Power Conditioning Efficiency - %	80	Same	85	Same
Power Conditioning Input - KW	25	41	40	52
Power Conditioning Weight	128	210	155	200
Power Conditioning Specific Weight - LB/KW Output	6.4	Same	4.7	Same

The values for pump efficiency are based on the D.C, condensate boost pump and the A.C. single phase primary coolant pump shown later in this report plus the A.C. induction pumps for radiator coolant shown in Quarterly Progress Report No. 2. These pumps are not all designed specifically for the thermionic plant applications. Therefore, some adjustment was made for the fact that efficiency improves with increasing pump size.

The original assumption that the D.C. pumps could be series connected to accept a power supply voltage of 5 volts now looks less likely. The compromise of reliability in the series arrangement cannot be avoided without severely reducing pump efficiency. The efficiency for power conditioning equipment producing D.C. at about one volt using present technology is not over 50%. Thus the A.C. pump is definitely favored in the thermionic power plant from the power conditioning standpoint.

E. Power Plant Integration

1. Introduction

Proper selection of pumps for each of the six applications must necessarily include consideration of the several interfaces between the pump and the rest of the power plant. Schematic diagrams of representative pumping systems were prepared and presented in Quarterly Progress Report No. 2 to aid in the power plant integration work. The principle items covered are power supply, power conditioning and pump cooling together with the associated weight penalties. Also to be considered are start up and control.

2. Pump Cooling

Sufficient study of the power supply and power conditioning requirements has been done to provide preliminary values for pumping system weights. During the past quarter pump cooling was studied with the result that four practical systems of pump cooling were devised. Each of these was evaluated in terms of weight penalty per KW of heat rejected. The results are tabulated in Table III-6.

As described in Quarterly Progress Report No. 2 the basic heat transfer arrangement within the EM pump is designed to deliver heat from electrical losses and from leakage through the duct insulation to a cooling coil bonded to the outer shell of the pump.

From the power plant systems viewpoint the heat must then be taken up by an alkali metal coolant and carried to a radiator for rejection to space.

TABLE III-6

EM PUMP COOLING WEIGHT PENALTIES

Pump Cooling Method	Coolant Temperature °F	Weight Penalties - lb/KW Heat Rejected: Coolant Pump	Coolant Pump Power	Regenerative Heat Exchanger	Coolant Radiator	Totals
Independent pump cooling loop powered by turbogenerator shaft mounted coolant pump	600	.1 #/KW	.2 #/KW		2.5 #/KW	2.8 #/KW
	1200	.1 #/KW	.2 #/KW		1.0#/KW	1.3 #/KW
Independent pump cooling loop powered by separate EM type cooling pump	600	2#/KW	.4 #/KW		2.5 #/KW	4.9 #/KW
	1200	2#/KW	.4 #/KW		1.0#/KW	2.5 #/KW
Regenerative heat exchanger type cooling loop powered by main EM pump	600	1.0#/KW	.4 #/KW	2#/KW	2.8 #/KW	6.2#/KW
	1200	1.0#/KW	.4 #/KW		1.4#/KW	2.8#/KW
Superfin type pump cooling	600				2.5 #/KW	2.5 #/KW
	1200				1.0#/KW	1.0#/KW

Two coolant temperatures were considered: 600°F and 1200°F. Although the lower temperature has been chosen as the basis for pump design, the higher temperature is not out of the question for some types of pumps. Therefore, it is of interest to determine the weight advantage to be gained using the 1200°F coolant.

To determine the approximate level of heat dissipation, it was estimated from experience with conventional EM pumps that about one half the power input to the pump would appear as heat in the coolant. The sources of heat to the coolant are I^2R losses in the windings, core losses in the magnetic structure, eddy currents in metal walls and heat leakage from the duct. This latter item is, of course, zero when the coolant and pumped fluid are at the same temperature. However, the pump designs include good thermal barriers at the ducts so the heat leakage will be small. From preliminary calculations, the I^2R loss in the windings will contribute 60-80% of the heat added to the coolant. For these reasons the heat addition will be considered the same for both coolant temperatures.

EM pump efficiencies are calculated to be between 10% and 20% in terms of the ratio of hydraulic power output to electrical power input. Taking a mean of 15% and looking at the hydraulic power requirements shown in Table II-I, the total plant pump power input is 44 KW for the thermionic system and 34 KW for the turboelectric system using lithium as both primary coolant and radiator coolant. Thus a radiator nominally sized for 20 KW heat rejection is adequate here.

Other pertinent assumptions were: a) the recirculation requirements for the auxiliary coolant loops must be 7% of the main loop flow and b) the regenerative heat exchanger handles 10 times the heat rejected at the auxiliary radiator with a heat exchange effectiveness of 85%.

To provide for simple evaluation of the pump cooling item in present preliminary work a rough estimate was selected of 2 lb./KW heat rejected for 1200°F cooling and 4 lb/KW for 600°F cooling based on an average of Table III-8.

The four system arrangements for pump cooling were:

1. Independent coolant loop and radiator with the recirculation pump driven by the turbogenerator shaft.
2. Independent coolant loop and radiator with the coolant driven by an all electrically powered EM pump.
3. Radiator loop fluid bled from a radiator loop EM pump and cooled by an auxiliary radiator and regenerative heat exchanger.
4. Two phase cooling by the refluxing or Superfin principle. Here the weight flow of coolant is drastically reduced by employing the latent heat of vaporization of the alkali metal coolant. No pump is required since the vapor moves from hot to cold surfaces by virtue of the volume change associated with the phase change. Condensate is returned to the hot surface by wick action.

The Superfin cooling system is now under development at General Electric - Evendale by Space Power and Propulsion Systems. Results to date are sufficiently promising to warrant its consideration in this study. A sketch of the system is shown in Figure E-1 as it might be applied to EM pump cooling.

3. Power Conditioning:

There was a need for an approximate weight value for power conditioning equipment. Study of this item included consideration of the basic equipment weight, the power losses associated with the components and the weight penalties incurred in dissipating the losses to maintain acceptable component temperatures. The weight penalties then assigned to power conditioning were 5 lb/KW for D.C. power input in the thermionic power plant when converting to either A.C. or low voltage D.C. and 2 lb/KW for the frequency changer in the turboelectric power plant.

4. Power Factor

Another source of weight increase associated with the A.C. pumps is the effect of low power factor. The additional current capacity required to supply the reactive KVA or KVAR in satisfying a low power factor load results in additional weight for all items handling the A.C. current. An estimated weight penalty of 1 lb./KVAR was assigned to this item.

5. Miscellaneous

In addition to the major weight items of power supply and EM pump cooling several other contributions to pumping system weights must be recognized. Two items not previously discussed were separate or extra shielding for the power conditioning equipment and the weight of cabling.

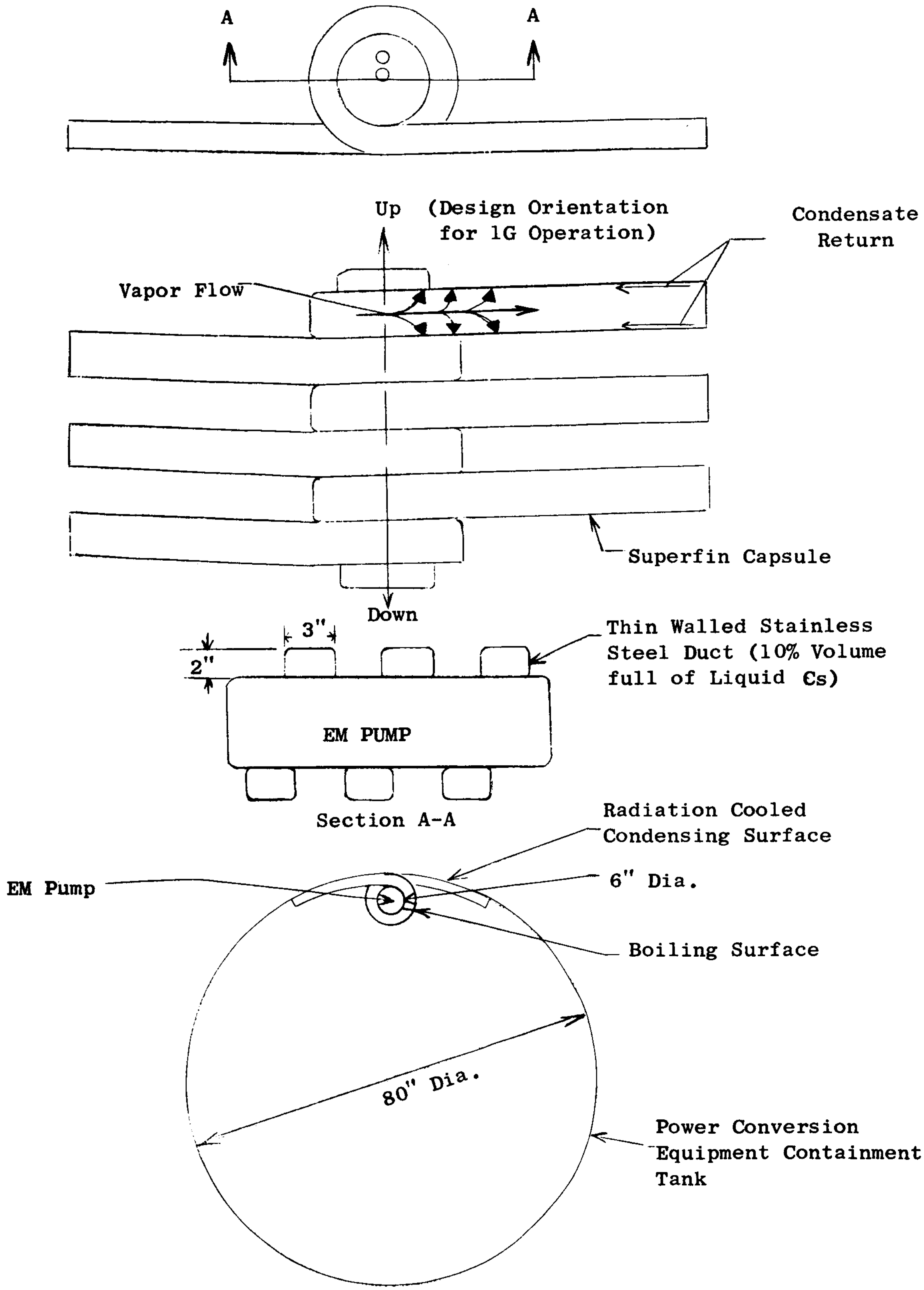

Figure E-1 Superfin Cooling Concept

This latter item is assumed negligible at this point of the study and would only become significant in a case where low voltage power were required in a situation that precluded short conductor lengths from P.C. equipment to pump. Likewise, the weight of extra shielding is being ignored at this time primarily because such power system design work is beyond the scope of this program.

6. Weight Penalty Summary

In order to facilitate the estimation of pumping system weights, a tabulation of all weight penalty items identified to date was prepared. The information is presented in Table III-7. As other items are identified, they will be added to the list.

TABLE III-7

EM PUMPING SYSTEM WEIGHTS

Item		Weight Penalty Thermionic System	Weight Penalty Turboelectric System
System Electric Power - lb/KW used (from main bus bar)		9	10
Power Conditioning - lb/KW output		5	2 (Freq. change only)
Pump Cooling - lb/KW Heat Rejected	-600°	4	4
	-1200°	2	2
Power Factor - lb/KVAR		1	1
Power Conditioning Shielding		Neglect	Neglect
Power Cable Weight		Neglect	Neglect

F. Reliability Considerations

1. Introduction

The strongest virtue of the EM pump for alkali metals systems is an inherently high reliability. Simplicity contributes most in providing the high reliability. Other factors are: few parts or components, no moving parts and no bearings or seals. However, EM pumps of certain types have failed in service in the past. These failures serve to point up certain reliability problems that must be considered in pump selection and design.

2. Relative Reliability

In the initial selection of EM pump types, reliability comparison has served as a guide. Here the number of failure mechanisms and the severity of failure have been the key considerations. A review of these considerations is given below:

a) Loss of pump cooling would adversely affect any of the pumps by increasing coil resistivities and reducing magnetic material performance. However, the polyphase configurations would be most susceptible because of greater complexity of coils and electrical insulation systems and because of their closer location to the hot duct.

b) Interruption of flow in the duct is most damaging to the conduction type of pump because of the high I^2R heat concentrated at the duct-to-bus connection. This type of failure is common in conduction pumps and usually results in duct leakage at the electrode connection.

c) Pressure fluctuations on the fluid side of the duct can fatigue the duct. The duct configuration most susceptible is that of the flat induction pump where the mechanical arrangement is inherently poorly suited to good duct wall stability. Very large conduction pumps with flat ducts must also fall into this problem. It should also be recognized here that the types of pumps which operate on single phase power generate considerably greater pulsation in their developed head than do any of the other types of pumps.

d) Overpressure inside the duct is not a serious threat to any but the moving magnet pumps since the ducts can readily be designed to accept, within allowable deformation limits, the same pressure as other components in the loop. However, the moving magnet pump duct is more difficult to support and, if deformed, will probably interfere with the rotor, thus causing pump failure.

e) Overtemperature in the pumped fluid, probably applicable only to the primary coolant, would reduce the performance and life of all types of pumps. However, the conduction pump would be most immediately affected and failure would most likely involve loss of main system fluid.

f) Mechanical damage causing misalignment of the rotor would be most likely to occur in the moving magnet pump due to the weight and complexity of the rotating magnetic structures. Since good pump performance demands a close clearance between the rotor and duct wall it is probable that duct damage and leakage would ensue.

g) Bearing lubricant or seal failure is applicable only to the moving magnet pumps and the failure mechanism is obvious here.

From the above it would appear that the single phase pump has, potentially, good reliability; however, it must be recognized that single phase pumps are relatively unknown. No operating experience is available to guide the reliability analyses. Nevertheless, the single phase pump does look promising from a reliability standpoint.

In addition to providing a guide for selection the foregoing analysis also points up those areas of weakness where design and development can mitigate or even eliminate the weakness. For example the development of an insulation system allowing the polyphase pump windings to reject heat to the 1200°F duct fluid would substantially improve reliability.

Further development of this analysis is now underway and will be guided toward selection and analysis of other failure mechanisms, identification of those pump types which offer best resistance to the various failure mechanisms and suggestions for design and development work to improve the problem areas.

G. Pump Selection and Design

1. Introduction

Selection of the optimum pump type for each application and the design of the specific pump to be applied will be based on the foregoing considerations presented in Sections A through F. Of particular importance are the power supply, the weight penalties and other power plant integration input and reliability ratings. The pump to be selected must necessarily be viewed as the principle component in a pumping system which in turn is a part of the overall power plant.

2. Pump Weight Improvement

Several preliminary pump designs have been presented in Quarterly Progress Report No. 2 and in the following pages of this report. The design information included estimated weights as well as pumping capability and efficiency. A logical next step, and a highly interesting one, was to compare the weights and efficiencies of the new designs with that of existing EM pumps. A number of pumps were found for which sufficient data were available for such a comparison. However, a basis for comparison of the many different pumps was needed.

It had been observed that in EM pumps designed on a consistent basis a fairly constant correlation exists between the weight of the various pumps and a parameter given by the product of flow, developed pressure and fluid electrical resistivity. This parameter has been designated the pump capability parameter. The degree to which correlation can be obtained with this parameter among pumps of widely varying capacities is illustrated in Figure G-1.

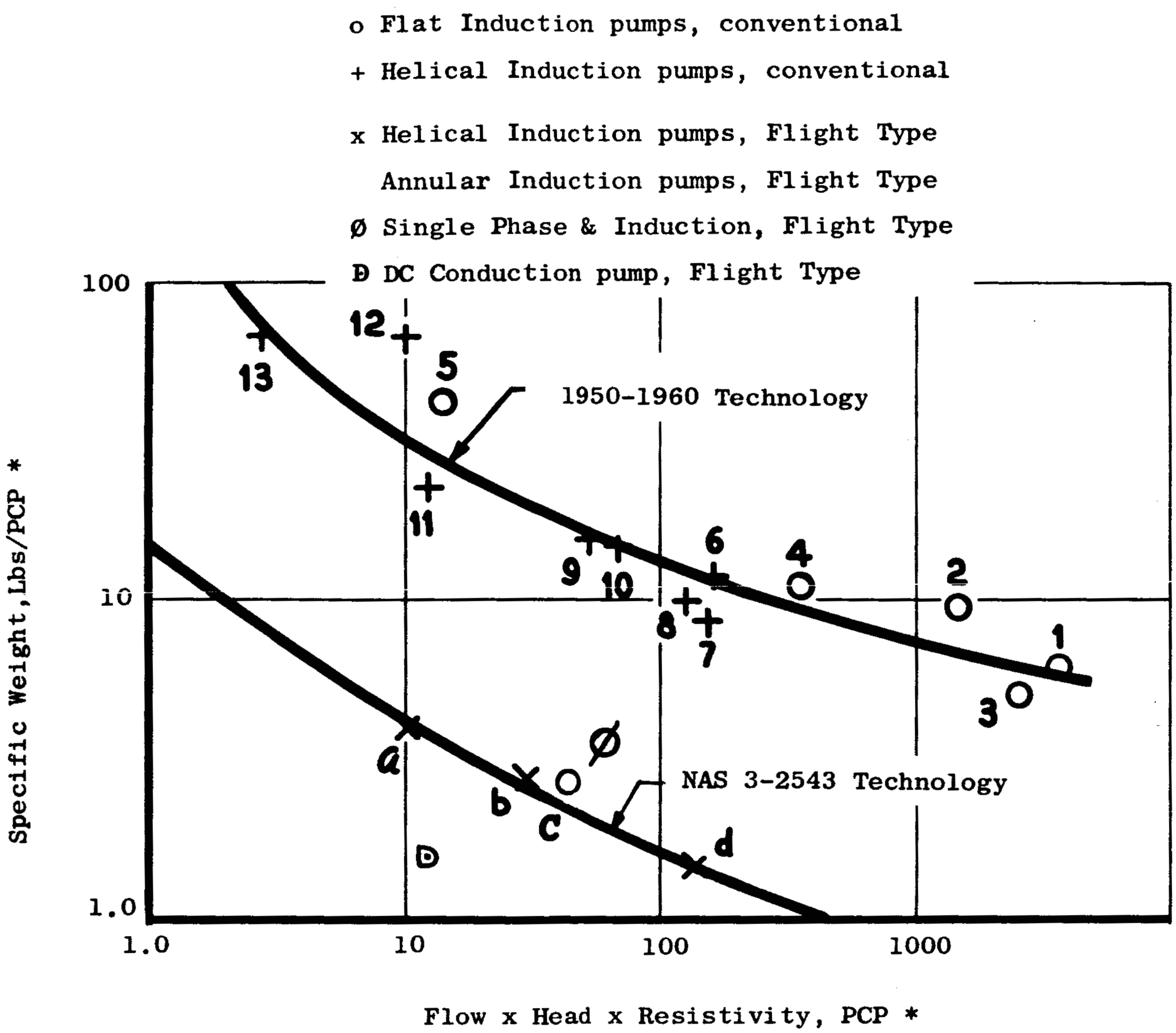

*PCP - Pump Capability Parameter = $\left(\frac{\text{gpm x PSI x MICRO-OHM-INCHES}}{1000}\right)$

Figure G-1 EM Pump Weight Improvement

In Figure G-1 the ratio of pump weight to this capability parameter is plotted against the capability parameter for a dozen induction pumps designed during the past 10 years and for six designs developed during the course of this study. The circles (o) represent flat induction pumps, and the crosses (+) represent helical induction pumps of prior construction. The x's (x), the square (□), the ∅ and the D, respectively, represent helical induction, annular induction, single phase induction and D.C. conduction pump designs developed during this study. The specific pump ratings shown on the chart are indicated in Table III-8. Many of the pumps in the group numbered 1 through 13 have operated tens of thousands of hours. These pumps have demonstrated outstanding reliability and have required no maintenance.

The observed correlation may be rationalized in the following manner. Assume a particular induction pumping configuration with a magnetic field of fixed peak amplitude moving at a fixed synchronous velocity. Now when various inducting fluids pass through the pump duct at a fixed velocity less than the velocity of the moving magnetic field, each fluid experiences a pressure rise inversely proportional to its electrical resistivity. Accordingly, since the flow is the same for all fluids for the assumed conditions, the product of flow, pressure, and electrical resistivity is constant for all the fluids. Thus, it may be said that the assumed pumping configuration has a capability related to the product of these three qualities: pressure, flow and

TABLE III-8

PUMP IDENTIFICATION, EM PUMP WEIGHT IMPROVEMENT CHART

Ident. No.	Weight lb.	Flow gpm	Head psi	.... Fluid .... Temp. °F	Resistivity -ohm-in.	Capability Parameter gpm-psi- ohm-in x 10^{-3}	Eff. %	Pump Type	Location or Application
Existing Pumps									
1.	18,500	6500	53	700 Na	8.5	2930	44	Flat Linear	EBR-2 Secondary Loop
2.	14,000	5000	40	700 Na	8.5	1700	40	Flat Linear	Argonne Nat'l Lab.
3.	11,400	3300	85	600 Na	7.1	1990	43	Flat Linear	U.S.S. Seawolf
4.	6,430	1200	40	700 Na	8.5	408	33	Flat Linear	KAPL Test Pump
5.	800	60	30	700 Na	8.5	15.3	15	Flat Linear	KAPL Service/EBR-2 Service
6.	2,250	500	40	900 Na	10.6	212	17	Helical Induction	LASL - in manufacture
7.	1,500	42	150	1600 K	35.0	220	10	Helical Induction	SPPS - Turbine Loop
8.	1,500	200	20	1850 K	37.5	150	6	Helical Induction	SPPS - 300KW Loop
9.	1,100	20	67	1850 K	37.5	50.1	5	Helical Induction	SPPS - 300KW Loop - maximum output rating
10.	1,000	50	50	1400 K	29.0	72.5	11	Helical Induction	AiResearch Corp.
11.	300	4	120	1400 K	29.0	13.9	3.5	Helical Induction	AiResearch Corp.
12.	570	3	75	2200 K	45.0	10.1	1	Helical Induction	SPPS - 100KW - Maximum output rating
13.	250	4	80	500 K	10.2	3.3	4	Helical Induction	SPPS - Bearing, Seal Service
Study Pumps									
a.	35	15.5	30	1200 K	23.5	10.9	12	Helical Induction	Turboelectric Condensate Boost Pump
b.	105	15.5	100	1200 K	23.5	36.5	14	Helical Induction	Turboelectric Boiler Feed Pump
c.	85	120	20	1200 Li	15.4	37.3	15	Annular Induction	Thermionic Radiator Coolant Pump
d.	310	80	100	1200 K	23.5	188	19	Helical Induction	Turboelectric Boiler Feed Pump
D.	18	15.7	30	1200 K	23.5	11.1	18	D.C. Conduction	Turboelectric Condensate Boost Pump
Ø	250	643	6	1700 Li	17.7	68.3	11	Single Phase Ind.	Thermionic Primary Coolant

electrical resistivity. The weight of the pump, therefore, is also a function of this same parameter.

$$W_t = f_1 (P\,Q/\rho) \text{ or}$$

$$W_t\,P\,G = f_2 (P\,Q/\rho)$$

Where:
W_t = Weight of Pump
P = Rated Developed Pressure
Q = Rated Flow
ρ = Fluid Resistivity
f_1, f_2 = function of

This neglects such significant variables as fluid temperature, density, viscosity, etc. Hence it should be used with care, particularly in comparing pumps for fluids with widely differing characteristics, or where the hydraulic requirements are highly dissimilar or where the pump design objectives and applications are substantially different. The order of magnitude difference between the two groups of pumps represented by the two curves of Figure G-1 illustrate this last point. A substantial difference exists between the two groups with regard to both design objectives and pump application.

The 10:1 weight reduction has been brought about by the virtual elimination of the pump frame, by the use of higher current and flux densities in the active portions of the pumps and by the use of a high temperature magnetic material providing a magnetic flux path in the duct bores.

The configuration chosen for designs for space application are cylindrical in form, permitting optimum utilization of material from a pressure containment viewpoint, thereby making it feasible to minimize the inactive materials used for structural purposes. The potential of this approach to weight minimization is illustrated by the EM pumps used in the Submarine U.S.S. Seawolf in which only 22% of the pump weight was active magnetic or conducting material.

Current densities in the designs proposed for space applications are approximately 4000-5000 amperes per square inch as compared to 2500-3500 amperes per square inch in earlier designs. Flux densities in EM pumps are usually low because of the large air gaps, particularly in high temperature helical induction pumps of the type installed in heat transfer loops at the Space Power and Propulsion Section. In the designs proposed for space applications, flux densities of about 90,000 lines per square inch are used in the magnetic material as compared with flux densities in the order of 40,000 lines per square inch in earlier pumps.

The use of a magnetic core in the stator bore, as compared to the nonmagnetic core construction used in the helical pumps presently in service at the Space Power and Propulsion Section, permits substantial reductions in stator conducting and magnetic material.

3. D.C. Conduction Pump Design

As a first trial of the D.C. pump design and performance prediction methods a D.C. conduction pump was designed for the turboelectric condensate boost application. A helical induction pump has already been designed for this application, thus permitting direct comparison.

The pump is illustrated in Figures G-2 and G-3. The comparison to the induction pump is shown in the next section under "Pumping System Weights". A detailed description of the D.C. conduction condensate boost pump follows:

Liquid pumped potassium at 1200°F.

Heat at entrance to pump - 10 ft., 2.98 psi.

Head rise developed by pump - 100 ft., 29.8 psi.

Flow - 1.5 lb.sec., 0.03495 cu. ft./sec., 15.70 gal./min.

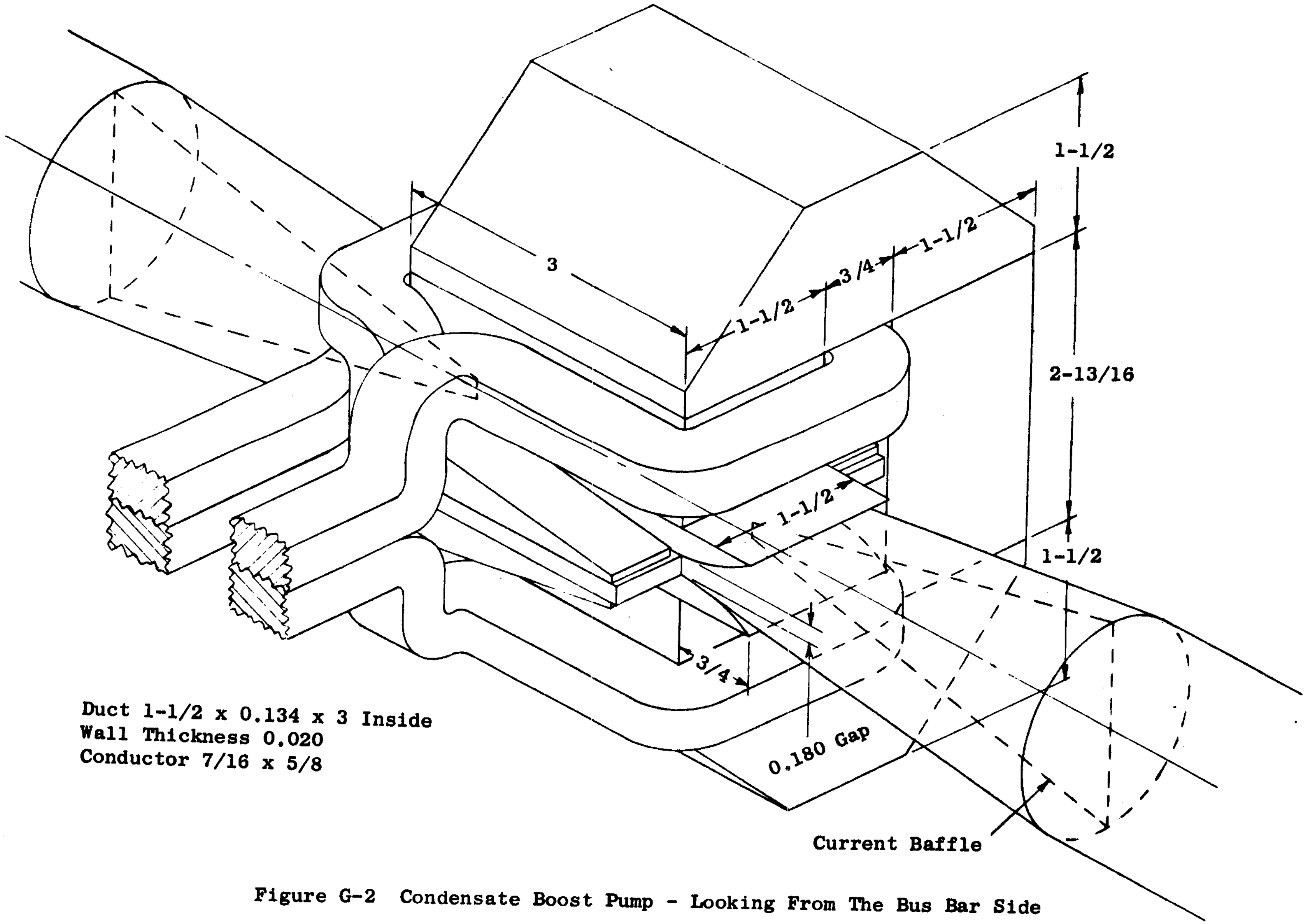

Figure G-2 Condensate Boost Pump - Looking From The Bus Bar Side

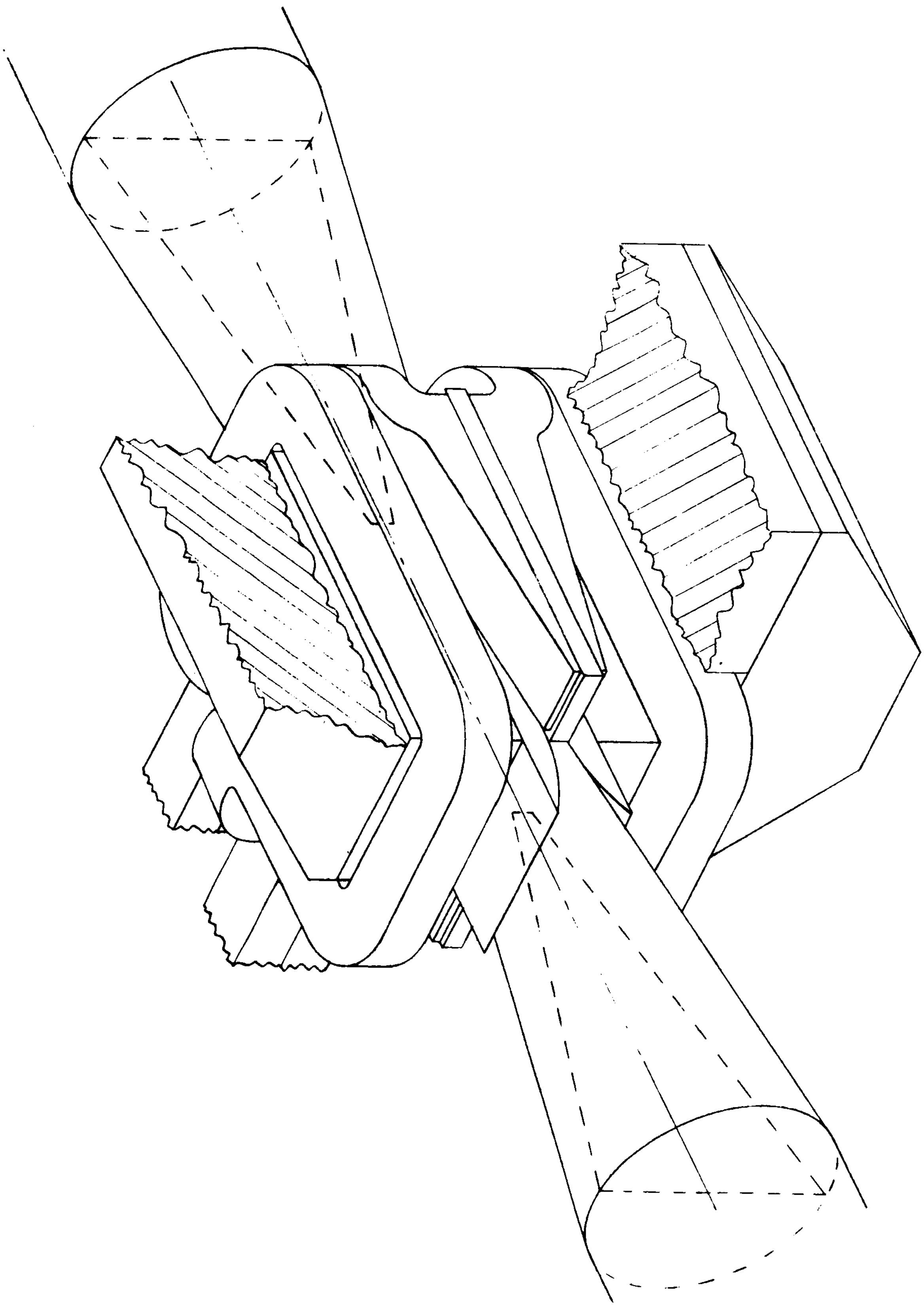

Figure G-3 Condensate Boost Pump - Looking From The Magnet Side

Characteristics of Principal Materials at 1200°F are as follows:

Potassium Density = 42.94 lb/cu ft = 0.0248 lb/cu in.

Potassium Viscosity = 0.350 lb/ft.-hr

Potassium Resistivity = 23.6×10^{-6} ohm-in.

Copper Resistivity at 1200°F = 2.37×10^{-6} ohm-in.

Copper Density = 0.32 lb/cu. in.

Iron Density in magnetic circuit = 0.28 lb/cu. in.

Stainless Steel Density in duct = 0.29 lb/cu. in.

Stainless Steel Resistivity in duct = 43×10^{-6} ohm-in.

The attached sketches show the proposed arrangement of duct, magnetic circuit, and electrical conductors, with some of the major dimensions. The pumping duct and diffusers are of nonmagnetic stainless steel, 0.020 in. thick. The duct is 3 in. long, 1.5 in. wide and 0.134 in. high inside. The diffusers are each 4 in. long, joining the rectangular duct to a circular cross section 2 in. in diameter inside. One fringe current baffle, or splitter, is located in each diffuser.

The magnet gap is 0.180 in. high to allow a small clearance for the duct with thin sheets of insulation on the outside, 1.5 in. wide, and uniform over a distance of 3 in. with 3/4 in. extensions on the pole pieces to provide a tapered fringing field at each end of the duct. The magnetic circuit has a cross section of 1.5 in. by 3.0 in. throughout, and encloses a window just large enough to contain the copper conductors with a small clearance.

The electrodes are copper plates welded or brazed to the edges of the duct. The electrodes are 3 in. long, 0.134 in. thick and 0.687 in. wide.

The current circuit is divided into two parallel circuits, one encircling each pole, to apply the magnetomotive force to the gap as symmetrically as possible. The copper conductors are of rectangular cross section, 5/8 in. wide by 7/16 in. high. The conductors completely encircle the poles once and are connected to the electrodes so that the electrode current effectively gives an additional half-turn.

The calculated characteristics for this DC conduction pump are:

Liquid pumped - Potassium at 1200°F.

Inlet pressure - 2.98 psi. (10 ft. head)

Velocity head at entrance to duct - 2.89 psi (9.7 ft. head)

Net pressure rise - 29.8 psi (100 ft. head)

Flow - 15.70 gpm

Current - 2270 amp.

Terminal voltage - 0.492 volts

Input power - 1120 watts.

Output hydraulic power - 203 watts.

Efficiency - 18.1%

Total weight - 18.2 lb., consisting of

Iron weight - 13.9 lb.

Copper weight - 4.0 lb.

Duct and diffuser weight - 0.3 lb.

Conductor and electrode power loss - 333 watts

Duct liquid electrical power loss - 92 watts

Fringe current power loss - 191 watts

Duct wall current power loss - 268 watts

Hydraulic power loss in duct and diffusers - 16 watts

Additional electrical power loss in duct due to the distortion of duct current by liquid flow - 17 watts.

Total power loss - 917 watts

Flux density across duct

at entering end	-	73.7 k./sq. in.
at center	-	55.3 kl/sq. in.
at exit end	-	36.9 kl/sq. in.

(neglecting distortion effects caused by liquid flow)

Flux density in magnetic circuit (approx.) - 90 kl/sq. in.

Current density in conductors - 4150 amp./sq. in.

Current density in electrodes at duct wall - 5650 amp./sq. in.

Current density in duct liquid between electrodes - 2350 amp./sq. in.

Duct current - 946 amp.

Fringe current - 550 amp.

Duct wall current - 774 amp.

4. Single Phase Induction Pump Design

The most promising pump type for the primary coolant application is the single phase induction pump illustrated in Figure G-4. The design is intended to meet the design point requirements of the thermionic power plant primary coolant pump:

Fluid - 1700°F lithium

Flow - 40 lb/sec

Inlet Pressure - 10 psia

Pressure Rise - 6 psi

Efficiency (Est) - 11%

Weight (Est) - 250 lb.

The primary advantage of this configuration is the simplicity of the coil. In the design shown the coil is made of tubing through which a coolant is passed. The coil is so located that it is easily isolated, thermally, from the hot duct. The magnetic structure and duct are relatively complicated but readily manufacturable. No mechanical support structure or containment envelope is shown on this design. The magnetic structure and duct are adequate for support. However, some additional cooling may be required for the laminated core and stator punchings. The design shown is presently being analyzed to determine performance characteristics.

5. Boiler Feed Pump

Although not specifically named in the work statement a boiler feed pump application looks very promising for the Rankine cycle turbo-electric system. This installation would be the prime-mover for the

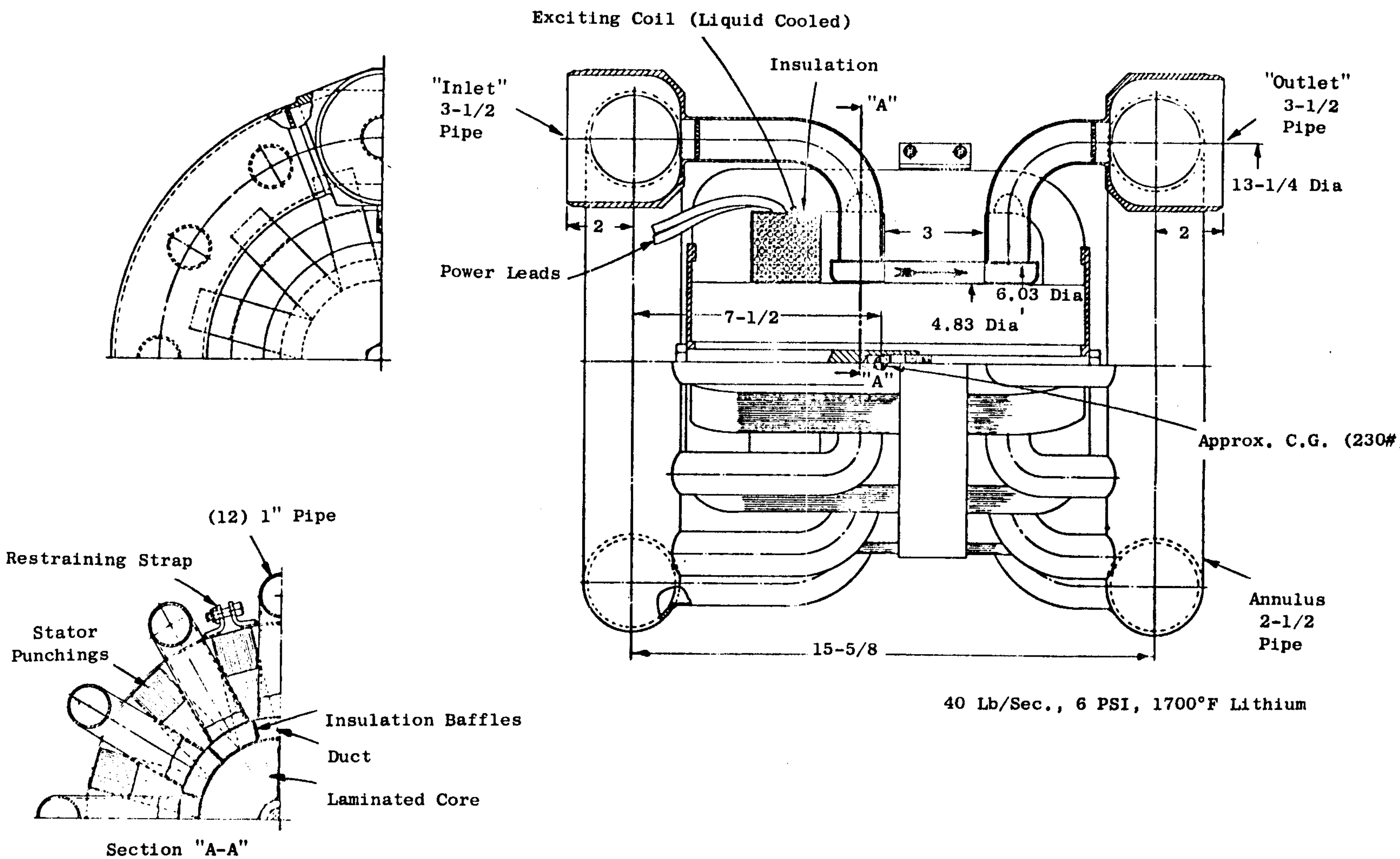

Figure G-4 Single Phase Induction Pump Primary Coolant, Thermionic System condensate to the boiler and would replace the earlier concept of a canned rotor pump and EM pump booster combination.

In analyzing the boost pump described above it became evident a helical induction EM pump could readily perform the complete task of feeding condensate to the boiler. A supplementary boost pump would be precluded and the highly reliable induction EM pump would be applied to the entire pumping job if it possesses adequate cavitation characteristics.

The pump requirements were derived from the flow specified for the boost application plus the boiler pressure demands of a typical turbogenerator power plant. Consequently, the design selected was 15.5 gpm at 100 psi developed head. The resultant design is illustrated in Figure G-5. The diameter is 6.5 inches; the length, 21 inches; the total weight, 105 pounds. Again, 3 phase 60 cycle power is employed. The pump, a two pole machine, uses 5 kw of power at 50% power factor with a 50% slip. Overall efficiency is approximately 12%. Comparing this pump to a canned motor pump with jet suction boost for a similar application, the EM pump is attractive. Below is the comparison based on information out of the AEC-SNAP 50 Office:

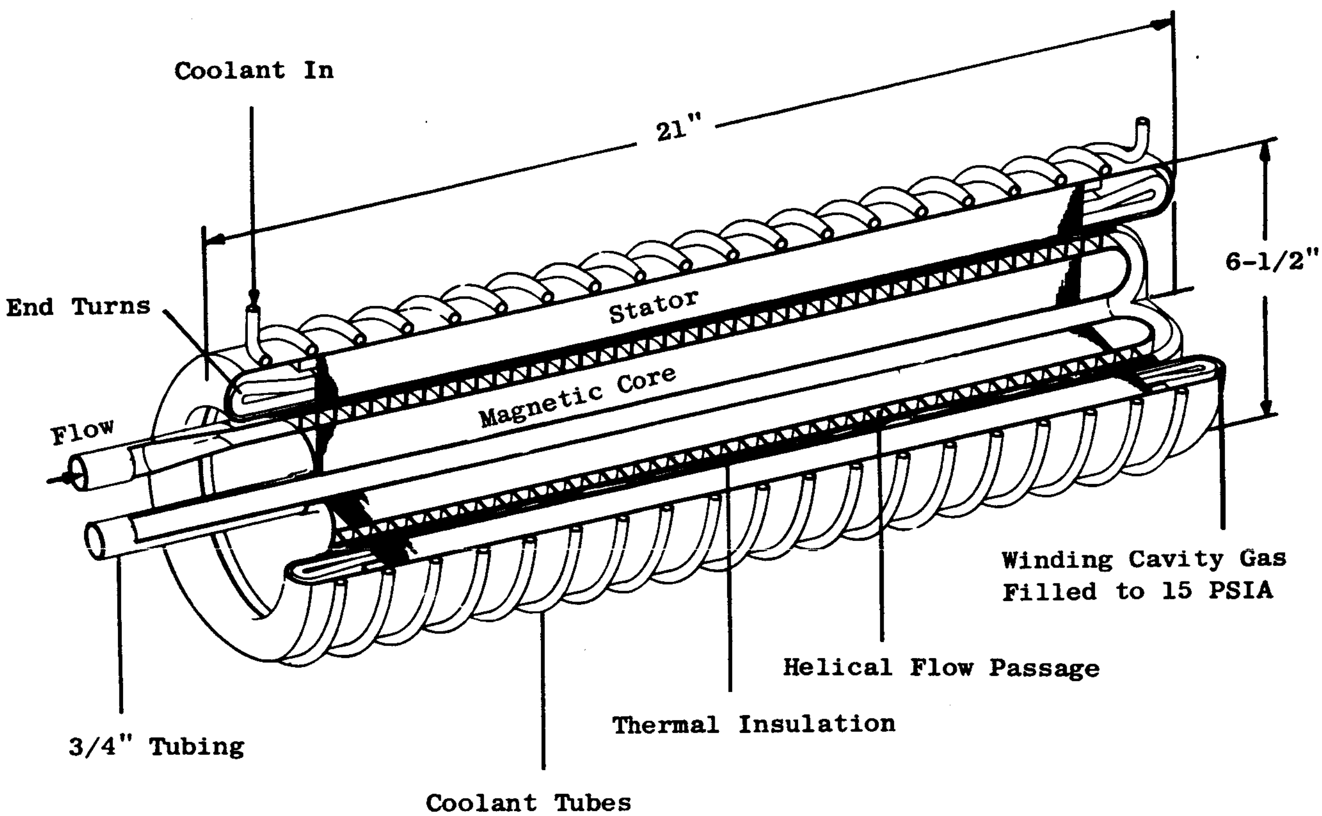

1200°F Potassium
15.5 GPM
100 PSI Dev. Head
2 Pole, 3 Phase, 60 CPS
5 KW, 0.5 PF
Est. Wt. = 105 Lbs.

Figure G-5 Helical Induction Boiler Feed Pump Turboelectric System

	EM Pump Boiler Feed	Canned Motor W/Jet Boost: SNAP-50 Size	Canned Motor W/Jet Boost: Scaled To EM Pump Size
Flow	1.5 pps	2 pps	1.5 pps
Head	100 psi	100 psi	100 psi
Weight (excl. penalties)	105 lb.	150 lb.	112 lb.
Power	10KVA, 60 ~	9KVA, 400 ~	7KVA, 400 ~
Efficiency	12%	17%	17%
Reliability	Good	Fair	Fair

Those materials selected for the two designs shown in Quarterly Progress Report No. 2 are also used here. Generally, the arrangement and configuration approximate those of the boost pump. The inlet nozzle design, however, has been improved hydraulically. The flow exit from the helical section is cleaner, the end turns have been shortened, and concurrently, the stator cavity has been reduced. To provide a secondary barrier against leakage, the thermal insulation is completely canned.

6. Pumping System Weights

Taking the information accumulated in past reports as well as this one, a preliminary tabulation of all the pump designs presented to date and the corresponding pumping system weights are given below.

a) Condensate Boost Application

Pump Characteristics	Hel. Ind.	D-C Cond.
Flow - pps	1.5	1.5
Head - psi	30	30
Power - KW	1.6	1.1
Weight - lb.	35	18
Efficiency - %	13	18
Slip - %	50	-
Power Factor - %	50	-
KVAR	2.8	-

Pumping System Wt. - lb.	Hel. Ind.	D-C Cond.
No. Pumps	4	4
Pump Wt.	140	72
Power Penalty	75	55
P.C. Wt.	13	22
Cooling Wt.:		
600F	13	
1200F		6
Power Fac. Penalty	11	
Total	252	155

b) NaK Radiator Application

Pump Characteristics	Ann. Ind.
Flow - pps	6
Head - psi	25
Power - KW	6.4
Weight - lb.	85
Efficiency - %	11
Slip - %	50
Power Factor - %	51
KVAR	10.8

Pumping System Wt. - lb.	Ann. Ind.
No. Pumps	16
Pump Wt.	1360
Pwr. Penalty	1210
P.C. Wt.	205
Cooling Wt.:	
600F	205
Pwr. Fac. Penalty	172
Total	3152

c) Li Radiator Applications

Pump Characteristics	Ann. Ind.	Ann. Ind.	Hel. Ind.
Flow - pps	8	2	2
Head - psi	20	20	20
Power - KW	6	2.2	2.2
Weight - lb.	85	40	48
Efficiency - %	15	12	12
Slip - %	50		40
Pwr. Fac. - %	53	51	70
KVAR	9.7	3.7	2.3

Pumping System Wt. - lb.	Ann. Ind.	Ann. Ind.	Hel. Ind
No. Pumps	4	16	16
Pump Wt.	340	640	768
Pwr. Penalty	282	412	412
P.C. Wt.	48	70	70
Cooling Wt.:			
600F	48	70	70
Pwr. Fac. Penalty	39	59	37
Total	757	1251	1357

d) Primary Coolant Application

Pump Characteristics	Single Phase
Flow - pps	40
Head - psi	6
Power - KW	21
Weight - lb.	250
Efficiency - %	11
Pwr. Fac - %	50 (assumed)
KVAR	36

Pumping System Wt. - lb.	Single Phase
No. Pumps	1
Pump Wt.	250
Pwr. Penalty	247
P.C. Wt.	42
Cooling Wt.	
1200F	21
Pwr. Fac. Penalty	36
Total	596

e) Boiler Feed Pump

Pump Characteristics

	Hel. Ind.
Flow - pps	15
Head - psi	100
Power - KW	5
Weight - lb.	105
Efficiency - %	12
Slip - %	50
Pwr. Fac. - %	50
KVAR	8.7

Pumping System Wt. - lb.

	Hel. Ind.
No. Pumps	4
Pump Wt.	420
Pwr. Penalty	236
P.C. Wt.	40
Cooling Wt. 600F	40
Pwr. Fac. Penalty	35
Total	771

H. Test Program

1. Introduction

Included in the Phase I work scope is the planning of Phase II which will be concerned with manufacture and testing of the pump types selected in this phase of the program.

In Quarterly Progress Report No. 2 an outline of a test program was presented along with a schematic and description of a test facility. Some additional work has been done during the past quarter, primarily to keep pace with the results of pump design work.

2. Phase II Schedule

As a first estimate a program involving one pumping application was scheduled as shown in Figure H-1 . It was assumed that two pumps approximately spanning the required test range of Table II-1 would suffice. The elapsed time was about 18 months. No endurance testing was included. To include it would require some additional test equipment to avoid tying up the main facility.

As additional pumps are included in the program the testing time will increase in direct proportion since more than one facility does not seem warranted. The other elements of the program would be covered by increased man hours and appropriate overlapping and sequencing so as not to add to the overall elapsed time for the program.

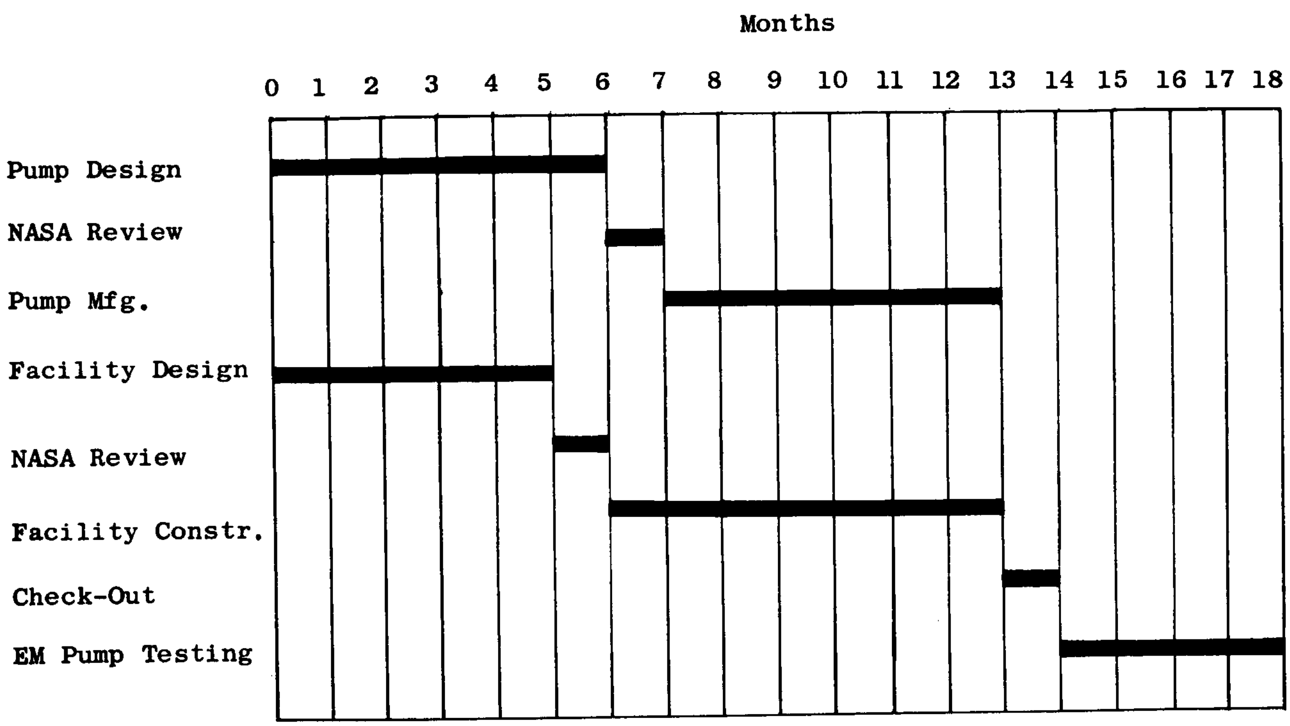

Figure H-1 EM Pump Program Phase II Schedule

IV. PROGRAM PLANS

A. Organization

During the past quarter two project meetings were held to review the progress to date in the various project functions. Plans were made to channel all effort towards final selection and analysis of pumps to be recommended for continued development. It will be necessary to summarize the selection process. A basis for comparison of pumps for each application is needed. Specific materials must be selected from all the data accumulated.

The moving magnet pump requires some additional study. It seems unlikely at this point that a preliminary design will be warranted, but some allowance will be made in the schedule for this eventuality.

B. Schedule

A contractual change has been consummated whereby the end date of Phase I was extended from June 27, 1964 to August 3, 1964. No additional work was involved. This allowed a shift of 5 weeks in the Final Report activity since it is to be complete within 30 days of the terminal date.

In addition the schedule has some minor changes in the activities of "Selection and Study" and "Preliminary Designs" to allow for additional work to be done on the moving magnet pump as described above. The "Test Program Layout" has been shifted since little additional work can be done until the "Second Selection" is further along. The revised schedule is shown in Figure J-1. The X portion of the bar for each element of the schedule indicates degree of completion of that activity. The slant line portion of the bar indicates the unfinished portion of the schedule. The dashed line portion indicates the changes since the last issue. To gain an estimate of the overall degree of progress vs. schedule, the total length of all bars is 53 months, the total length of all X portions is 33 months giving 63% completion. Nine of the 13 months have passed or 69% of the allotted time. Thus the program is approximately on schedule, even though certain activities may be lagging.

C. Projection

During the coming month the single phase pump design shown above will be analyzed and a number of design calculations for the thermionic primary coolant application will be made in order to approach the optimum.

A tabular form for summarizing the pump selection process will be made. In the materials area review of the accumulated data for final selection of pump materials will begin.

During the quarter which ends June 27, 1964 a d-c conduction pump design will be made for each of the six applications. Helical induction designs will

Revised 3/27/64

FIGURE J-1

SCHEDULE

EM PUMP PROGRAM

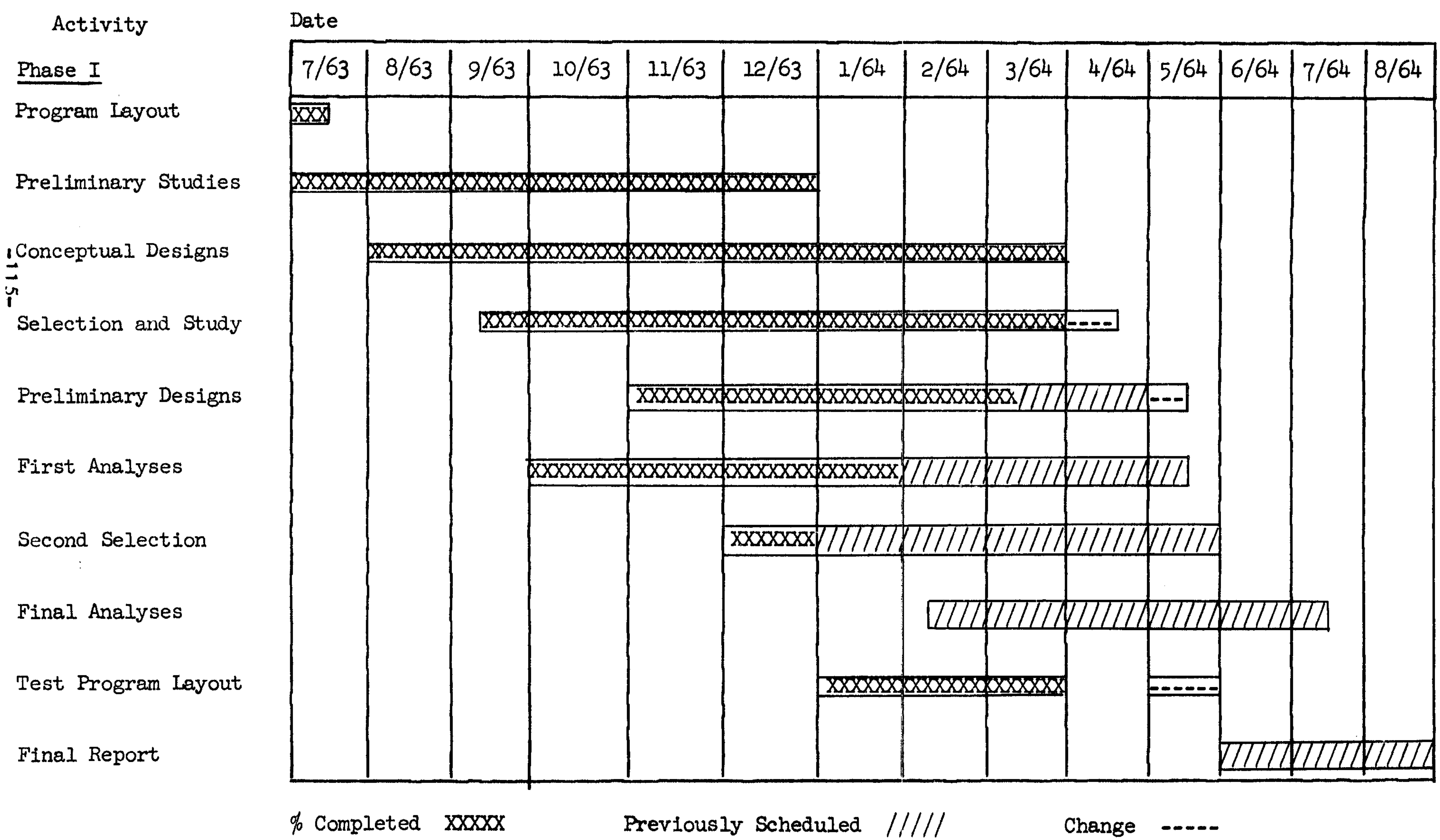

be made for all but the primary coolant application and annular induction designs will be made for the radiator coolant applications.

The selection chart mentioned above will be completed. Final materials selection will be made and the final pump selections will be made. Final analysis and performance predictions for the selections will begin.

V. BIBLIOGRAPHY

(1) Die Thermoelektromagnetische Pumps, Von S. Hufnagel, Aus dem Institut fur Thermodynamik der Technischen Hochschule Munchen (Translation).

(2) A Toroidal Thermoelectric - Magnetic Liquid Metal Pump for Space Application, D.C. Miley, July 1959, General Electric Company No. R59-FPD-624.

(3) Heat Transmission, W. H. McAdams, McGraw Hill Book Company, New York.

(4) Mechanical Engineering Handbook, L. S. Marks, McGraw Hill Book Company, New York.

(5) Magnetohydrodynamics, T. G. Cowling, Interscience Publishers, New York.

(6) Boundary Layer Theory, H. Schlichting, McGraw Hill Book Company, New York.

(7) Hydrodynamics, H. Lamb, Cambridge University Press, London.

(8) Permanent Magnets and Their Application, Parker and Studders, John Wiley and Sons, Inc.

(9) Electro-Magnetic Devices, Roters, John Wiley and Sons, Inc.

(10) Conduction and Induction Pumps for Liquid Metals, L. R. Blake, Proceedings IEE, Vol. 104, Part A, 1957.

(11) The Design of Electromagnetic Pumps for Liquid Metals, D. A. Watt, Proceedings IEE, Vol. 106, Part A, 1959.

(12) The D-C Electromagnetic Pump for Liquid Metals, J. Woodrow, A.E.R.E., E/R 452.

(13) Direct Current Electromagnetic Pumps, A. H. Barnes, Nucleonics, January 1953.

(14) A Single Phase Annular Induction Pump for Liquid Metals, D. A. Watt, AERE CE/R 1090, January 1953.

(15) A Single Phase Annular Induction Pump for Liquid Metals, D. A. Watt, AERE ED/R 1844, Harwell, Berks, January 1956.

(16) Bozorth, R. M., "Ferromagnetism", 1951, New York, D. Van Nostrand.

(17) Becker, J. J., "Recent Development in Magnetic Metals and Alloys," Metallurgical Rev. 1962, 7, 28 (371).

(18) Metals Handbook, Vol. 1, 1961, ASM.

(19) Goldberg, M. E. and Hamre, H. G., "Electronic Component Parts Research for 500°C Operation", WADC TR-57-362, Feb., 1958.

(20) Pasnak, M. and Lundsten, R. H., "Effects of Extremely High Temperature on Magnetic Properties of Core Material," NAVORD Report 6132, 10 July, 1958.

(21) Pavlik, N., "High Temperature Stability of Magnetic Materials", J. App. Phys., Suppl. Vol. 32 No. 3, March 1961.

(22) Chen, G. W., "Temperature Dependence of Magnetic Properties of Silicon Iron", J. App. Phys, Vol. 29, No. 9, p. 1337, 1958.

(23) Harms, H. B. and Fraser, J. C., "Ultra High Temperature (500°C) Transformers and Inductors", WADC TR 59-348, July, 1959.

(24) "Hiperco Soft Magnetic Alloy for High Flux Levels", Tech. Data Bulletin 52-163, p. 1-4, Westinghouse Elec. Co., March, 1963.

(25) Greene, C. K., Lee, R. E., Lietzov, K. E., "Evaluation of Magnetic Cores at Ultra High Temperatures", WADC TR 58-483, April, 1959.

(26) Harms, H. B. and Fraser, J.C., "Ultra High Temperature Miniaturized Power Transformers and Inductor Materials", WADC TR 57-492, V1 and V2, May, 1958.

(27) Clark, J. J. and Fritz, J. F., "The Effect of Temperature on the Magnetic Properties of Silicon Iron, Cobalt Iron and Aluminum Iron Alloys", WADC TR-59-240, July, 1959.

(28) "Hiperco Soft Magnetic Alloy for High Flux Levels", Hiperco 35, Tech. Data Bulletin 52-163, March 1962, p. 5-8, Westinghouse Elec. Co.

(29) Young, F. T. and Schenk, H. L., "Method for Measuring Iron Losses in Elliptically Polarized Magnetic Fields", J. App., Suppl. to Vol 31, No. 5, May, 1960.

(30) Kaplan, Asa, "Magnetic Core Losses Resulting from a Rotating Flux", J. App. Phys., Supp. Vol. 32, No. 3, March, 1961.

(31) Stratton, R. D. and Young, F. J. "Iron Losses in Elliptically Rotating Fields", J. App. Phys., Supp. to Vol. 33, No. 3.

(32) Graham, Jr., C. C., "Temperature Dependence of Anisotropy and Saturation Magnetism in Iron and Iron Silicon Alloys, J. App. Phys., Supp. to Vol. 30, No. 5.

(33) Sery, R. S., Fischell, R. E. and Gordon, D. I., "Effect of Nuclear Irradiation on Magnetic Properties of Core Materials", NAVORD 4381, December 19, 1956.

(34) Sery, R. S. and Gordon, D. I., "Nuclear Irradiation Effects on Ferromagnetic Core Materials", NAVORD 6127, June 3, 1958.

(35) Javitz, A. E. and Barkan, H. E., "Transformer Materials for Extreme Environments", Elec. Mfg., Conover-Mast Tech. Publg. Corp., 1960.

(36) Helms, Jr., H. H., "Adaptability of Iron-Silicon Magnetic Alloys for Special Environments", NAVWEPS Report 7331, October 26, 1960.

(37) Helms. Jr., H. H., "Review of Aluminum-Iron Magnetic Alloys and Associated Systems", NOL Technical Report 62-144, Oct. 23, 1962.

(38) Gordon, B. I., "Magnetic Cores and Permanent Magnets in Hyper-Environments", 1960 Proceedings of Institute of Environmental Silicon, Nat'l. Meeting April, 1960, Los Angeles, Cal. pp. 205-228.

(39) Schindler, A. I. and Salkovitz, E. I., Effect of Applying a Magnetic Field During Neutron Irradiation on Magnetic Properties of Fe-Ni Alloys, J. App. Phys., Supp. Vol. 31, No. 5, May, 1960.

(40) Lauriente, M. and Lyon, G. E., "Characteristics of Supermendur at 500°C,". J. App. Phys., p. 372S, Supp. to Vol. 32, No. 3, March, 1961.

(41) Talaat, M.E., "Direct Energy Conversion", Ind. Research, May 1964.

(42) SNAP 2 Quarterly Progress Reports, Atomic International, NAA-SR-8091, 8391, 8691, 8991. Confidential RD.

(43) Daring, J. E. and Crowe, A. W., " Electric Strength of Saturated Hydrocarbon Gases", J. Chem. Phys. Vol. 25, No. 5 (1956) p. 1053.

(44) Sharbaugh, A. H., Private Communication.

VI. DISTRIBUTION FOR QUARTERLY AND FINAL REPORTS FOR CONTRACT NAS 3-2543

National Aeronautics and Space Administration
Lewis Research Center
21000 Brookpark Road
Cleveland, Ohio 44135
Attention: Librarian (3-7) (2)

National Aeronautics and Space Administration
Lewis Research Center
21000 Brookpark Road
Cleveland, Ohio 44135
Attention: H.O. Slone (86-5)

National Aeronautics and Space Administration
Lewis Research Center
21000 Brookpark Road
Cleveland, Ohio 44135
Attention: Dr. B. Lubarsky (86-1)

National Aeronautics and Space Administration
Lewis Research Center
21000 Brookpark Road
Cleveland, Ohio 44135
Attention: R.T. Wainwright (86-5) (25)

National Aeronautics and Space Administration
Lewis Research Center
21000 Brookpark Road
Cleveland, Ohio 44135
Attention: J.E. Dilley (86-1)

National Aeronautics and Space Administration
Lewis Research Center
21000 Brookpark Road
Cleveland, Ohio 44135
Attention: Patent Counsel (77-1)

National Aeronautics and Space Administration
Lewis Research Center
21000 Brookpark Road
Cleveland, Ohio 44135
Attention: Office of Reliability and Quality Assurance (21-4)

National Aeronautics and Space Administration
Lewis Research Center
21000 Brookpark Road
Cleveland, Ohio 44135
Attention: M.J. Hartman (5-9)

National Aeronautics and Space Administration
Lewis Research Center
21000 Brookpark Road
Cleveland, Ohio 44135
Attention: C.H. Hauser (5-9)

National Aeronautics and Space Administration
Lewis Research Center
21000 Brookpark Road
Cleveland, Ohio 44135
Attention: D.C. Reemsnyder (5-9)

National Aeronautics and Space Administration
Lewis Research Center
21000 Brookpark Road
Cleveland, Ohio 44135
Attention: T.R. Mariani (0-5)

National Aeronautics and Space Administration
Lewis Research Center
21000 Brookpark Road
Cleveland, Ohio 44135
Attention: A. Vary (106-1)

National Aeronautics and Space Administration
Lewis Research Center
21000 Brookpark Road
Cleveland, Ohio 44135
Attention: C.S. Corcoran (100-1)

National Aeronautics and Space Administration
Lewis Research Center
21000 Brookpark Road
Cleveland, Ohio 44135
Attention: J.J. Ward (100-1)

National Aeronautics and Space Administration
Lewis Research Center
21000 Brookpark Road
Cleveland, Ohio 44135
Attention: R.F. Mather (86-5)

National Aeronautics and Space Administration
Lewis Research Center
21000 Brookpark Road
Cleveland, Ohio 44135
Attention: D.W. Bitler (100-1)

National Aeronautics and Space Administration
Lewis Research Center
21000 Brookpark Road
Cleveland, Ohio 44135
Attention: R.E. Schwirian (5-9)

National Aeronautics and Space Administration
Lewis Research Center
21000 Brookpark Road
Cleveland, Ohio 44135
Attention: G.M. Thur (86-5)

National Aeronautics and Space Administration
Washington, D.C. 20546
Attention: Dr. F. Schulman (RNP)

National Aeronautics and Space Administration
Washington, D.C. 20546
Attention: J.J. Lynch (RNP)

National Aeronautics and Space Administration
Langley Research Center
Langley Station
Hampton, Virginia 23365
Attention: Librarian

National Aeronautics and Space Administration
Ames Research Center
Moffett Field, California 94035
Attention: Librarian

National Aeronautics and Space Administration
Ames Research Center
Moffett Field, California 94035
Attention: V.J. Rossow

National Aeronautics and Space Administration
George C. Marshall Space Flight Center
Huntsville, Alabama 35812
Attention: Librarian

National Aeronautics and Space Administration
Goddard Space Flight Center
Greenbelt, Maryland 20771
Attention: Librarian

Jet Propulsion Laboratory
4800 Oak Grove Drive
Pasadena, California 91103
Attention: Librarian

National Aeronautics and Space Administration
Scientific and Technical Information Facility
Box 5700
Bethesda, Maryland 20014
Attention: NASA Representative (2 copies plus reproducible)

Argonne National Laboratory
P.O. Box 299
Lemont, Illinois 60439
Attention: Librarian

Brookhaven National Laboratory
Upton, Long Island, New York 11973
Attention: Dr. O.E. Dwyer

Brookhaven National Laboratory
Upton, Long Island, New York 11973
Attention: Librarian

Oak Ridge National Laboratory
Oak Ridge, Tennessee 37831
Attention: Librarian

Oak Ridge National Laboratory
Oak Ridge, Tennessee 37831
Attention: A.G. Grindell

U.S. Atomic Energy Commission
Division of Technical Information Extension
P.O. Box 62
Oak Ridge, Tennessee 37831 (2)

Air Force Systems Command
Aeronautical Systems Division
Wright-Patterson Air Force Base, Ohio 45433
Attention: Librarian, D. Warnock

Defense Documentation Center
Arlington Hall Station
Arlington, Virginia 22212 (2)

National Aeronautics and Space Administration
Western Operation Office
150 Pico Boulevard
Santa Monica, California 90406
Attention: Librarian

U.S. Atomic Energy Commission
New York Operations Office
376 Hudson Street
New York, New York 10014
Attention: Librarian

SNAP 50 SPUR Project Office
U.S. Atomic Energy Commission
Washington, D.C. 20545
Attention: H.D. Rochen
NASA-AEC Deputy

SNAP 50 SPUR Project Office
U.S. Atomic Energy Commission
Germantown, Maryland 20545
Attention: G. Leighton
NASA-AEC Deputy

U.S. Atomic Energy Commission
CANEL Project Office
P.O. Box 1102
Middletown, Connecticut 06458
Attention: C.E. McColley

Hydronautics, Incorporated
Pindell School Road, Howard County
Laurel, Maryland 20810
Attention: P. Eisenberg

University of Michigan
North Campus
Ann Arbor, Michigan 48103
Attention: Dr. F.G. Hammitt

General Electric Company
Valley Forge Space Technology Center
P.O. Box 8555
Philadelphia, Pennsylvania 19101
Attention: T.F. Widmer

The Martin Company
Nuclear Division
Advanced Programs Department
P.O. Box 5042
Baltimore, Maryland 21220
Attention: W.P. Haass

MSA Research Corporation
Callery, Pennsylvania 16024
Attention: R.C. Werner

Westinghouse Electric Corporation
Aerospace Electrical Division
Lima, Ohio 45801
Attention: J.D. Miner

Westinghouse Electric Corporation
Astronuclear Laboratory
P.O. Box 10864
Pittsburgh, Pennsylvania 15236
Attention: Librarian

Thompson Ramo Wooldridge
Rankine Cycle Power Systems
7209 Platt Avenue
Cleveland, Ohio 44104
Attention: J.A. Rudy

AiResearch Manufacturing Company
9851-9951 Sepulveda Boulevard
Los Angeles, California 90045
Attention: R.C. Byloff

Atomics International
8900 DeSoto Avenue
Canoga Park, California 91303
Attention: R.S. Baker

Atomics International
8900 Desoto Avenue
Canoga Park, California 91303
Attention: S. Sudar

Southwest Research Institute
8500 Culebra Road
San Antonio, Texas 78206
Attention: W.D. Weatherford, Jr.

Pratt and Whitney Aircraft
CANEL
P.O. Box 611
Middletown, Connecticut 06458
Attention: G.M. Wood

Pratt and Whitney Aircraft
CANEL
P.O. Box 611
Middletown, Connecticut 06458
Attention: J. Walton

Allis-Chalmers Manufacturing Company
Atomic Power Section
Milwaukee, Wisconsic 53201
Attention: E.F. Brill

General Atomic Division
John Jay Hopkins Laboratory
P.O. Box 608
San Diego, California 92112
Attention: Dr. R.W. Pidd

Radio Corporation of America
Electron Tube Division
Lancaster, Pennsylvania 17601
Attention: F.G. Block

Stanford University
Department of Electrical Engineering
Palo Alto, California 94305
Attention: R. Panholzer

Massachusetts Institute of Technology
Naval Supersonic Laboratory
Cambridge, Massachusetts 02139
Attention: E.E. Covert

The Bendix Corporation
Bendix Systems Division
Ann Arbor, Michigan 48103
Attention: Librarian

Thompson Ramo Wooldridge, Inc.
New Product Research Department
23555 Euclid Avenue
Cleveland, Ohio 44117
Attention: A.C. Eckert

Aerojet-General Corporation
P.O. Box 296
Azusa, California 91703
Attention: Librarian

Aerojet-General Nucleonics
P.O. Box 77
San Ramon, California 94583
Attention: Librarian

AiResearch Manufacturing Company
Sky Harbor Airport
402 South 36th Street
Phoenix, Arizona 85009
Attention: L.D. Six

Hughes Aircraft Company
Aerospace Division
11940 West Jefferson Boulevard
Culver City, California 90230
Attention: Librarian

Pratt and Whitney Aircraft
400 Main Street
East Hartford, Connecticut 06108
Attention: W.J. Lueckel

Rocketdyne
Canoga Park, California 91303
Attention: Librarian

Byron Jackson Pumps, Incorporated
P.O. Box 2017, Terminal Annex
Los Angeles, California 90054
Attention: Librarian

U.S. Atomic Energy Commission
Division of Reactor Development
Army Reactors Branch
Washington, D.C. 20545
Attention: C.A. Vansant

Iowa State University
Ames, Iowa 50010
Attention: F.H. Spedding

Hughes Aircraft Company
Hughes Research Laboratories Division
3011 Malibu Canyon Road
Malibu, California 70265
Attention: James. R. Golledge

Sundstrand Aviation
2480 West 70th Avenue
Denver, Colorado 80221
Attention: Librarian

Westinghouse Electric Corporation
Atomic Equipment Division
Cheswick, Pennsylvania 15024
Attention: R.L. Nixon

Allison Division
General Motors Corporation
Indianapolis, Indiana 46206
Attention: L. Tipton